RESTRICTED UNCLASSIFIED

COPY NO. 96

RM No. E8F09b

Inactive
Auth. J. W. Crowley 3/25/54
per change 1961 NACA 4/1/54

NACA

RESEARCH MEMORANDUM

ALTITUDE-WIND-TUNNEL INVESTIGATION OF A 4000-POUND-THRUST AXIAL-FLOW TURBOJET ENGINE

III - PERFORMANCE CHARACTERISTICS WITH THE HIGH-FLOW COMPRESSOR

By William A. Fleming and Richard L. Golladay

CLASSIFICATION CANCELLED

Authority J. W. Crowley Date 12/14/53
E.O. 10501
By NACA 1/15/54 See NACA
RM 1961

CLASSIFIED DOCUMENT

This document contains classified information affecting the National Defense of the United States within the meaning of the Espionage Act, USC 50:31 and 32. Its transmission or the revelation of its contents in any manner to an unauthorized person is prohibited by law. Information so classified may be imparted only to persons in the military and naval services of the United States, appropriate civilian officers and employees of the Federal Government who have a legitimate interest therein, and to United States citizens of known loyalty and discretion who of necessity must be informed thereof.

LIBRARY COPY

JAN 7 1954

LANGLEY AERONAUTICAL LABORATORY
LIBRARY, NACA
LANGLEY FIELD, VIRGINIA

NATIONAL ADVISORY COMMITTEE
FOR AERONAUTICS

WASHINGTON
August 5, 1948

RESTRICTED UNCLASSIFIED

NASA Technical Library
3 1176 01435 5334

UNCLASSIFIED

NATIONAL ADVISORY COMMITTEE FOR AERONAUTICS

RESEARCH MEMORANDUM

ALTITUDE-WIND-TUNNEL INVESTIGATION OF A 4000-POUND-THRUST AXIAL-FLOW TURBOJET ENGINE

III - PERFORMANCE CHARACTERISTICS WITH THE HIGH-FLOW COMPRESSOR

By William A. Fleming and Richard L. Golladay

SUMMARY

An investigation was conducted in the Cleveland altitude wind tunnel to determine the performance of an axial-flow turbojet engine having a thrust rating of 4000 pounds with a high-flow compressor. The range of the investigation extended from pressure altitudes of 5000 to 40,000 feet with ram pressure ratios from 1.00 to 1.82. The data presented cover a range of pressure altitudes from 20,000 to 40,000 feet and ram pressure ratios from 1.09 to 1.75. A comparison is made between the engine performance with high-flow and low-flow compressors. The data presented also show how the performance is affected by enlarging the tail-pipe-nozzle area. Methods of generalizing the data discussed in a previous investigation are applied to the data obtained in this investigation.

Installation of a high-flow compressor in the engine in place of a low-flow compressor, at a corrected engine speed of 7600 rpm and a ram pressure ratio of 1.40 gave an increase in corrected jet thrust of 11 percent, in corrected net thrust of 6.5 percent, in corrected net thrust horsepower of 6.5 percent, in corrected fuel consumption of 14 percent, and in corrected air flow of 12 percent. With the high-flow compressor, the specific fuel consumption based on net thrust horsepower was slightly increased above the values obtained with the low-flow compressor. Increasing the tail-pipe-nozzle area resulted in a reduction in thrust with a small increase in specific fuel consumption based on jet thrust and on net thrust horsepower. An increase in airspeed resulted in a corresponding decrease in specific fuel consumption based on net thrust horsepower. At a pressure altitude of 30,000 feet and an engine speed of 7500 rpm, the specific fuel consumption based on net thrust horsepower was 1.03 at 480 miles per hour and 0.80 at

UNCLASSIFIED

630 miles per hour. The methods of generalizing the data discussed in a previous investigation are further substantiated by the data presented in this report.

INTRODUCTION

An investigation has been conducted in the Cleveland altitude wind tunnel to determine the operational and performance characteristics of an axial-flow turbojet engine. The investigations with a high-flow compressor were conducted over a range of pressure altitudes from 5000 to 40,000 feet and ram pressure ratios from 1.00 to 1.82 with tunnel temperatures from 60° to -50° F. The tunnel temperatures were held at approximately NACA standard values for each altitude condition. Performance and windmilling drag characteristics of the engine with the low-flow compressor are presented in reference 1. Tests were also run with a high-flow compressor installed in the engine to increase the thrust without increasing the size or the weight of the engine. Operational characteristics of the engine with a low-flow compressor and with a high-flow compressor are discussed in reference 2.

The high-flow compressor unit reported herein does not represent any engine contemplated for production by the engine manufacturer, but does represent the initial attempt of the engine manufacturer to obtain increased performance by modifying a standard unit with the quickest and simplest methods available at the time of the 4000-pound-thrust axial-flow turbojet engine investigation.

The results of performance investigations on the engine with the high-flow compressor over a range of pressure altitudes from 20,000 to 40,000 feet and ram pressure ratios from 1.09 to 1.75 is presented. Measurements of thrust, horsepower, fuel consumption, and air flow were made at several pressure altitudes and ram pressure ratios throughout the range of operable engine speeds. A comparison is made of the performance of the engine in the standard configuration with the low-flow compressor and in the revised configuration with the high-flow compressor. The effect of tail-pipe-nozzle area on engine performance is discussed. A further check was made on the applicability of the methods discussed in reference 1 that were used to generalize the data.

The engine configuration was changed several times during the investigation with the high-flow compressor in an attempt to obtain satisfactory engine operation. Two tail-pipe nozzles, one 18 inches

and the other $19\frac{1}{2}$ inches in diameter, and standard and large-size turbine nozzles were used. A further description of the engine configurations is presented in reference 2.

553

Air was introduced into the engine through a duct at pressures corresponding to ram pressures for various flight speeds. Extensive instrumentation was installed on the engine to obtain detailed information on the individual components of the engine as well as the over-all engine performance.

SYMBOLS

The following symbols are used in the report:

F_j	jet thrust, pounds
F_n	net thrust, pounds
H_1	total pressure at cowl inlet, station 1, pounds per square foot absolute
H_1/p_0	ram pressure ratio
N	engine speed, rpm
p_0	tunnel ambient pressure, pounds per square foot absolute
thp	net thrust horsepower
W_a	air flow, pounds per second
W_f	fuel consumption, pounds per hour
W_f	fuel consumption, pounds per second
W_f/W_a	fuel-air ratio
W_f/F_j	specific fuel consumption based on jet thrust, pounds per hour per pound thrust
W_f/thp	specific fuel consumption based on net thrust horsepower, pounds per thrust horsepower-hour (same as corrected value)

δ ratio of absolute total pressure at compressor inlet to absolute static pressure at NACA standard atmospheric conditions at sea level

θ ratio of absolute total temperature at compressor inlet to absolute static temperature of NACA standard atmospheric conditions at sea level

The following generalized engine and performance parameters are obtained by correcting the data to NACA standard atmospheric conditions at sea level.

F_j/δ corrected jet thrust, pounds

F_n/δ corrected net thrust, pounds

$N/\sqrt{\theta}$ corrected engine speed, rpm

$thp/(\delta\sqrt{\theta})$ corrected net thrust horsepower

$(W_a\sqrt{\theta})/\delta$ corrected air flow, pounds per second

$W_f/(\delta\sqrt{\theta})$ corrected fuel consumption, pounds per hour

$W_f/(F_j\sqrt{\theta})$ corrected specific fuel consumption based on jet thrust, pounds per hour per pound thrust

$w_f/(W_a\theta)$ corrected fuel-air ratio

WIND-TUNNEL INSTALLATION AND PROCEDURE

Description of Engine

Because the J33 turbojet engine had not been operated with the high-flow compressor before its installation in the wind tunnel, no static sea-level rating was available for the engine in this configuration. The high-flow compressor differed from the low-flow compressor in that the blade angles of the rotor and stator blades were increased approximately 5°. The change of blade angle increased the air-flow rate 12 percent above that obtained with the low-flow compressor at maximum engine speed (7600 rpm). With the high-flow compressor the engine has the same physical dimensions and weight as with the low-flow compressor. The over-all length of the engine is approximately 14 feet; the maximum diameter, 36 inches; and the total weight, 2300 pounds. The high-flow compressor has 11 axial-flow

553

553

stages and provides a pressure ratio of about 5 at 7600 rpm. On the engine are eight individual combustion chambers, each of which is joined to the adjacent chambers by small interconnecting tubes for cross ignition. A single-stage turbine drives the compressor. Two tail-pipe nozzles were used during the runs with the high-flow compressor; one nozzle was 18 inches in diameter and the other was $19\frac{1}{2}$ inches. A standard turbine nozzle having an area of 106.7 square inches was used with the 18-inch-diameter tail-pipe nozzle, and a turbine nozzle having an area of 121.0 square inches was used with the $19\frac{1}{2}$-inch-diameter tail-pipe nozzle. The runs with the $19\frac{1}{2}$-inch-diameter tail-pipe nozzle and part of the runs with the 18-inch-diameter tail-pipe nozzle were conducted with a tail pipe on the engine that contained a row of vanes immediately behind the turbine. These vanes were installed in an attempt to reduce the swirl in the jet.

Installation and Procedure

Installation of the engine with the high-flow compressor was the same as with the low-flow compressor (reference 1). The description is repeated in this section.

The engine was supported on a 7-foot-chord airfoil installed in the 20-foot-diameter test section of the wind tunnel (fig. 1). The cowling extended back only as far as the rear of the compressor; the combustion chambers and the tail pipe were thus cooled by the movement of the air in the test section. Inlet pressures corresponding to flight at high speeds were obtained by introducing dry refrigerated air from the tunnel make-up air system throttled from approximately sea-level pressure to the desired pressure at the engine inlet. The wind-tunnel pressure and temperature corresponding to the test altitude were maintained. The make-up air duct was connected to the engine intake by means of a slip joint located 40 feet upstream of the engine (fig. 2, station X). The use of a slip joint permitted engine-thrust and installation-drag measurements to be made with the tunnel scales. An orifice for measuring the air flow is shown in the ram-pipe installation, but the results obtained were not sufficiently accurate to be used. The velocity in the tunnel test section varied from 40 to 100 feet per second, as induced by the ejector effect of the jet and by the tunnel-exhauster scoop located immediately downstream of the test section.

The engine was extensively instrumented as shown in figure 3. Temperature and pressure measurements of the air and the gases were

made at eight stations in the engine (fig. 4). Thrust was measured by the balance scales and was also calculated from pressure and temperature measurements obtained with the tail-pipe-nozzle rake. (See fig. 5.) In order to correct the scale thrust measurements, power-off drag investigations were conducted with the engine inlet covered so that the external drag coefficient of the installation could be determined.

- 553

METHODS OF CALCULATION

The thrust was determined by two methods: (1) measurement directly on the balance scales and (2) calculation from temperature and pressure measurements obtained with the tail-rake survey (fig. 5) located at the tail-pipe-nozzle exit. The thrust values measured by the second method are presented because they give more consistent results than some of the measurements with the balance scales. The jet thrust calculated with the tail-rake survey was multiplied by the factor 0.985, which was discussed in reference 1, in order to obtain the actual jet thrust. This factor was further substantiated by data obtained with the high-flow compressor.

The rate of engine air flow was determined by two methods: (1) calculation from temperatures and pressures obtained with the tail-rake survey at station 8 and (2) calculation from temperatures and pressures obtained with the cowl-inlet survey at station 1. The values obtained from the tail-rake survey are presented because they more closely agree with heat balances made through the engine. The methods and the equations used to determine the engine performance are presented in reference 1.

RESULTS AND DISCUSSION

Effect of Altitude, Tail-Pipe-Nozzle Area, and Ram Pressure Ratio on Engine Performance

Effect of altitude. - The performance data for the engine at a ram pressure ratio of approximately 1.40 are presented for the 18-inch tail pipe at pressure altitudes of 20,000 and 30,000 feet and for the $19\frac{1}{2}$-inch tail pipe at pressure altitudes of 20,000, 30,000, and 40,000 feet. The jet thrust (fig. 6), the net thrust

(fig. 7), the net thrust horsepower (fig. 8), and the fuel consumption (fig. 9) decreased as the altitude increased owing to the reduced density of the air and the consequent reduced mass air flow through the engine at altitude (fig. 10).

In the upper range of engine speeds, the specific fuel consumption based on jet thrust (fig. 11) fell on a single curve for pressure altitudes of 20,000 and 30,000 feet but was slightly higher at 40,000 feet. In the range of lower engine speeds, the increase in specific fuel consumption as the altitude became higher is attributed to lower component efficiencies at high altitude.

The specific fuel consumption based on net thrust horsepower decreased slightly with increasing altitude (fig. 12). As the altitude was increased from sea level and the ambient temperature was correspondingly decreased at constant engine speed and ram pressure ratio, the compressor pressure ratio slightly increased. The improvement in cycle efficiency accompanying the increased compressor pressure ratio resulted in a slight decrease in specific fuel consumption based on net thrust horsepower at high altitudes. As the ambient temperature was reduced at a constant ram pressure ratio, the airspeed decreased in proportion to the square root of the ratio of free-stream total temperature at altitude to sea-level ambient temperature $\sqrt{\theta}$. This reduction in airspeed thereby resulted in a reduction in net thrust horsepower and fuel consumption proportional to $\sqrt{\theta}$. The net thrust horsepower and the fuel consumption decreased proportionately, therefore the specific fuel consumption based on net thrust horsepower was not dependent on air temperature.

The fuel-air ratio increased slightly with altitude throughout the entire range of engine speeds. (See fig. 13.)

Effect of tail-pipe-nozzle area. - A comparison of the engine performance shows that with the $19\frac{1}{2}$-inch nozzle at an engine speed of 7600 rpm there were reductions of approximately 20 percent in jet thrust (fig. 6), 30 percent in net thrust (fig. 7), 30 percent in net thrust horsepower (fig. 8), and 19 percent in fuel consumption (fig. 9). The tail-pipe temperatures were lower with this nozzle than with the 18-inch nozzle for corresponding engine speeds. The weight air flow was slightly lower with the $19\frac{1}{2}$-inch nozzle (fig. 10). The air flow measured by both the tail-pipe survey and

the cowl-inlet survey was lowest with the $19\frac{1}{2}$-inch nozzle. No explanation for these results is known.

The specific fuel consumption based on jet thrust was about the same with both tail-pipe nozzles at 7600 rpm and pressure altitudes of 20,000 and 30,000 feet (fig. 11). At lower engine speeds the specific fuel consumption was considerably higher with the $19\frac{1}{2}$-inch nozzle. The specific fuel consumption based on net thrust horsepower was higher with the $19\frac{1}{2}$-inch nozzle throughout the entire range of engine speeds (fig. 12). At 7600 rpm the specific fuel consumption was approximately 1.03 with the 18-inch nozzle and 1.16 with the $19\frac{1}{2}$-inch nozzle. With the $19\frac{1}{2}$-inch tail-pipe nozzle, the pressure at the compressor outlet was lower than with the 18-inch nozzle, and the compressor pressure ratio was correspondingly decreased. The reduced compressor pressure ratio resulted in a lower cycle efficiency and therefore higher specific fuel consumptions based on jet thrust and on net thrust horsepower.

The fuel-air ratio (fig. 13) was lower with the $19\frac{1}{2}$-inch nozzle throughout the entire range of engine speeds. With this nozzle and the large turbine nozzles, the back pressure on the turbine was reduced. In both cases the pressure ratio across the turbine was approximately the same and, consequently, the back pressure on the compressor was also lower; the work required to drive the compressor was therefore less. The result was that the engine could be operated at each speed with a lower turbine-inlet temperature and consequently with a lower fuel-air ratio when the large tail-pipe and turbine nozzles were used.

Effect of ram pressure ratio. - Performance data were obtained at a pressure altitude of 30,000 feet and ram pressure ratios of 1.09, 1.40, and 1.75 with the 18-inch tail-pipe nozzle and standard turbine nozzles. The jet thrust increased with ram pressure ratio throughout the entire range of engine speeds (fig. 14) owing chiefly to the corresponding increase in weight air flow (fig. 15) and jet velocity. The fuel consumption also increased with ram pressure above 6000 rpm (fig. 16), but at lower engine speeds the fuel consumption was less at high ram pressures. The net thrust (fig. 17) and the net thrust horsepower (fig. 18) increased with ram pressure ratio at high engine speeds but at low engine speeds both were lower at high ram pressure ratios. The fuel-air ratio was lower at high ram pressures throughout the entire range of engine speeds (fig. 19). The fuel-air raio is dependent on the temperature required at the turbine inlet to drive the turbine. As the ram pressure ratio is

increased, the pressure ratio across the compressor becomes less, but the pressure ratio across the turbine changes negligibly. The work per pound of air flow required to drive the compressor is less at high ram pressure ratios and the temperature rise required per pound of air through the combustion chamber is therefore lower because a lower gas temperature is required to drive the turbine. This reduction in temperature rise per pound of air at high ram pressure ratios gives the corresponding reduction in fuel-air ratio.

The specific fuel consumption based on jet thrust (fig. 20) and net thrust horsepower (fig. 21) rapidly decreased as the ram pressure ratio was increased. At an engine speed of 7500 rpm and a ram pressure ratio of 1.40, corresponding to a true airspeed of about 480 miles per hour at a pressure altitude of 30,000 feet, the specific fuel consumption based on net thrust horsepower was 1.03. For the same engine speed and a ram pressure ratio of 1.75, corresponding to a true airspeed of about 630 miles per hour at a pressure altitude of 30,000 feet, the specific fuel consumption based on net thrust horsepower was 0.80.

Effect of Altitude and Ram Pressure Ratio on Generalized Performance

Effect of altitude. - As previously discussed in reference 1, an analysis of jet-engine performance data has given reduction parameters that generalize experimental performance data taken at any altitude in order that these data may serve to estimate jet-engine performance at all altitudes. The application of the reduction factors θ and δ to the engine performance parameters give the following generalized parameters: corrected engine speed $N/\sqrt{\theta}$, corrected jet thrust F_j/δ, corrected net thrust F_n/δ, corrected net thrust horsepower $thp/(\delta\sqrt{\theta})$, corrected air flow $(W_a\sqrt{\theta})/\delta$, corrected fuel consumption $W_f/(\delta\sqrt{\theta})$, corrected specific fuel consumption based on jet thrust $W_f/(F_j\sqrt{\theta})$, specific fuel consumption based on net thrust horsepower W_f/thp, and corrected fuel-air ratio $w_f/(W_a\theta)$.

Applications of some of these reduction factors are shown in curves of generalized performance obtained at pressure altitudes of 20,000, 30,000, and 40,000 feet at a ram pressure ratio of approximately 1.40. Data were obtained with the 18-inch tail-pipe nozzle at pressure altitudes of 20,000 and 30,000 feet and with the $19\frac{1}{2}$-inch nozzle at pressure altitudes of 20,000, 30,000, and

40,000 feet. Performance of the low-flow compressor at a pressure altitude of 40,000 feet and a ram pressure ratio of 1.41 is shown on the generalized curves for the 18-inch tail-pipe nozzle. These performance data with the low-flow compressor are presented in reference 1. Jet thrust (fig. 22), net thrust (fig. 23), net thrust horsepower (fig. 24), and air flow (fig. 25) reduce to single curves. These results further substantiate the data presented in reference 1, which show that such curves can be generalized.

The corrected fuel consumption (fig. 26) measured at pressure altitudes of 20,000, 30,000, and 40,000 feet and an approximate ram pressure ratio of 1.40 lie on a single curve. Reference 1 shows that the fuel consumption in the low range of engine speeds increased with altitude. The engine was not operated at sufficiently low engine speeds in this series of investigations to show clearly the effect of altitude on fuel consumption.

The corrected specific fuel consumption based on jet thrust (fig. 27) shows more clearly the effect of altitude on fuel consumption than figure 26. At high engine speeds the corrected specific fuel consumption based on jet thrust fell on a single curve for all altitudes; whereas at low engine speeds the specific fuel consumption increased with altitude. Altitude had a very small effect on the specific fuel consumption based on net thrust horsepower (fig. 28), as discussed in reference 1.

The corrected fuel-air ratio reduces to a single curve throughout the entire range of engine speeds with the 18-inch tail-pipe nozzle (fig. 29(a)). With the $19\frac{1}{2}$-inch tail-pipe nozzle, however, the corrected fuel-air ratio reduces to a single curve only at high engine speeds (fig. 29(b)). In the range of low engine speeds, the fuel-air ratio is higher at high altitudes.

Effect of ram pressure ratio. - In general, the effect of ram pressure ratio on performance as determined from these investigations substantiates the results presented in reference 1. An increase in ram pressure ratio resulted in a corresponding increase in corrected jet thrust (fig. 30). The corrected net thrust was lower at a ram pressure ratio of 1.40 than at 1.09, but above a corrected engine speed of 7000 rpm the corrected net thrust was higher at a ram pressure ratio of 1.75 than at 1.40 (fig. 31). The corrected net thrust horsepower increased with ram pressure ratio throughout most of the operating range (fig. 32); in the lower portion of the operating range, however, the corrected net thrust horsepower was lower at high ram pressure ratios. The corrected fuel consumption was

553

lower at high ram pressure ratios throughout a large part of the operating range (fig. 33), but above a corrected engine speed of 7900 rpm the corrected fuel consumptions for ram pressure ratios of 1.09, 1.40, and 1.75 were of equal value. The generalization factors correct the air flow to a single curve at corrected engine speeds above 5000 rpm for all ram pressure ratios (fig. 34). The high idling speed of the engine at high airspeeds and at a pressure altitude of 30,000 feet prevented predicting whether the correction will also apply in the lower range of engine speeds. Calculated data presented in the manufacturer's installation manual indicate that a family of curves will diverge in the low range of engine speeds, showing an increase in air flow with airspeed.

These data, the generalized data presented for several altitudes, and the data presented in reference 1 show that runs at several ram pressure ratios give generalized data, which fall on a family of curves and show that data must be obtained at each ram pressure ratio in order to determine the family of generalized curves representative of the performance at all airspeeds.

Increased ram pressure ratios resulted in an appreciable reduction in the corrected specific fuel consumption based on jet thrust (fig. 35) and the corrected specific fuel consumption based on net thrust horsepower (fig. 36). The corrected fuel-air ratios for ram pressure ratios of 1.09, 1.40, and 1.75 determine a single curve above a corrected engine speed of 7500 rpm (fig. 37). Below this engine speed, the corrected fuel-air ratio is lower at high ram pressure ratios.

Comparison of Generalized Performance with High-Flow and Low-Flow Compressors

Generalized performance data obtained at a ram pressure ratio of approximately 1.4 are compared for the engine equipped with the high-flow and the low-flow compressors. Data are presented for the low-flow compressor with the $16\frac{3}{4}$-inch tail-pipe nozzle and for the high-flow compressor with the 18-inch tail-pipe nozzle. These data were chosen for the comparison because in both cases the turbine-inlet temperatures at maximum engine speed were close to the maximum allowable limit. The data for the high-flow compressor were obtained at pressure altitudes of 20,000 and 30,000 feet and the data for the low-flow compressor, which were presented in reference 1, were obtained at a pressure altitude of 40,000 feet. Data obtained at a

pressure altitude of 40,000 feet for the low-flow compressor are used here because they are also presented in reference 1. These data can be logically compared with the data for the high-flow compressor at pressure altitudes of 20,000 and 30,000 feet because the main portion of the generalized performance reduces to a single curve throughout the entire range of engine speeds. The corrected values of jet thrust, net thrust, net thrust horsepower, fuel consumption, and air flow were higher with the high-flow compressor throughout the entire range of engine speeds. At a corrected engine speed of 7600 rpm with the high-flow compressor, the corrected jet thrust was 11 percent higher (fig. 22(a)), the corrected net thrust was 6.5 percent higher (fig. 23(a)), the corrected net thrust horsepower was 6.5 percent higher (fig. 24(a)), the corrected fuel consumption was 14 percent higher (fig. 26(a)), and the corrected air flow was 12 percent higher (fig. 25(a)). The curves of the corrected values of jet thrust, net thrust, and net thrust horsepower for the high-flow compressor change in slope between 6500 and 7000 rpm but with the low-flow compressor they were practically straight above 7000 rpm. The fuel-consumption curves for both compressors did not change in slope and their shapes were very similar. The air-flow curve for the high-flow compressor began to level off at an engine speed approximately 1000 rpm lower than for the low-flow compressor. The thrust and horsepower curves changed in slope because the air flow leveled off at a lower engine speed and the compressor efficiency was lower at high engine speeds with the high-flow compressor.

Curves are presented for corrected specific fuel consumption based on jet thrust (fig. 27(a)) and net thrust horsepower (fig. 28(a)) plotted against corrected engine speed. The corrected specific fuel consumption based on jet thrust (fig. 38) and net thrust horsepower (fig. 39) are also plotted with corrected jet thrust and corrected net thrust horsepower, respectively, as the ordinate. The corrected specific fuel consumption based on jet thrust is approximately the same with both compressors throughout the entire range of engine speeds (cf. figs. 27(a) and 38) except that at high engine speeds the engine had a slightly lower corrected specific fuel consumption based on jet thrust when operating with the low-flow compressor. The specific fuel consumption based on net thrust horsepower is slightly lower at high engine speeds for the low-flow compressor (fig. 28(a)), but at lower speeds the specific fuel consumption based on net thrust horsepower is about the same with both compressors. Figure 39 shows the specific fuel consumption based on net thrust horsepower to be slightly lower with the low-flow compressor throughout the entire range of thrust horsepower values for the engine. These results indicate that increasing

553

553

the thrust of the engine by using the high-flow compressor slightly increased the specific fuel consumption based on net thrust horsepower and did not change the corrected specific fuel consumption based on jet thrust.

The fuel-air ratio with both the high-flow and the low-flow compressors (fig. 29(a)) was approximately the same at low engine speeds, but at high engine speeds the fuel-air ratio was slightly higher with the high-flow compressor.

SUMMARY OF RESULTS

From an investigation of the performance characteristics of a 4000-pound-thrust axial-flow turbojet engine with high-flow and low-flow compressors at pressure altitudes from 20,000 to 40,000 feet and ram pressure ratios from 1.09 to 1.75, the following results were obtained:

1. The use of a high-flow compressor in place of a low-flow compressor in the engine at a corrected engine speed of 7600 rpm and a ram pressure ratio of approximately 1.4 gave an increase in corrected jet thrust of 11 percent, in corrected net thrust of 6.5 percent, in corrected net thrust horsepower of 6.5 percent, in corrected fuel consumption of 14 percent, and in corrected air flow of 12 percent. Changing the compressor had a negligible effect on the corrected specific fuel consumption based on jet thrust for all values of corrected jet thrust. The specific fuel consumption based on net thrust horsepower was raised slightly with the high-flow compressor for all values of corrected net thrust horsepower.

2. Increasing the tail-pipe-nozzle area from that of an 18-inch-diameter tail-pipe nozzle to that of a $19\frac{1}{2}$-inch-diameter tail-pipe nozzle resulted in an approximate reduction of 20 percent in jet thrust, 30 percent in net thrust, 30 percent in net thrust horsepower, and 19 percent in fuel consumption. The specific fuel consumption based on jet thrust was approximately the same at maximum engine speed (7600 rpm) for both tail-pipe nozzles, but at lower speeds the specific fuel consumption based on jet thrust was higher with the larger tail-pipe nozzle. The specific fuel consumption based on net thrust horsepower was higher throughout the entire range of engine speeds with the $19\frac{1}{2}$-inch-diameter tail-pipe nozzle.

3. The specific fuel consumption based on net thrust horsepower decreased markedly as the airspeed was increased; at a pressure altitude of 30,000 feet and an engine speed of 7500 rpm, the

specific fuel consumption based on net thrust horsepower was 1.03 at 480 miles per hour and 0.80 at 630 miles per hour.

4. The specific fuel consumption of the engine in the upper range of engine speeds at a given ram pressure ratio remained essentially the same with variation in altitude. In the lower engine-speed range the specific fuel consumption increased slightly with an increase in altitude.

5. Methods of generalizing the data discussed in a previous investigation are further substantiated by the data presented in this paper.

Flight Propulsion Research Laboratory,
National Advisory Committee for Aeronautics,
Cleveland, Ohio.

REFERENCES

1. Fleming, William A.: Altitude-Wind-Tunnel Investigation of a 4000-Pound-Thrust Axial-Flow Turbojet Engine. I - Performance and Windmilling Drag Characteristics. NACA RM No. E8F09, 1948.

2. Fleming, William A.: Altitude-Wind-Tunnel Investigation of a 4000-Pound-Thrust Axial-Flow Turbojet Engine. II - Operational Characteristics. NACA RM No. E8F09a, 1948.

553

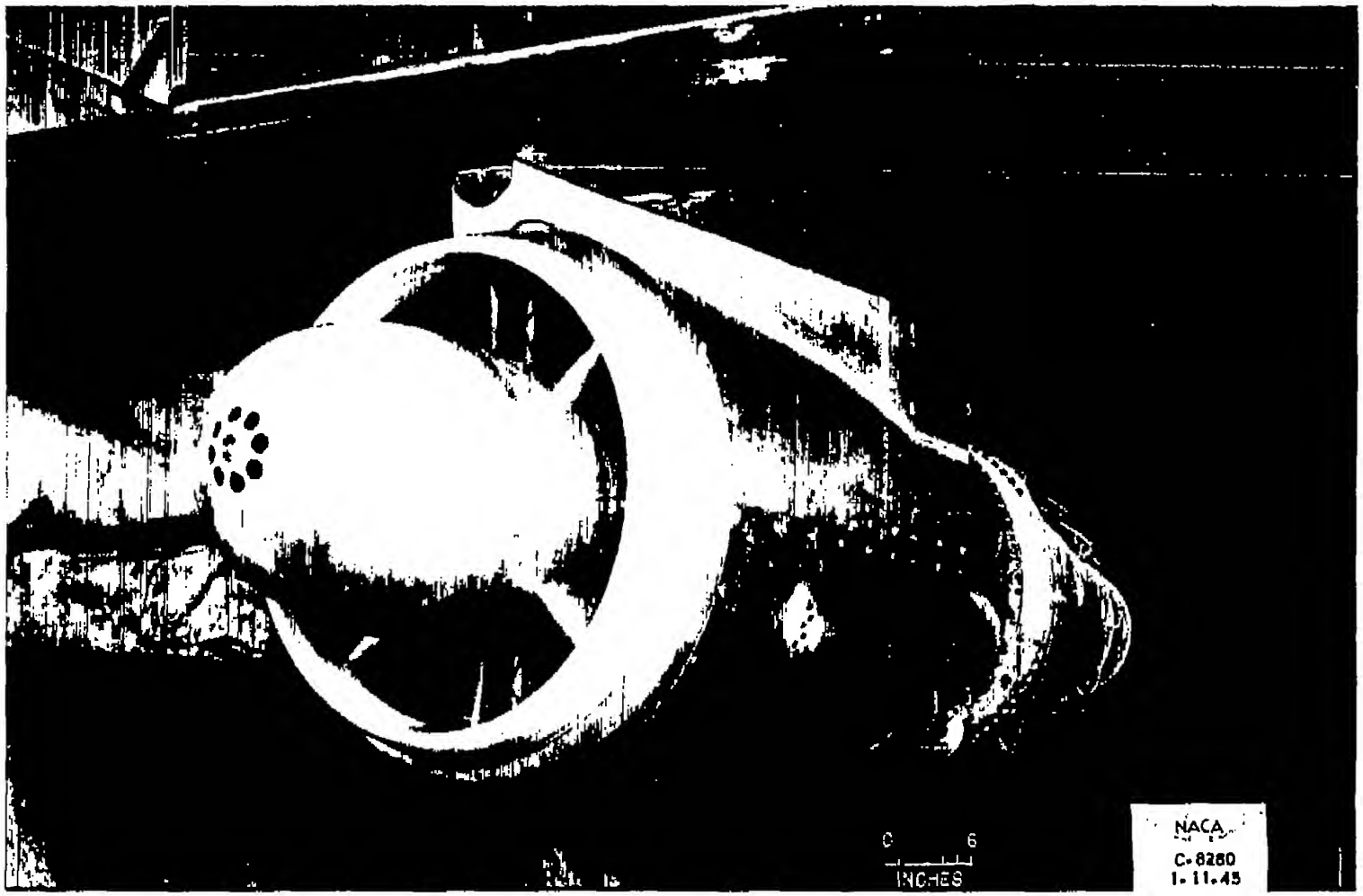

(a) Left-side view with cowling installed.

Figure 1. - Installation of 4000-pound-thrust axial-flow turbojet engine in altitude wind tunnel.

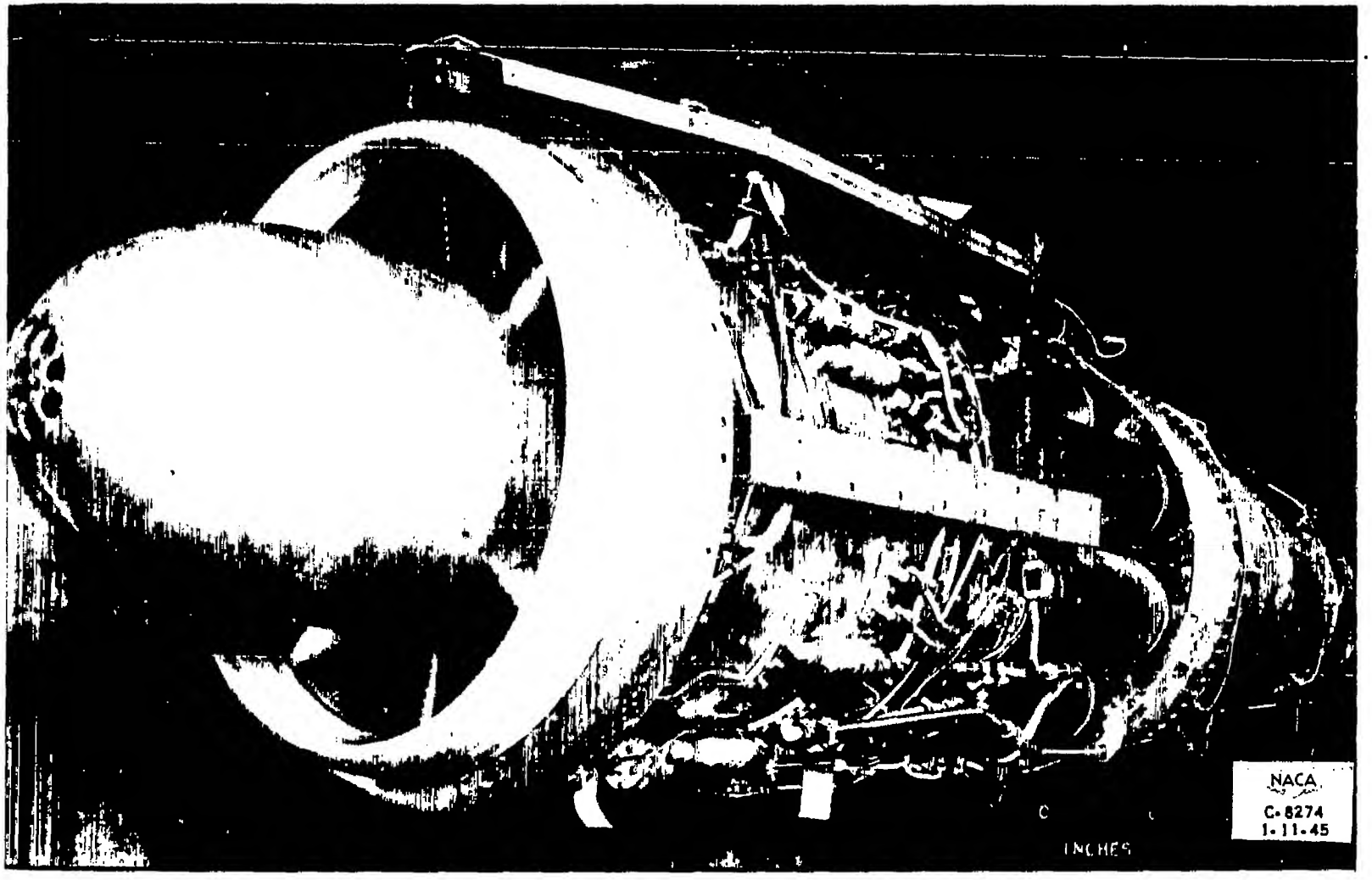

(b) Left-side view with cowling removed.

Figure 1. - Concluded.

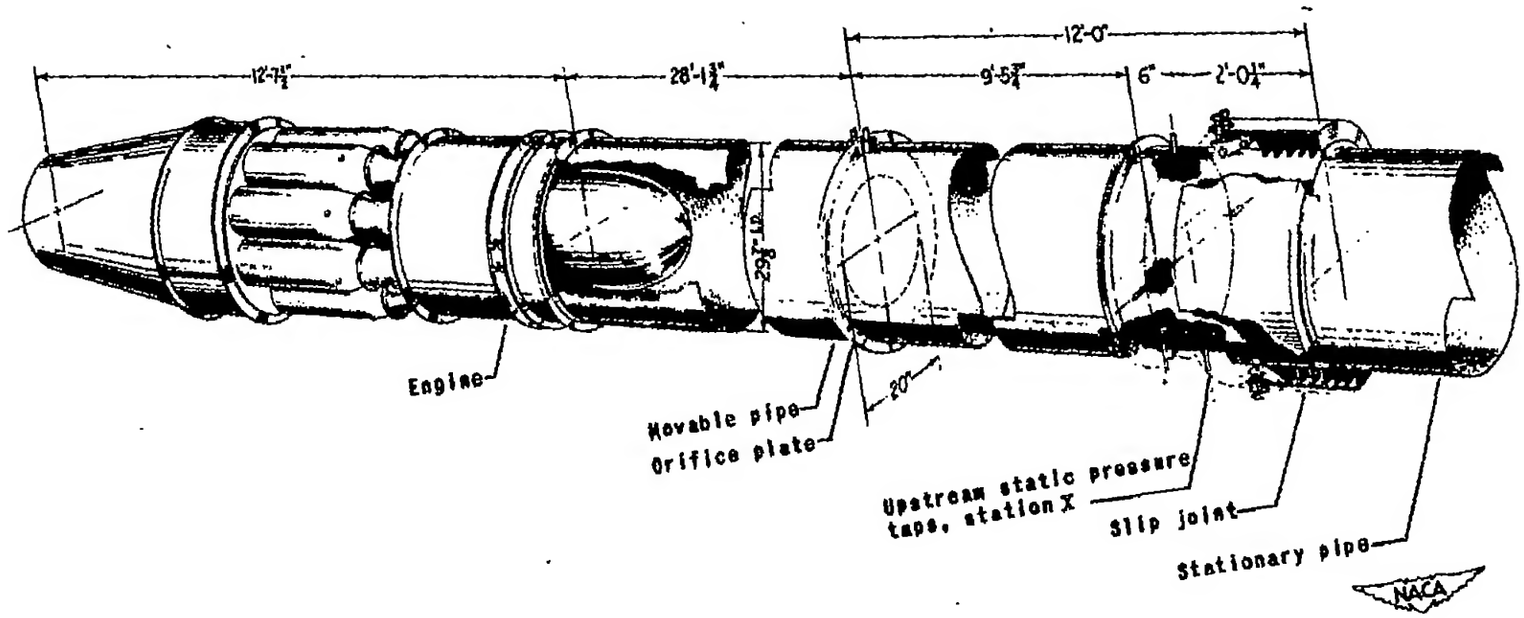

Figure 2. - Installation of closed duct from tunnel make-up air system to engine inlet for supplying air at ram pressures.

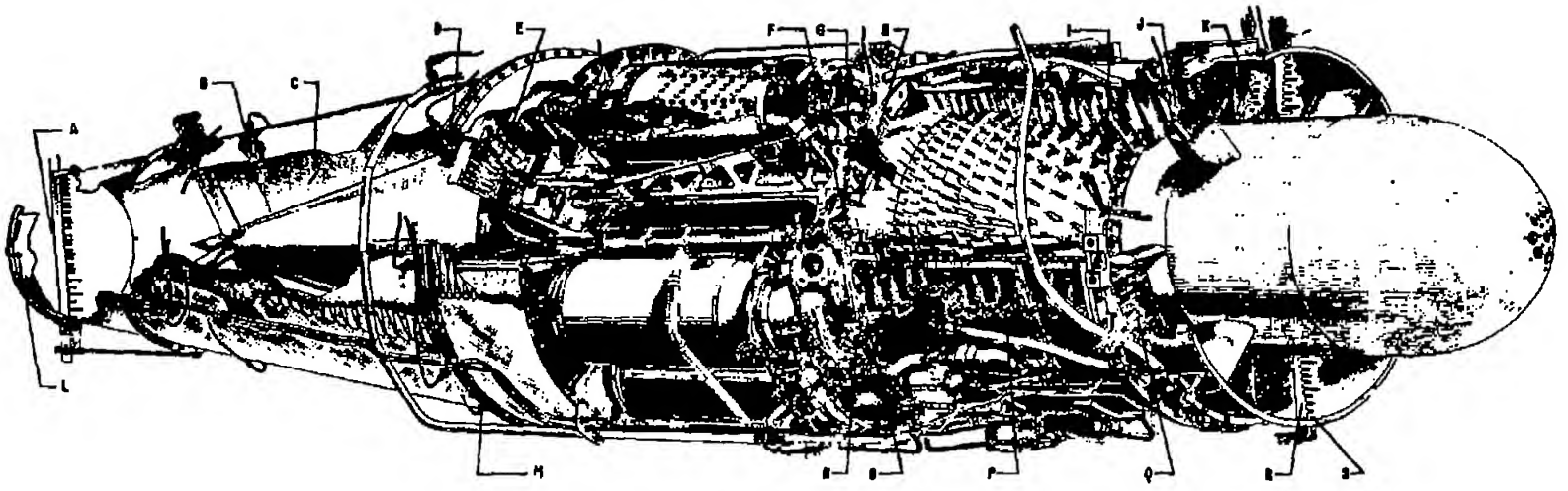

A Tail-pipe-discharge total and static-pressure and temperature survey rake (NACA)
B Tail-pipe total-pressure tube
C Tail-pipe thermocouple
D Turbine-outlet thermocouple
E Turbine-inlet total-pressure tube
F Compressor-outlet total-pressure tube
G Compressor-outlet static-pressure wall orifice (NACA)
H Compressor-outlet total-pressure and temperature survey rake (NACA)
I Compressor-inlet static-pressure wall orifice
J Compressor-inlet thermocouple
K Compressor-inlet total- and static-pressure survey rake (NACA)
L Tail-pipe-discharge static-pressure wall orifice (NACA)
M Turbine-outlet static-pressure wall orifice
N Compressor-outlet thermocouple
O Compressor-outlet static-pressure survey rake (NACA)
P Compressor-interstage static-pressure wall orifices
Q Compressor-inlet total-pressure tube
R Cowl-inlet total- and static-pressure and temperature survey rake (NACA)
S Cowl-inlet static-pressure wall orifice (NACA)

(NACA) Instrumentation installed by NACA for altitude-wind-tunnel tests.

NACA

Figure 3. – Instrumentation of axial-flow turbojet engine for altitude-wind-tunnel investigations.

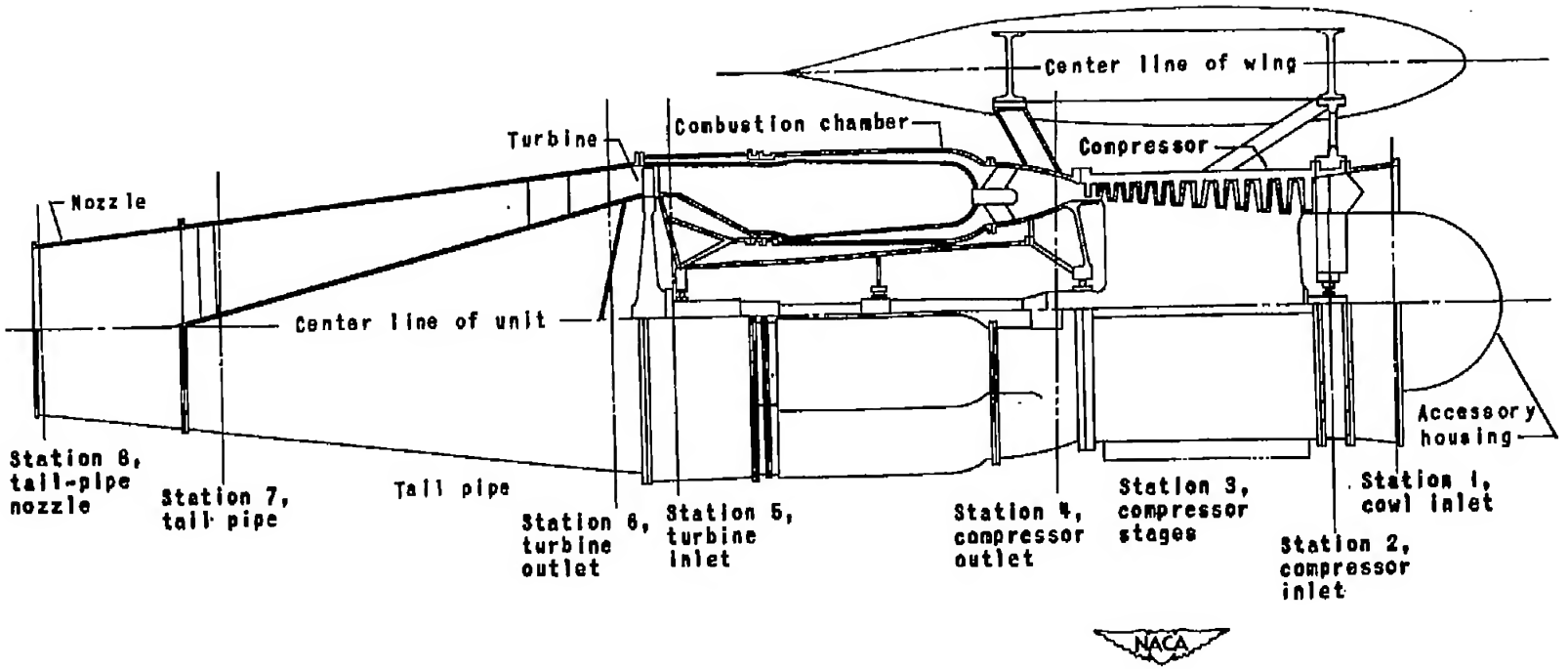

Figure 4. – Side view of turbojet installation showing measuring stations.

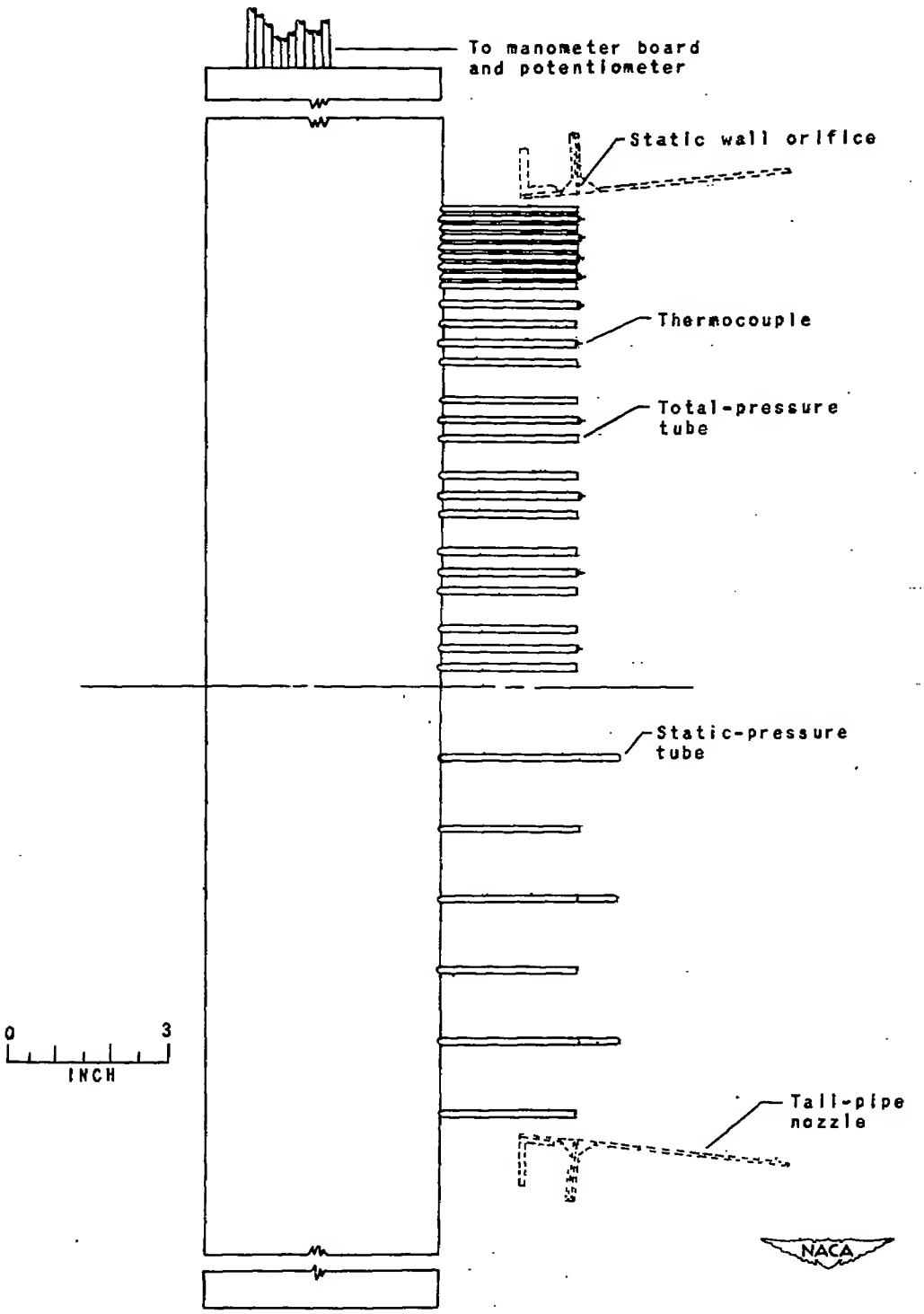

Figure 5. - Details of total- and static-pressure-tube and thermocouple installation at nozzle outlet.

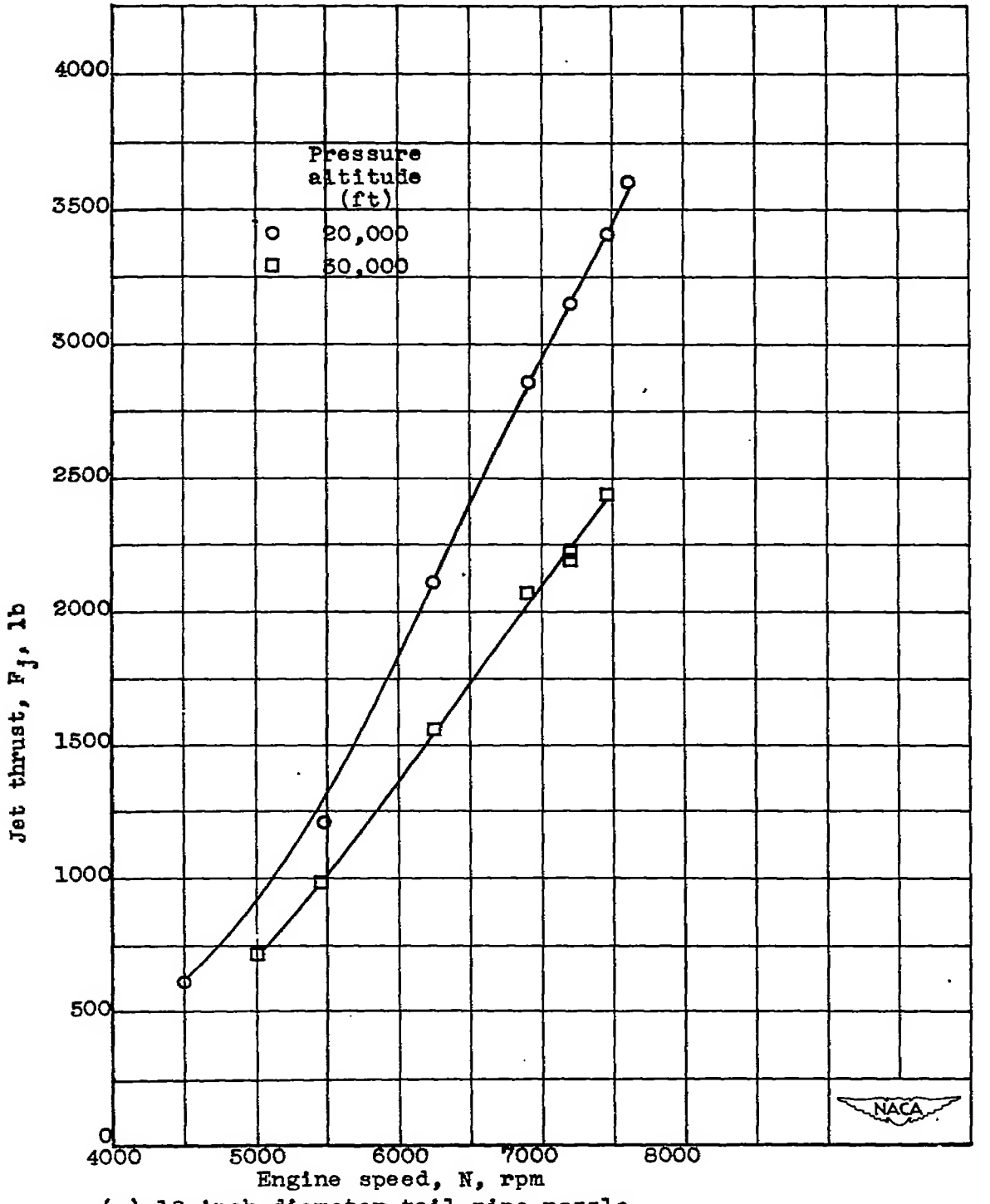

(a) 18-inch-diameter tail-pipe nozzle.

Figure 6.- Effect of engine speed and pressure altitude on jet thrust at a ram pressure ratio of approximately 1.40 with high-flow compressor.

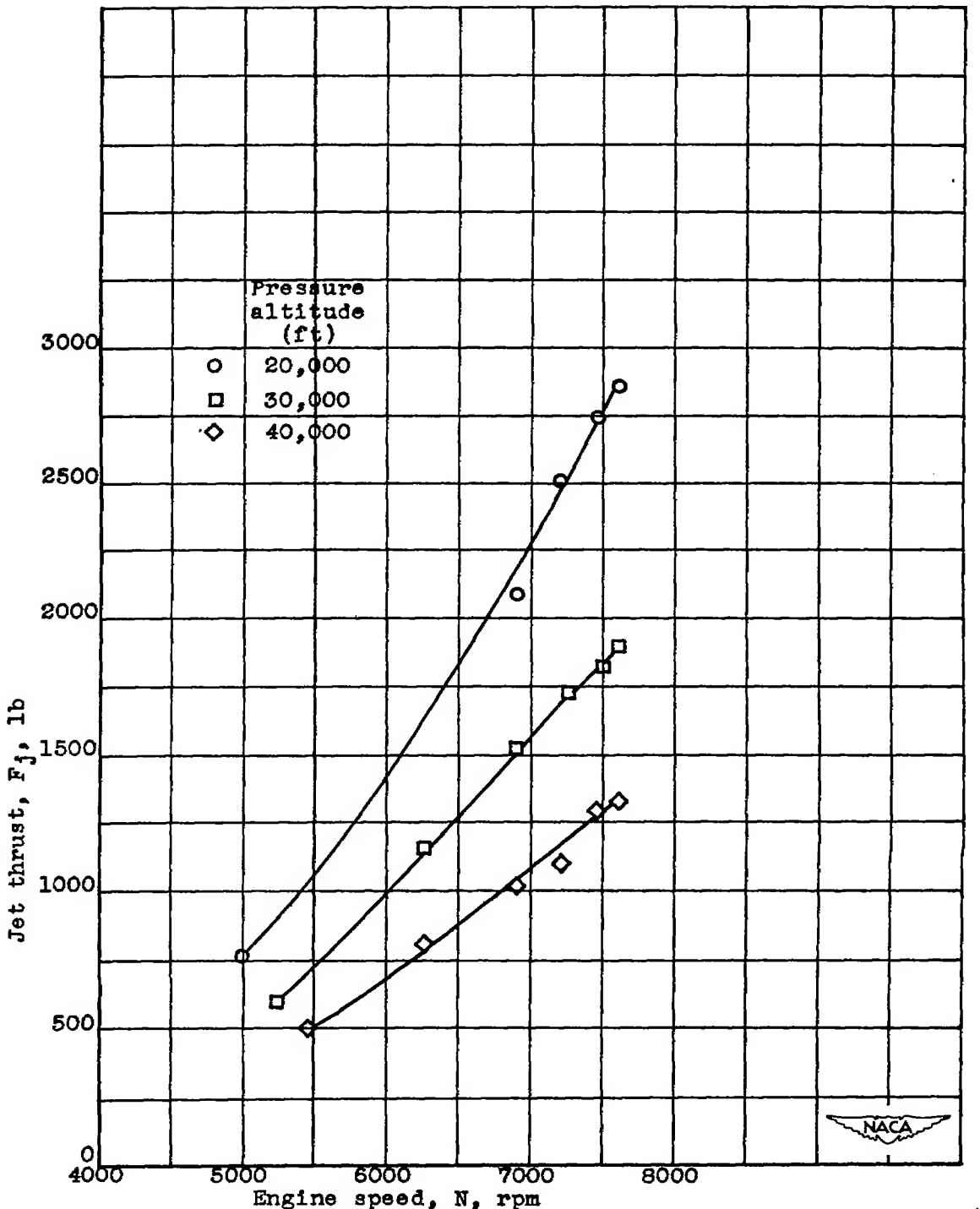

(b) $19\frac{1}{2}$-inch-diameter tail-pipe nozzle.

Figure 6.- Concluded.

553

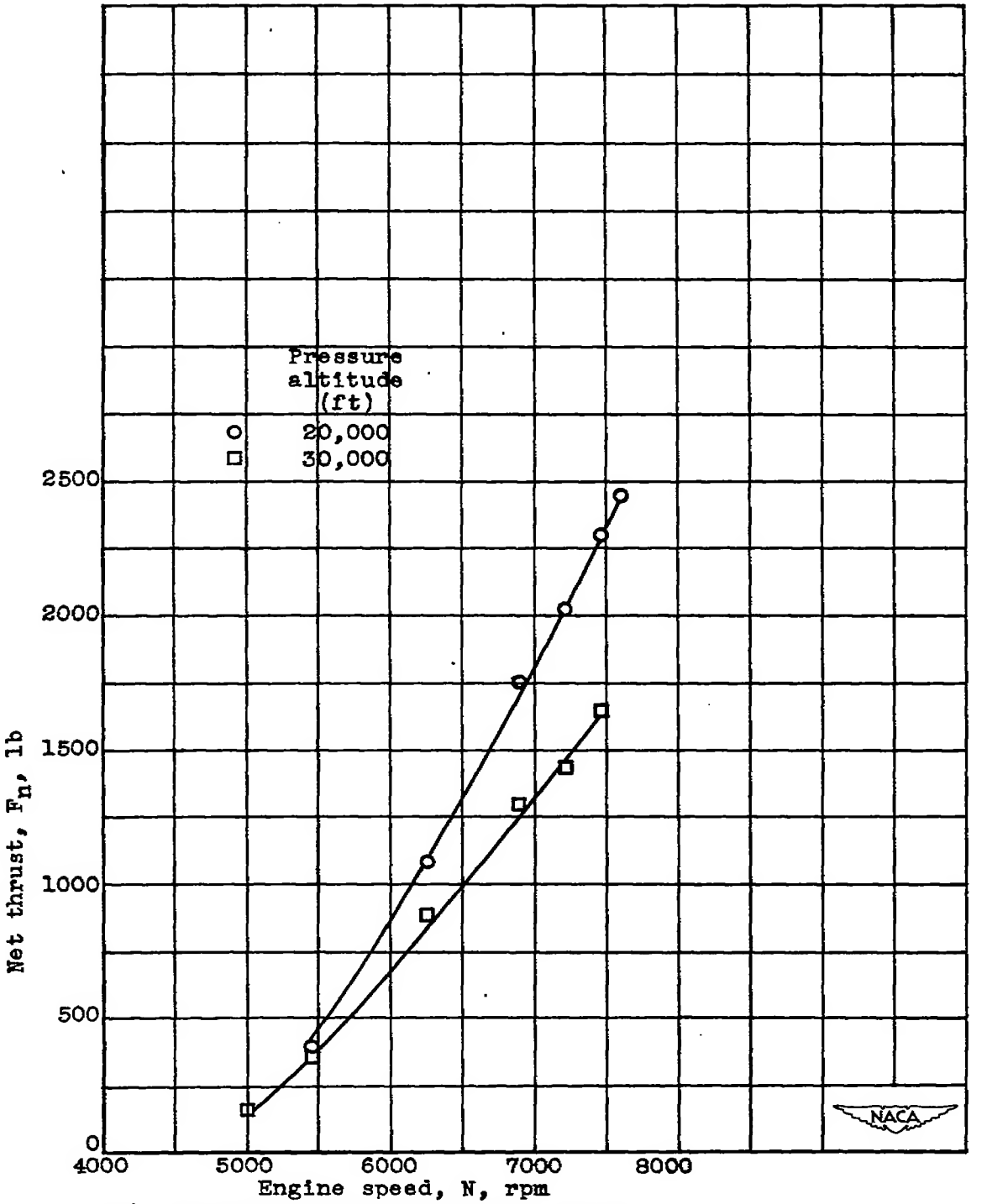

(a) 18-inch-diameter tail-pipe nozzle.

Figure 7.- Effect of engine speed and pressure altitude on net thrust at a ram pressure ratio of approximately 1.40 with high-flow compressor.

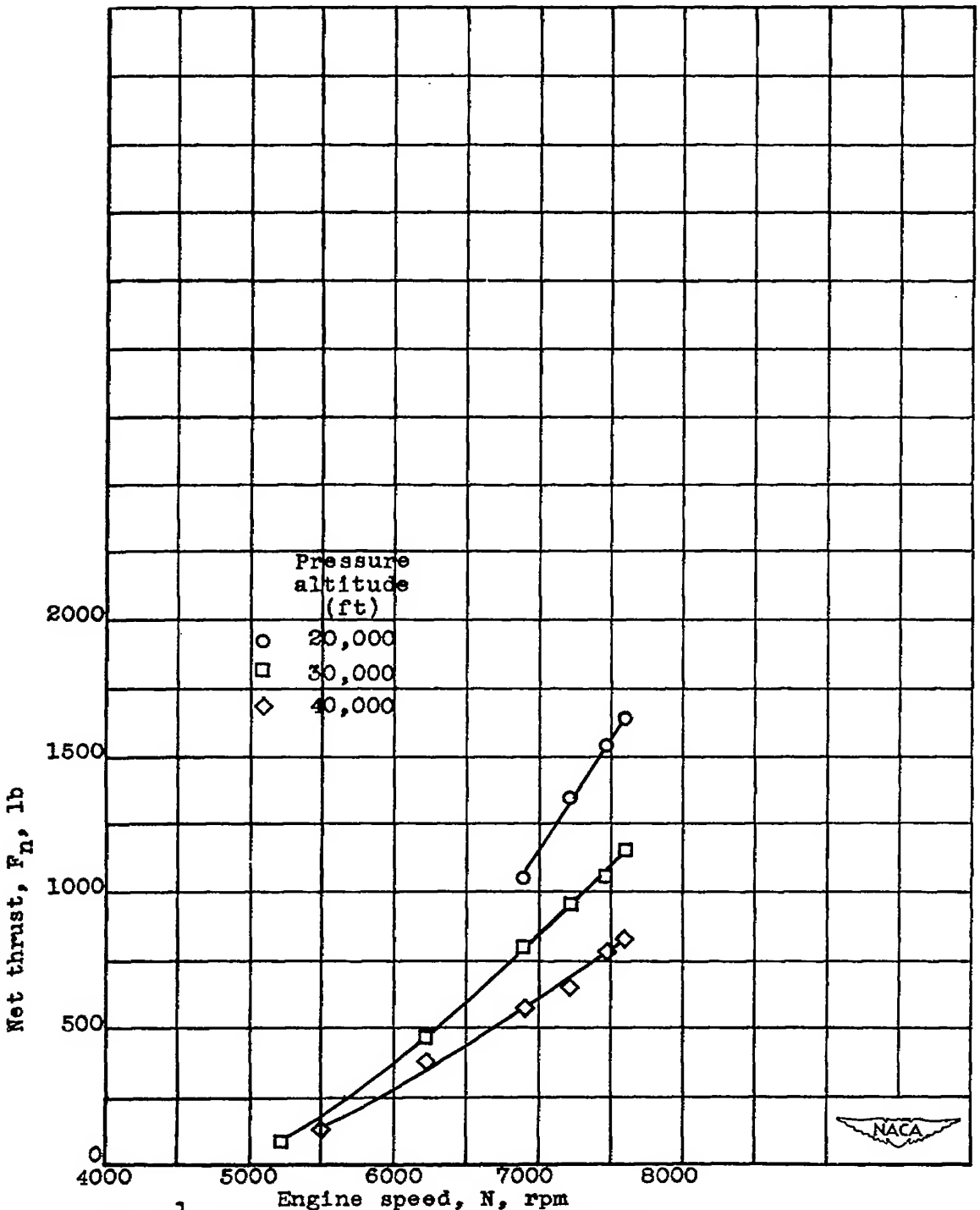

(b) $19\frac{1}{2}$-inch-diameter tail-pipe nozzle.

Figure 7.- Concluded.

553

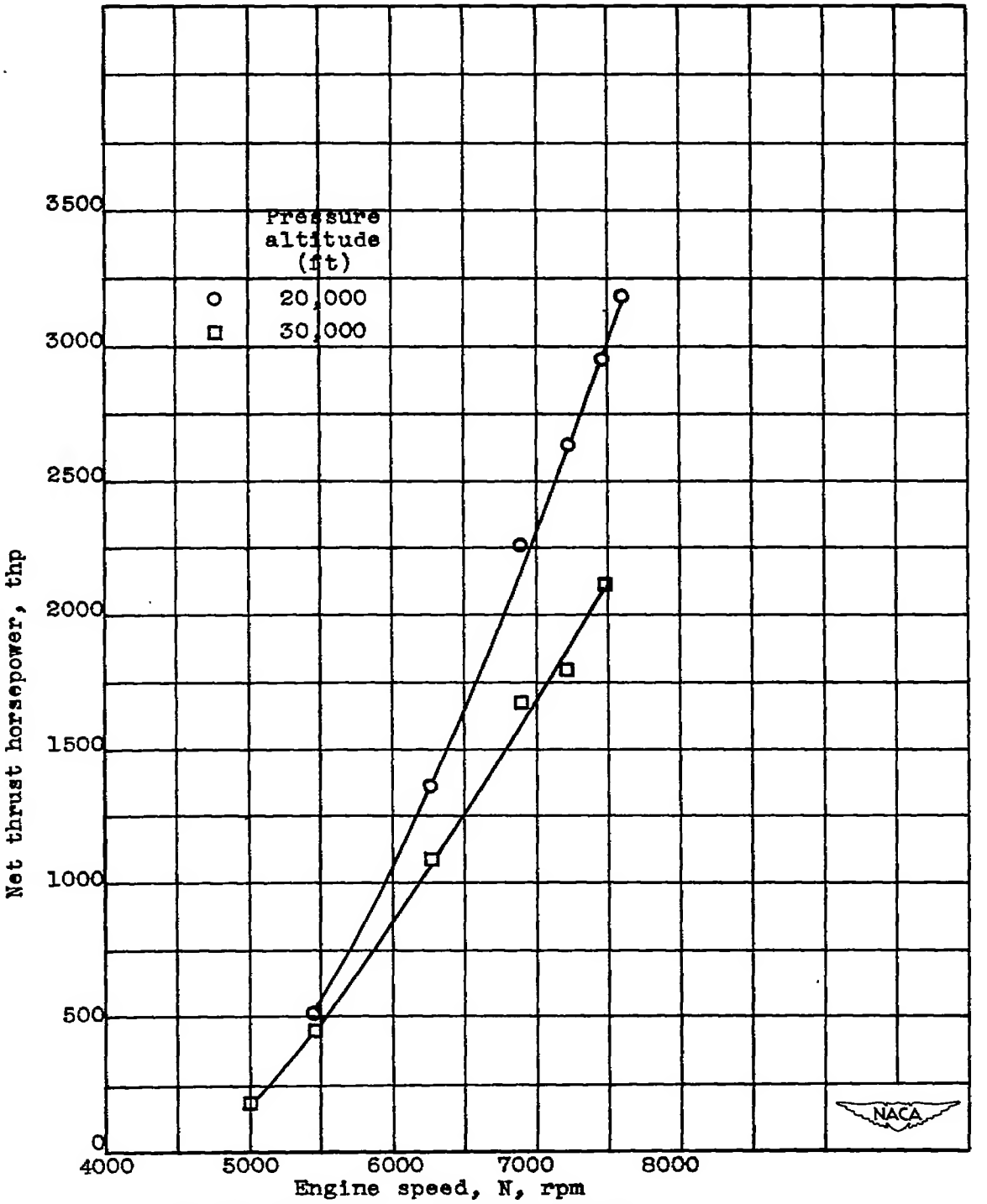

(a) 18-inch-diameter tail-pipe nozzle.

Figure 8.- Effect of engine speed and pressure altitude on net thrust horsepower at a ram pressure ratio of approximately 1.40 with high-flow compressor.

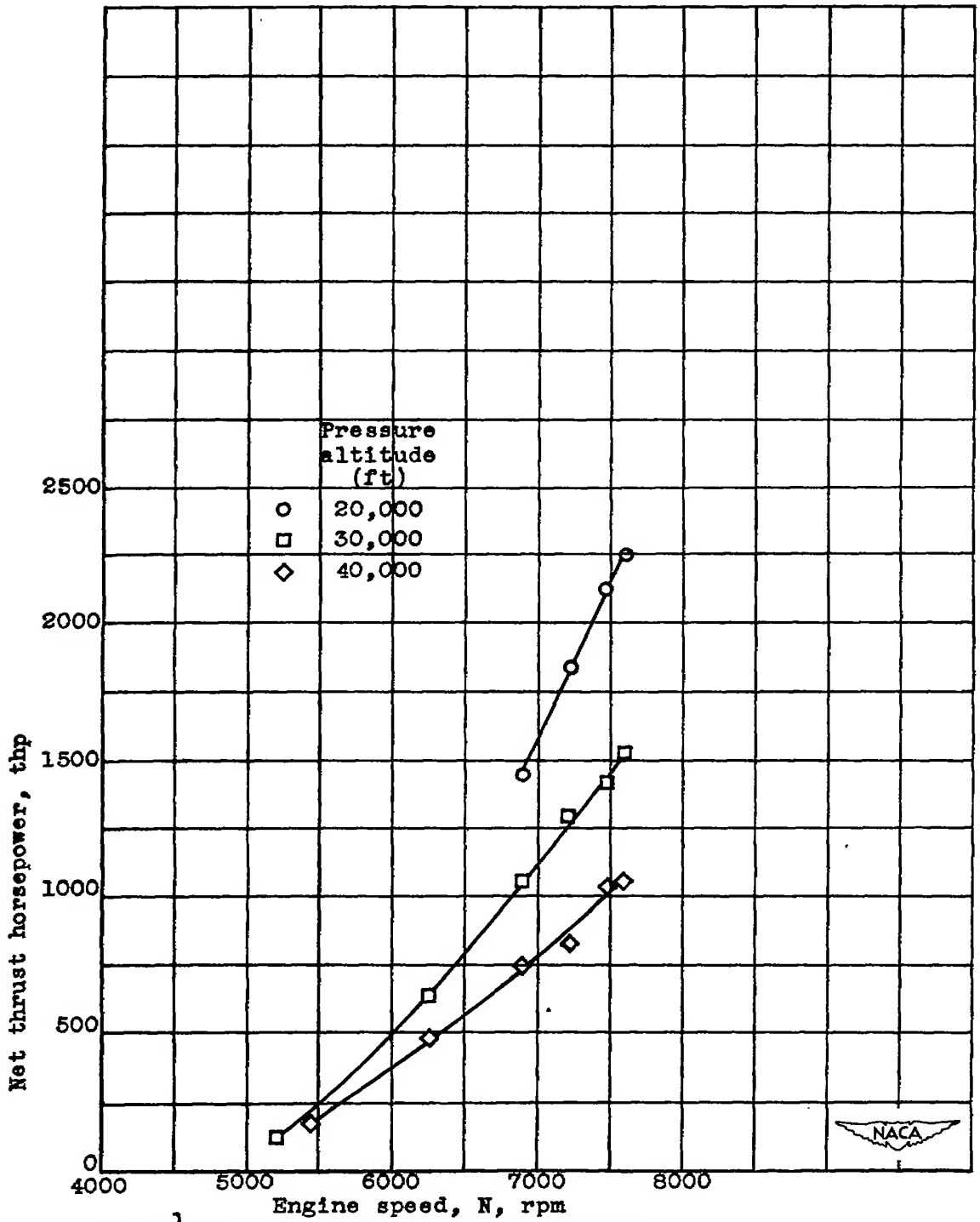

(b) $19\frac{1}{2}$-inch-diameter tail-pipe nozzle.

Figure 8.- Concluded.

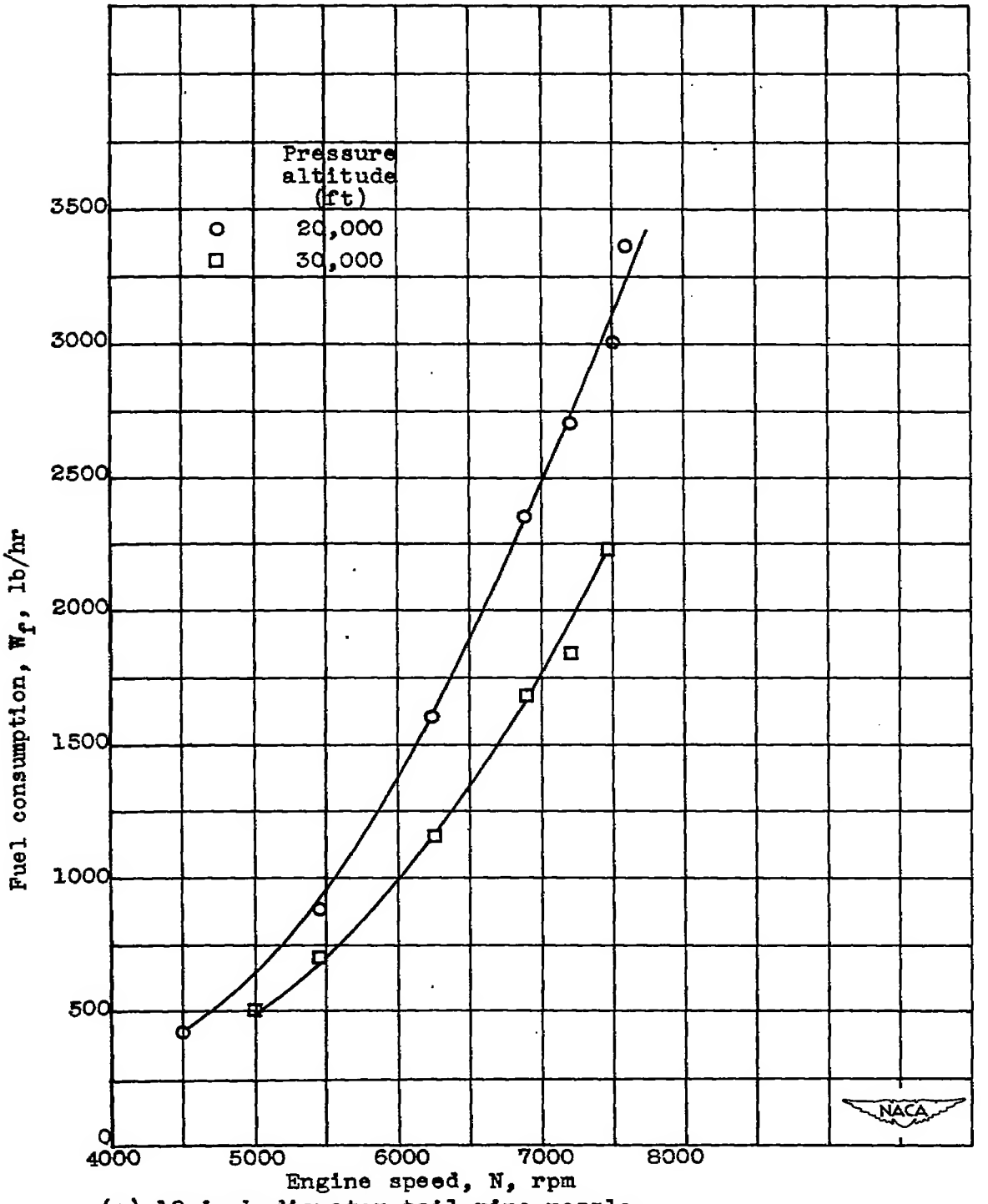

(a) 18-inch-diameter tail-pipe nozzle.

Figure 9.- Effect of engine speed and pressure altitude on fuel consumption at a ram pressure ratio of approximately 1.40 with high-flow compressor.

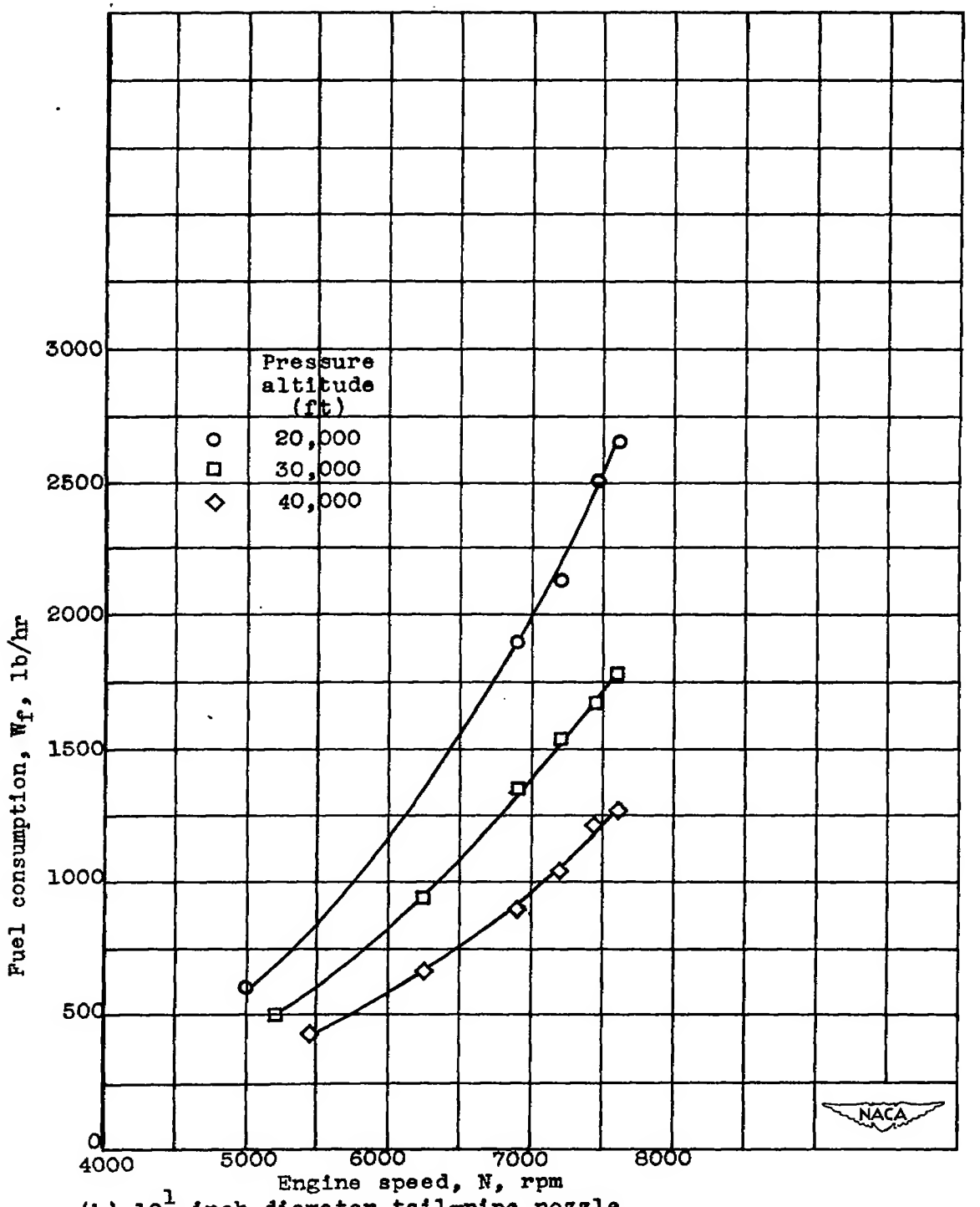

(b) 19½-inch-diameter tail-pipe nozzle.

Figure 9.- Concluded.

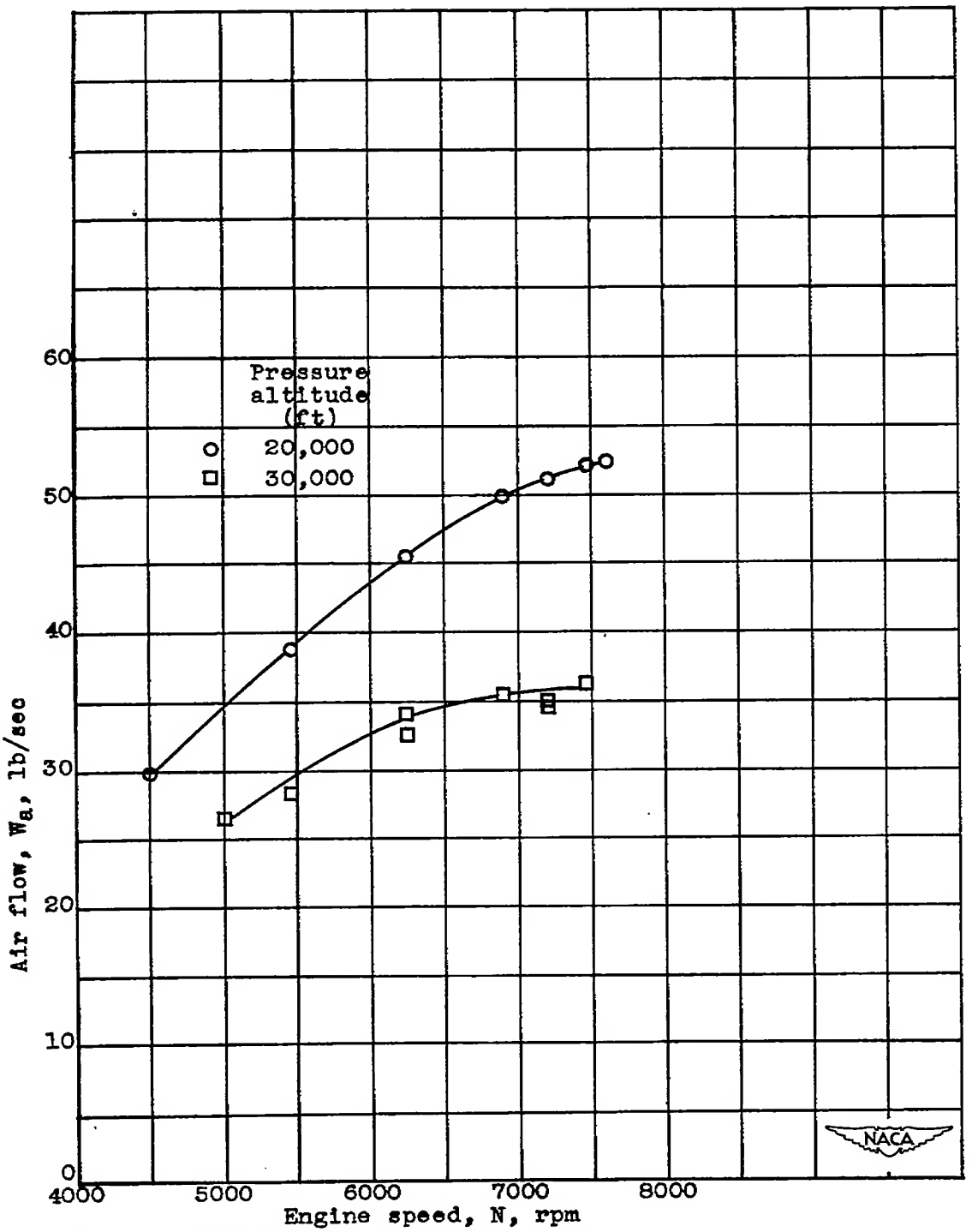

(a) 18-inch-diameter tail-pipe nozzle.

Figure 10.- Effect of engine speed and pressure altitude on air flow at a ram pressure ratio of approximately 1.40 with high-flow compressor.

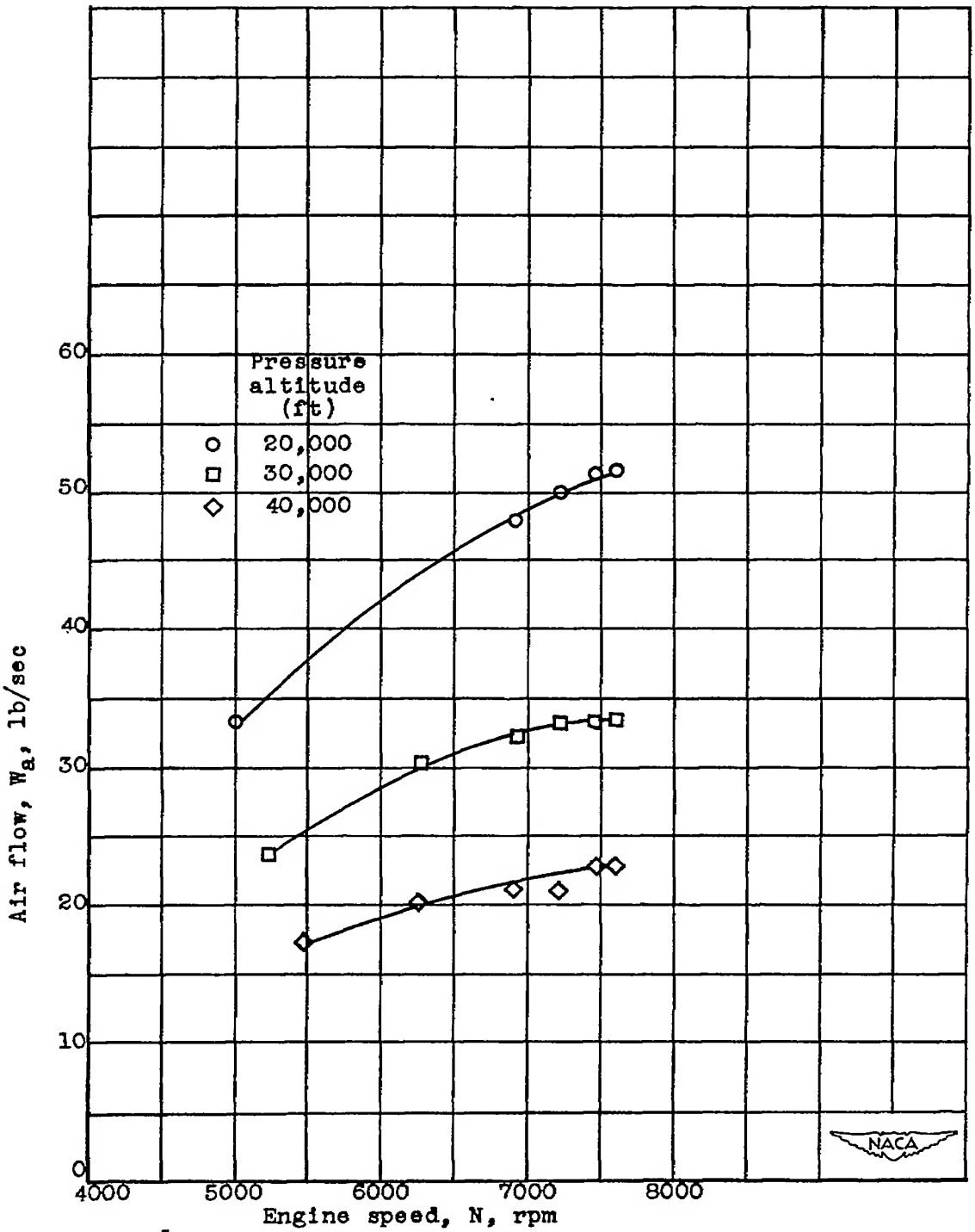

(b) $19\frac{1}{2}$-inch-diameter tail-pipe nozzle.

Figure 10.- Concluded.

553

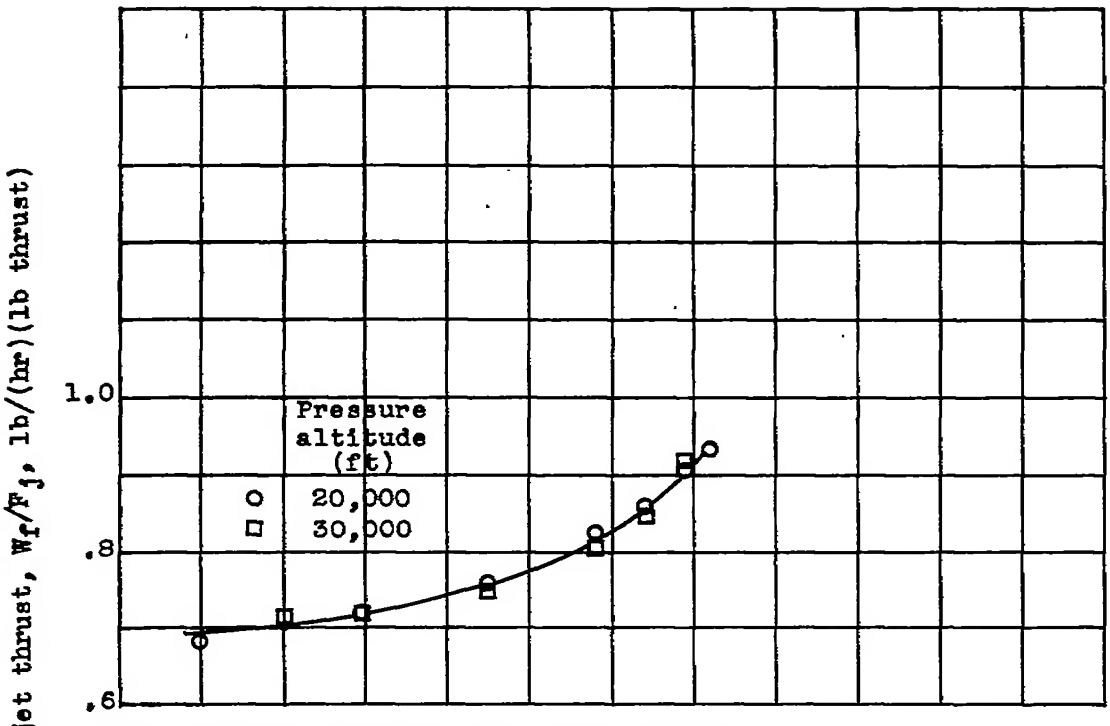

(a) 18-inch-diameter tail-pipe nozzle.

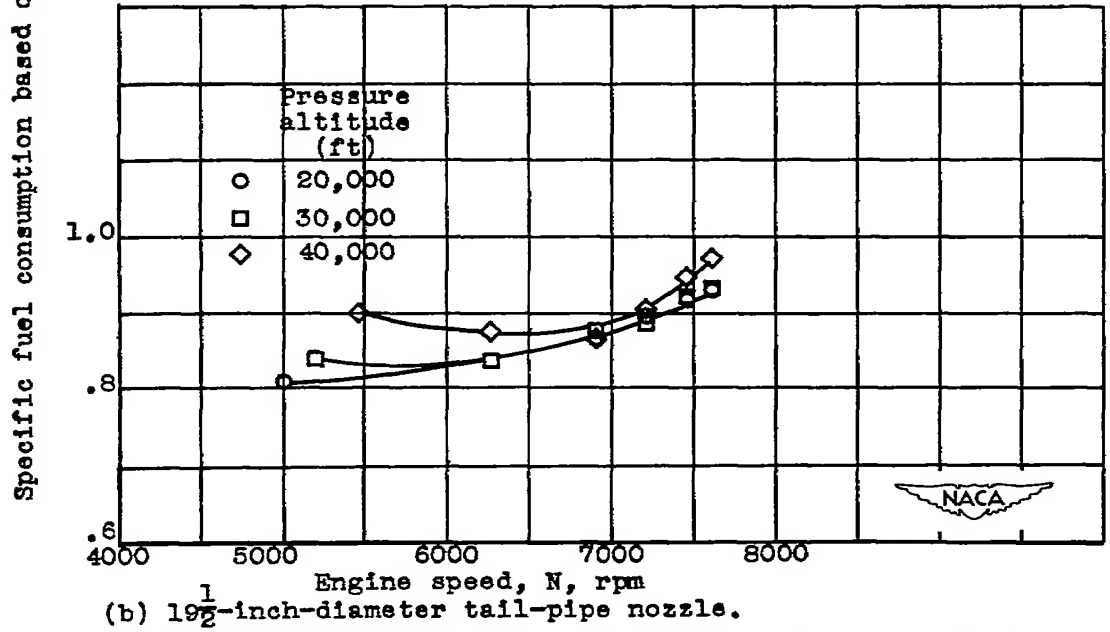

(b) $19\frac{1}{2}$-inch-diameter tail-pipe nozzle.

Figure 11.- Variation of specific fuel consumption based on jet thrust with engine speed and pressure altitude at a ram pressure ratio of approximately 1.40 with high-flow compressor.

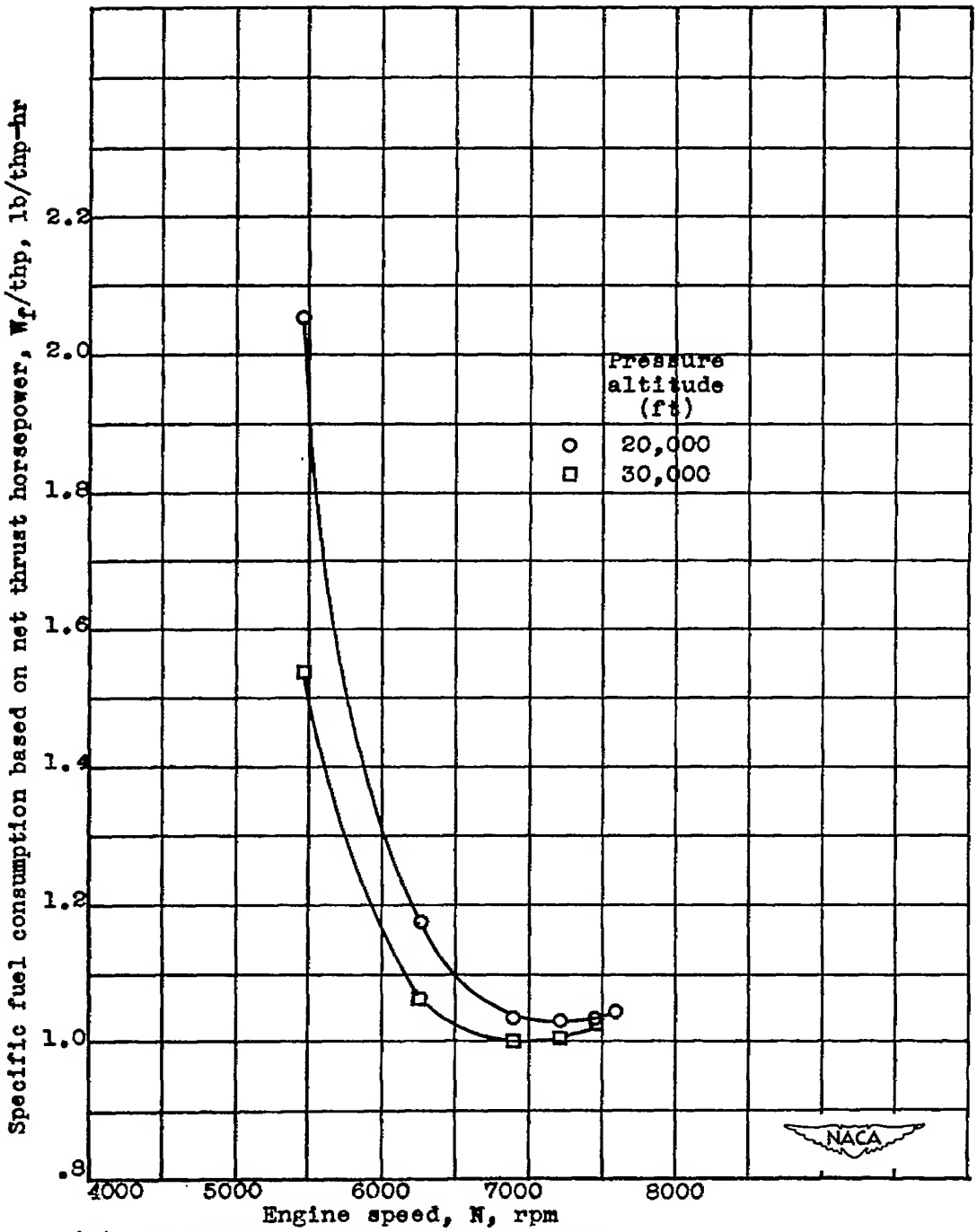

(a) 18-inch-diameter tail-pipe nozzle.

Figure 12.- Variation of specific fuel consumption based on net thrust horsepower with engine speed and pressure altitude at a ram pressure ratio of approximately 1.40 with high-flow compressor.

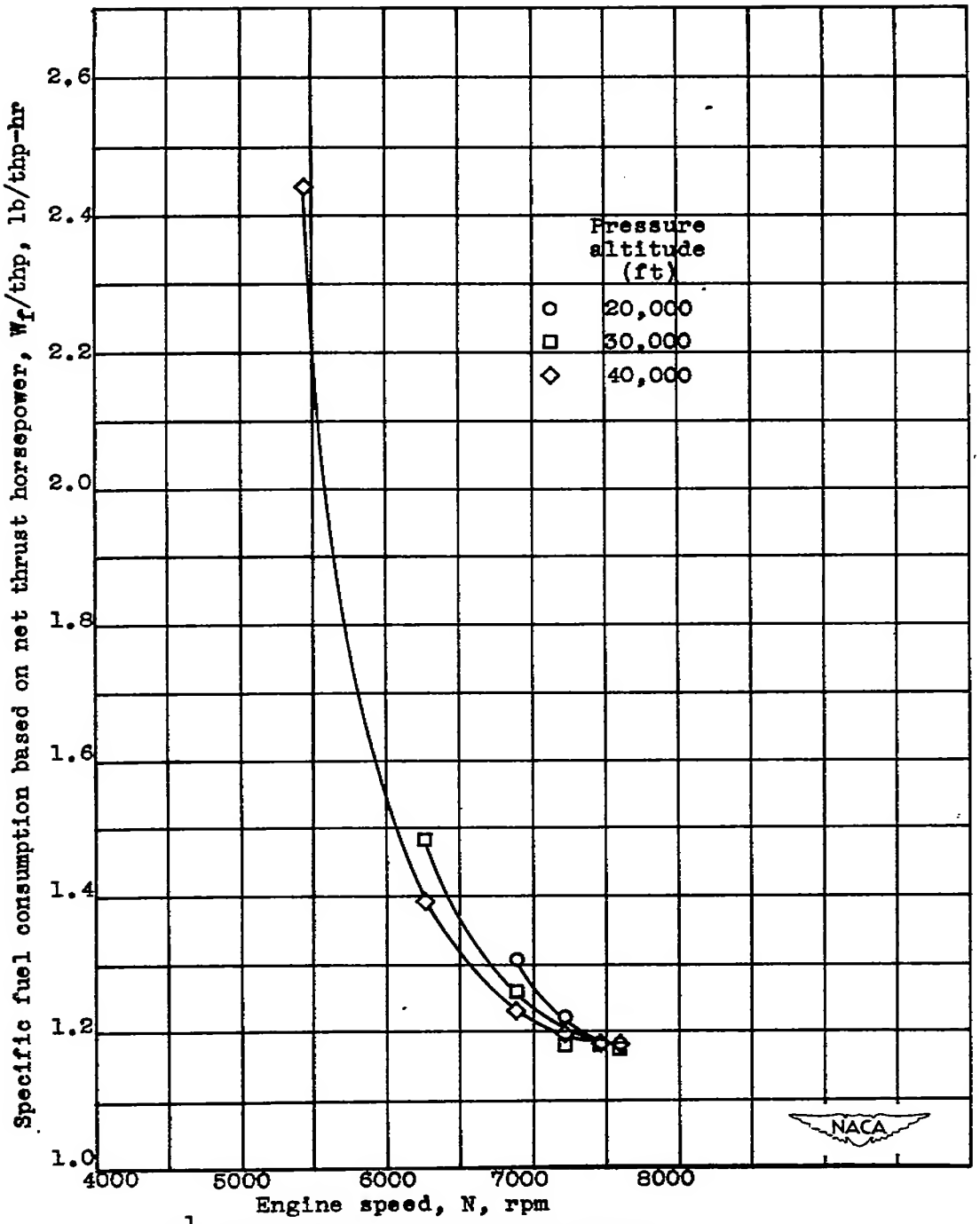

(b) $19\frac{1}{2}$-inch-diameter tail-pipe nozzle.

Figure 12.- Concluded.

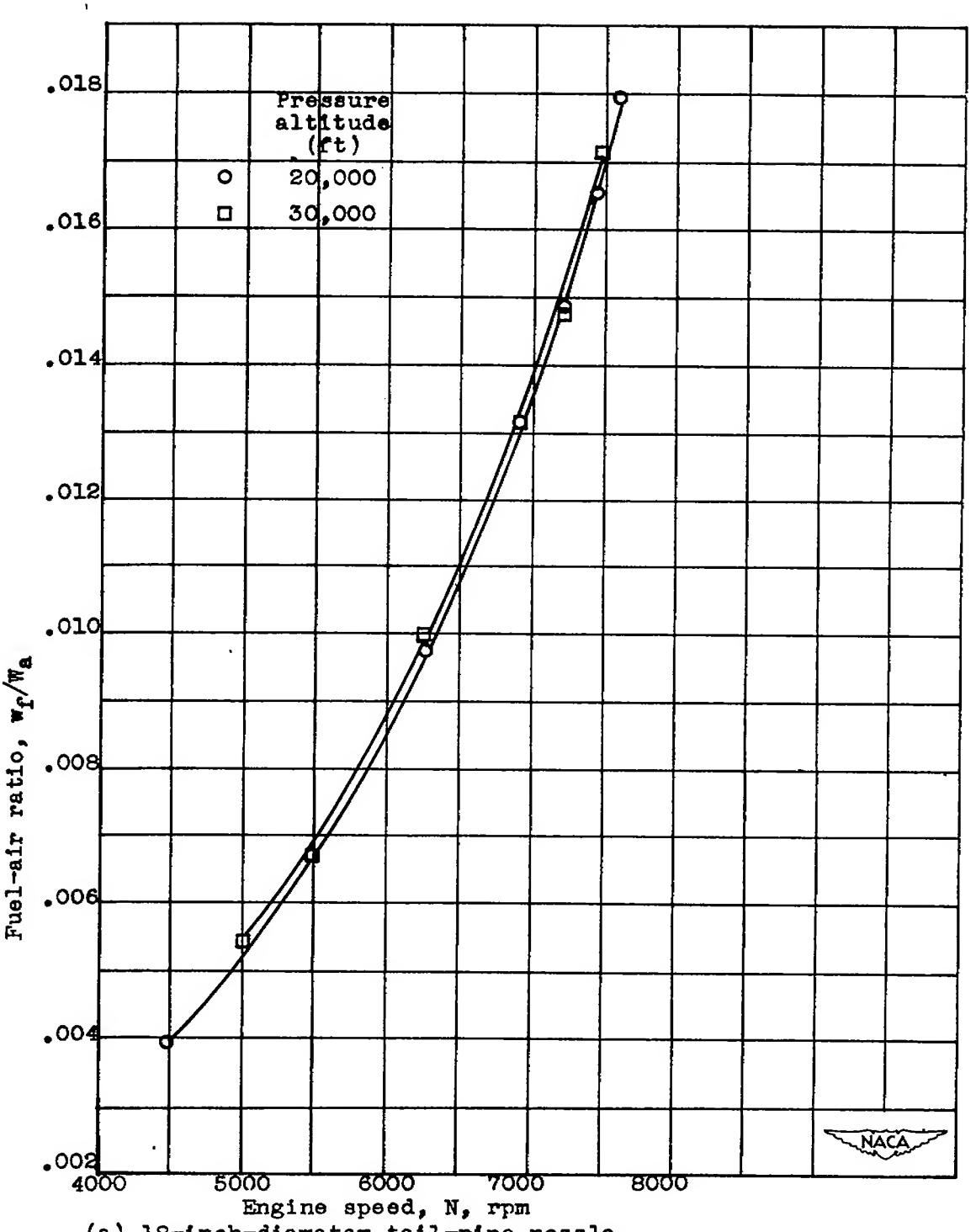

(a) 18-inch-diameter tail-pipe nozzle.

Figure 13.- Effects of engine speed and pressure altitude on fuel-air ratio at a ram pressure ratio of approximately 1.40 with high-flow compressor.

553

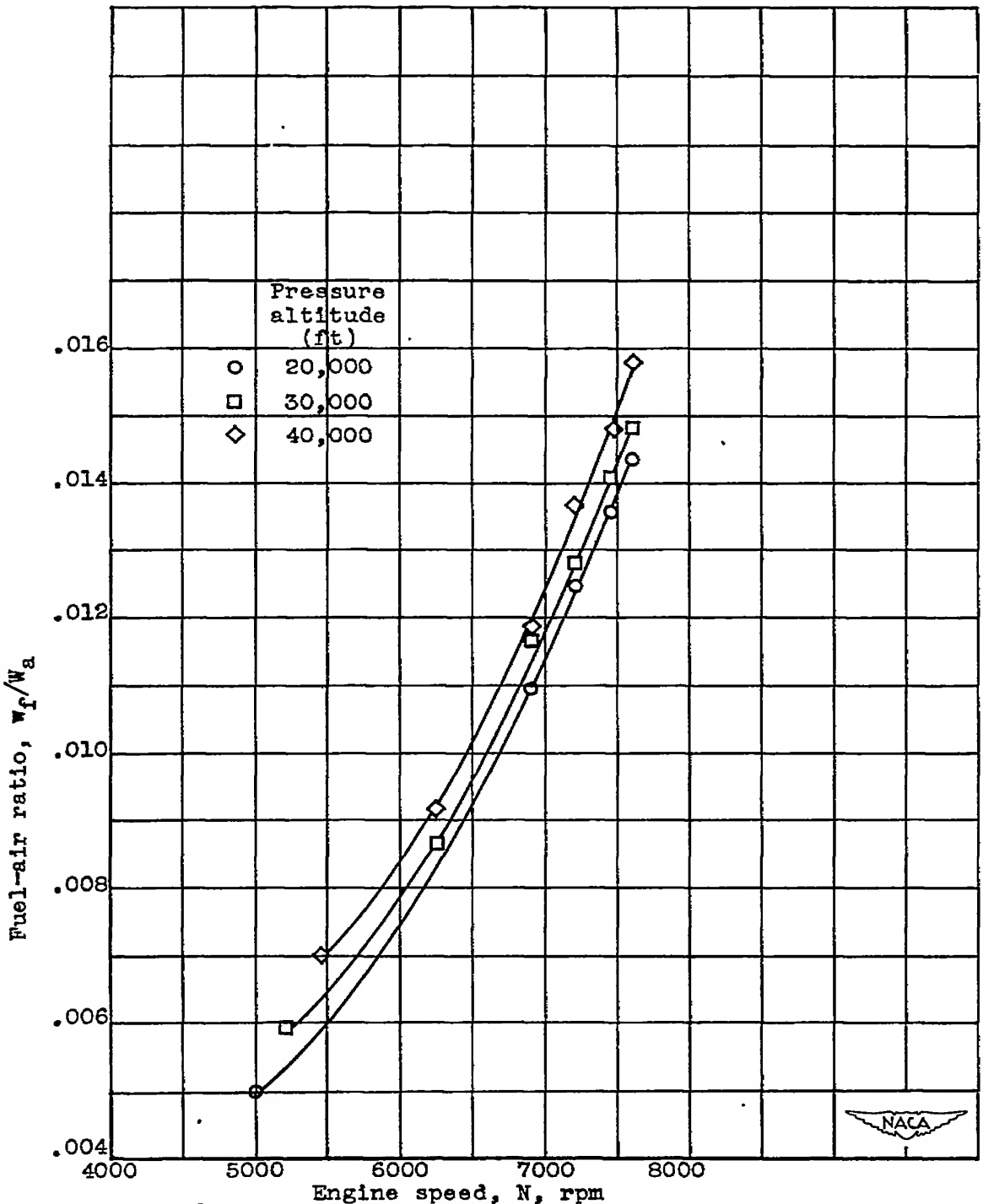

(b) $19\frac{1}{2}$-inch-diameter tail-pipe nozzle.

Figure 13.- Concluded.

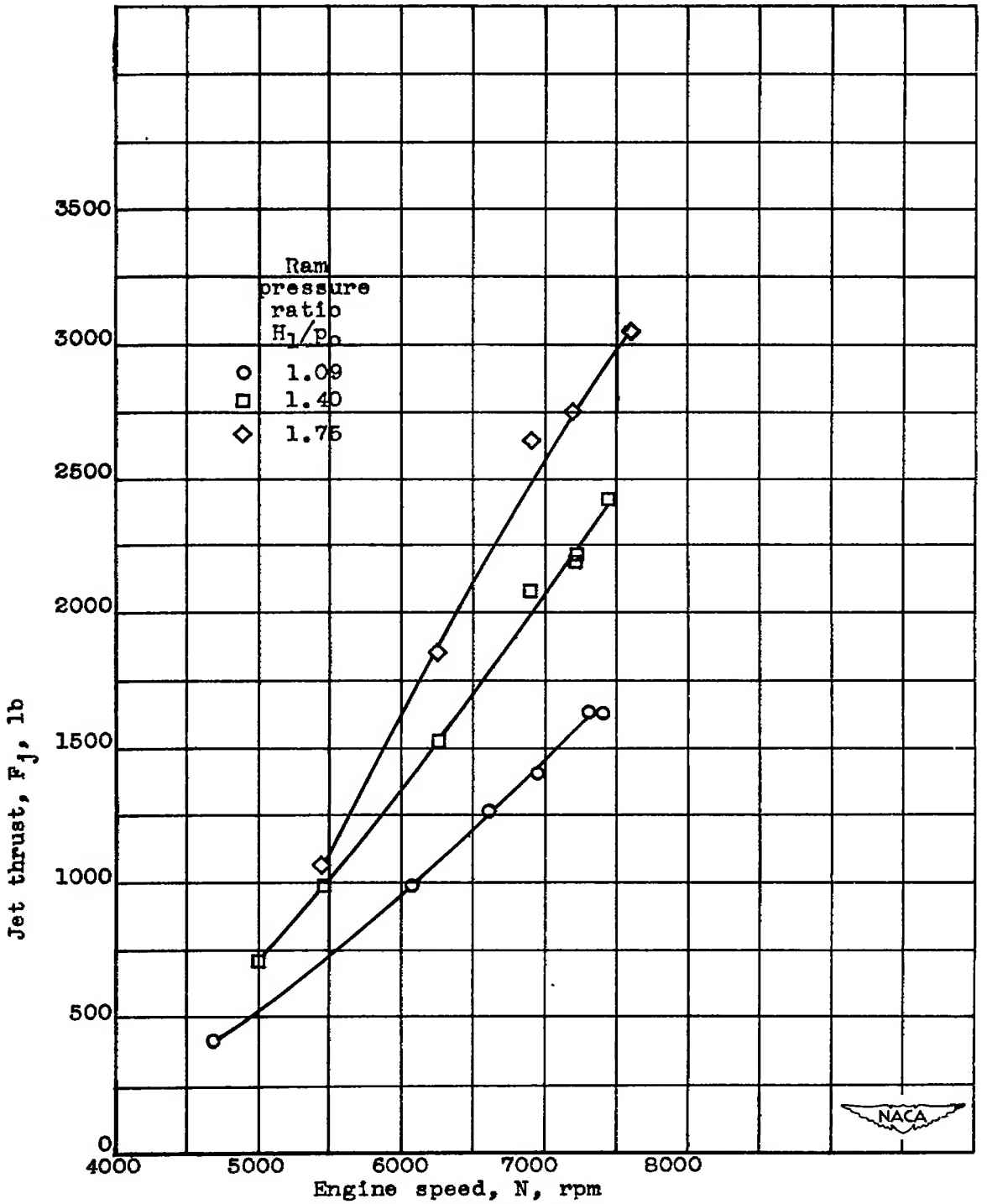

Figure 14.- Effect of engine speed and ram pressure ratio on jet thrust at a pressure altitude of 30,000 feet with high-flow compressor and 18-inch-diameter tail-pipe nozzle.

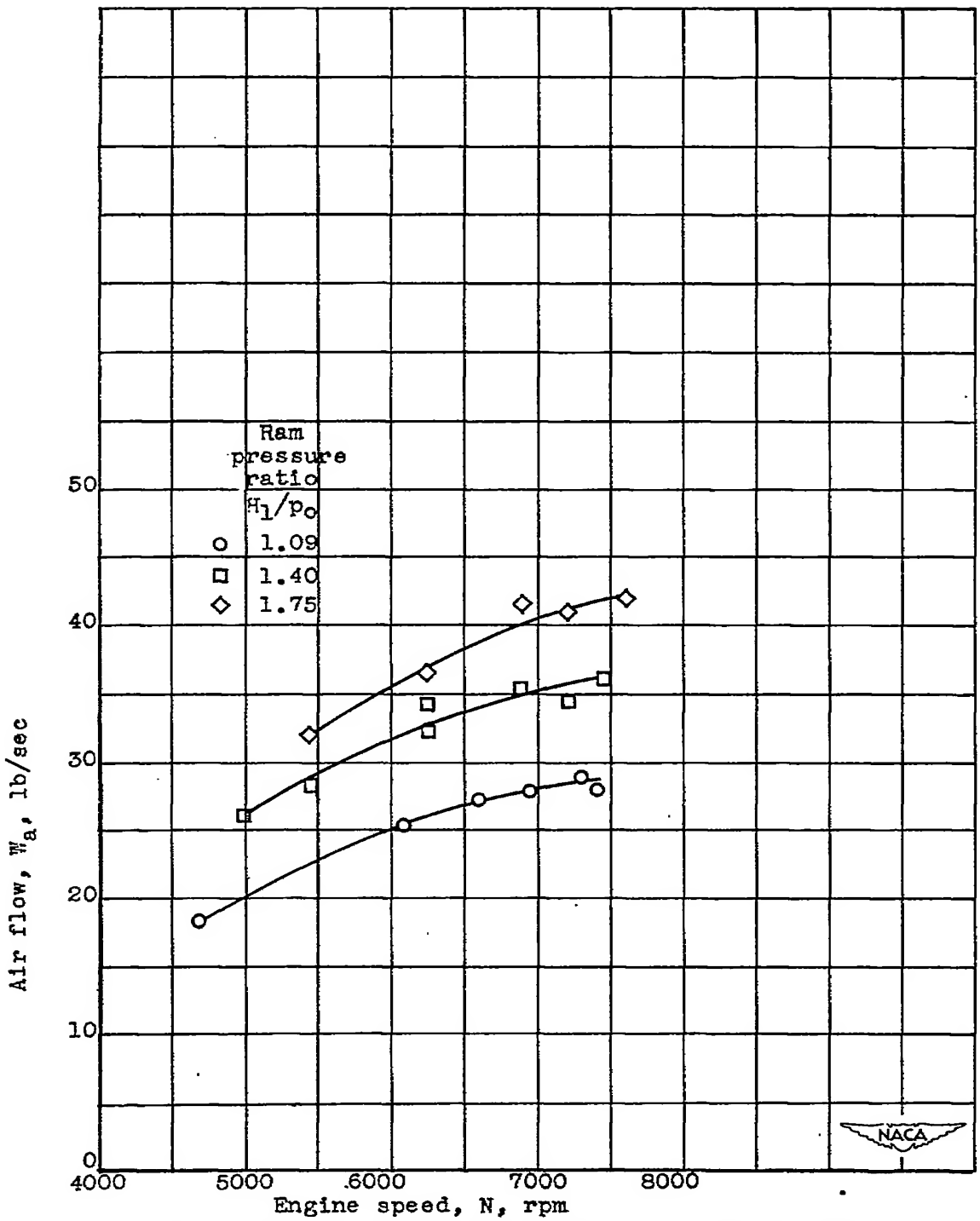

Figure 15.- Effect of engine speed and ram pressure ratio on air flow at a pressure altitude of 30,000 feet with high-flow compressor and 18-inch-diameter tail-pipe nozzle.

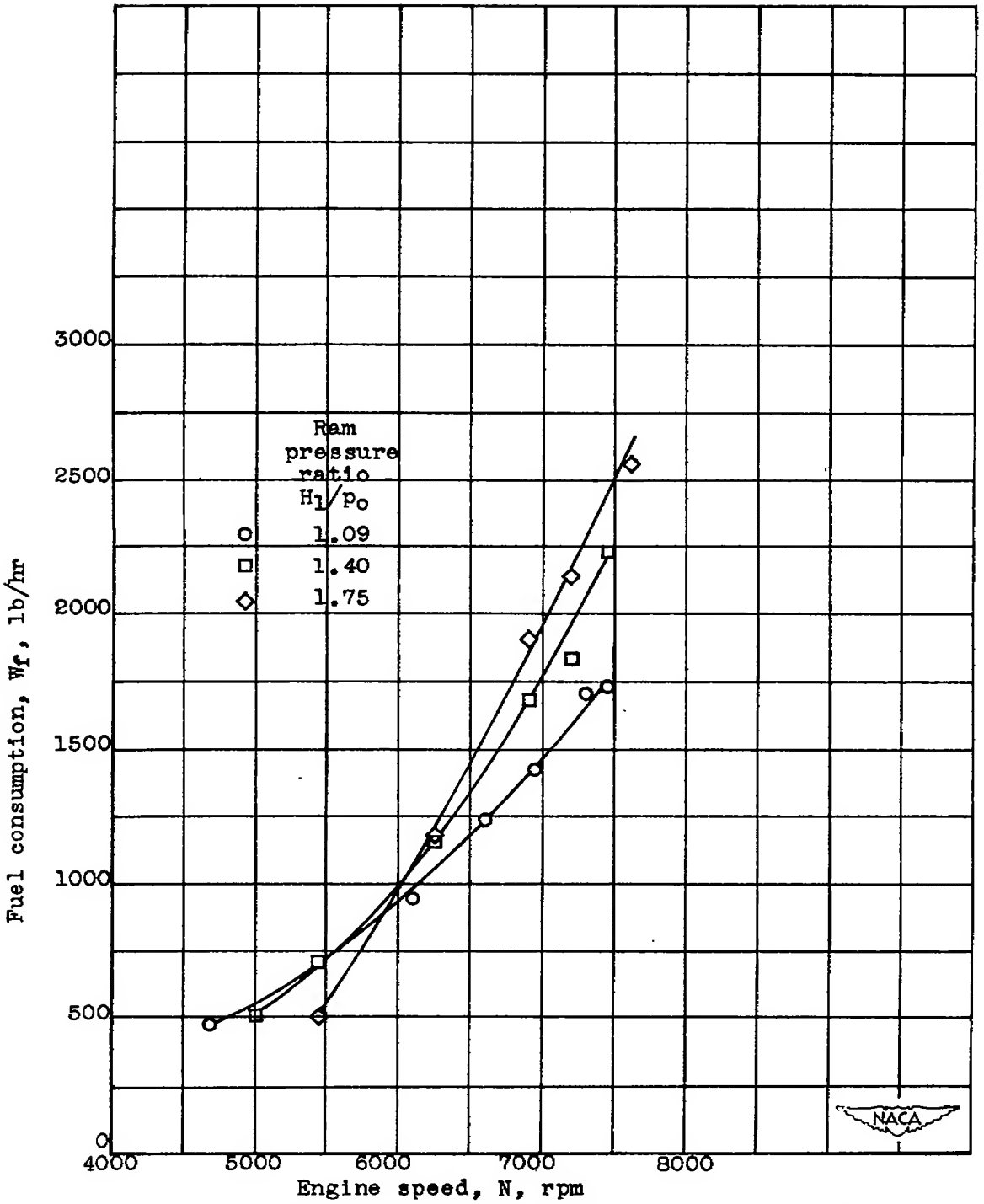

Figure 16.- Effect of engine speed and ram pressure ratio on fuel consumption at a pressure altitude of 30,000 feet with high-flow compressor and 18-inch-diameter tail-pipe nozzle.

553

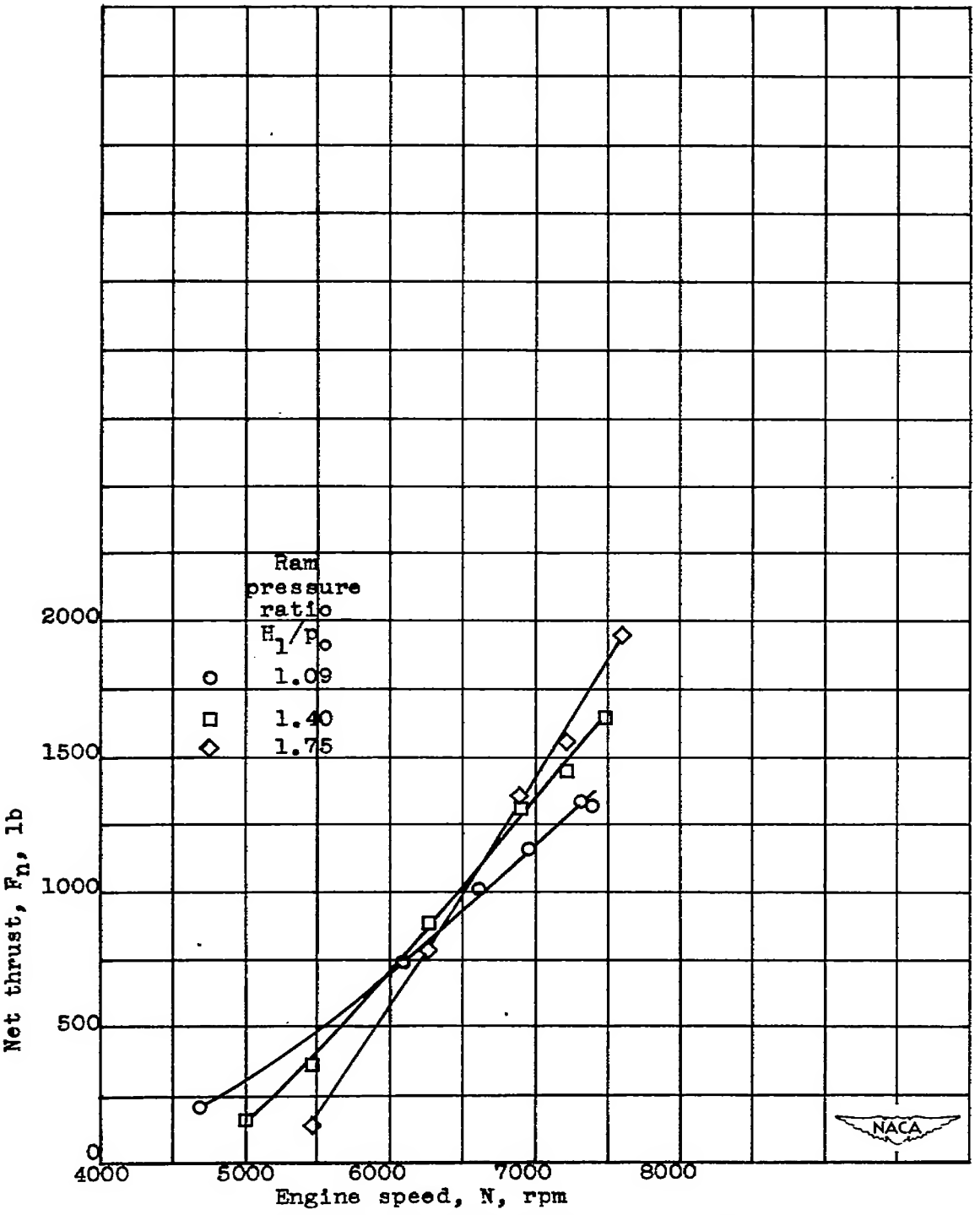

Figure 17.- Effect of engine speed and ram pressure ratio on net thrust at a pressure altitude of 30,000 feet with high-flow compressor and 18-inch-diameter tail-pipe nozzle.

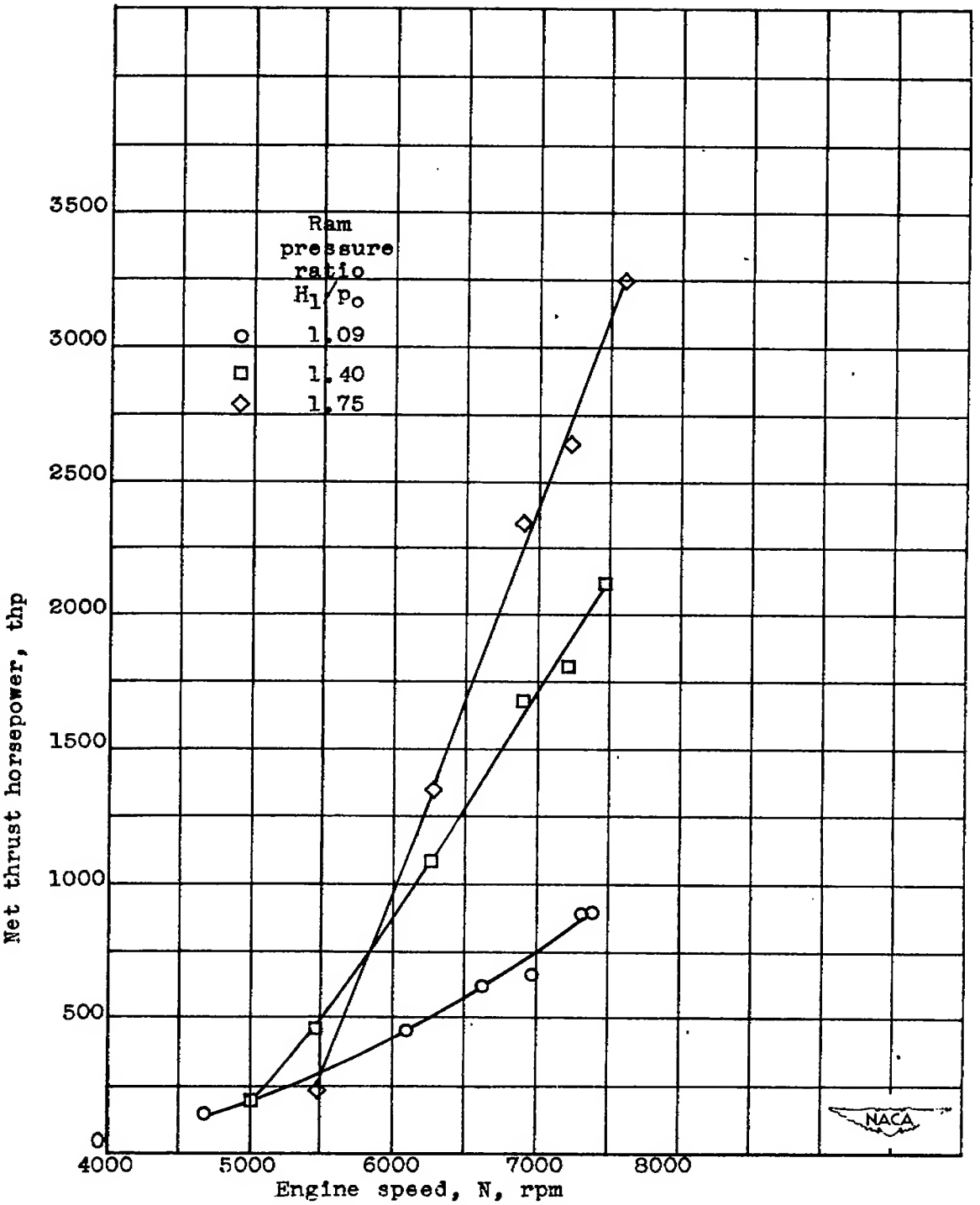

Figure 18.- Effect of engine speed and ram pressure ratio on net thrust horsepower at a pressure altitude of 30,000 feet with high-flow compressor and 18-inch-diameter tail-pipe nozzle.

553

553

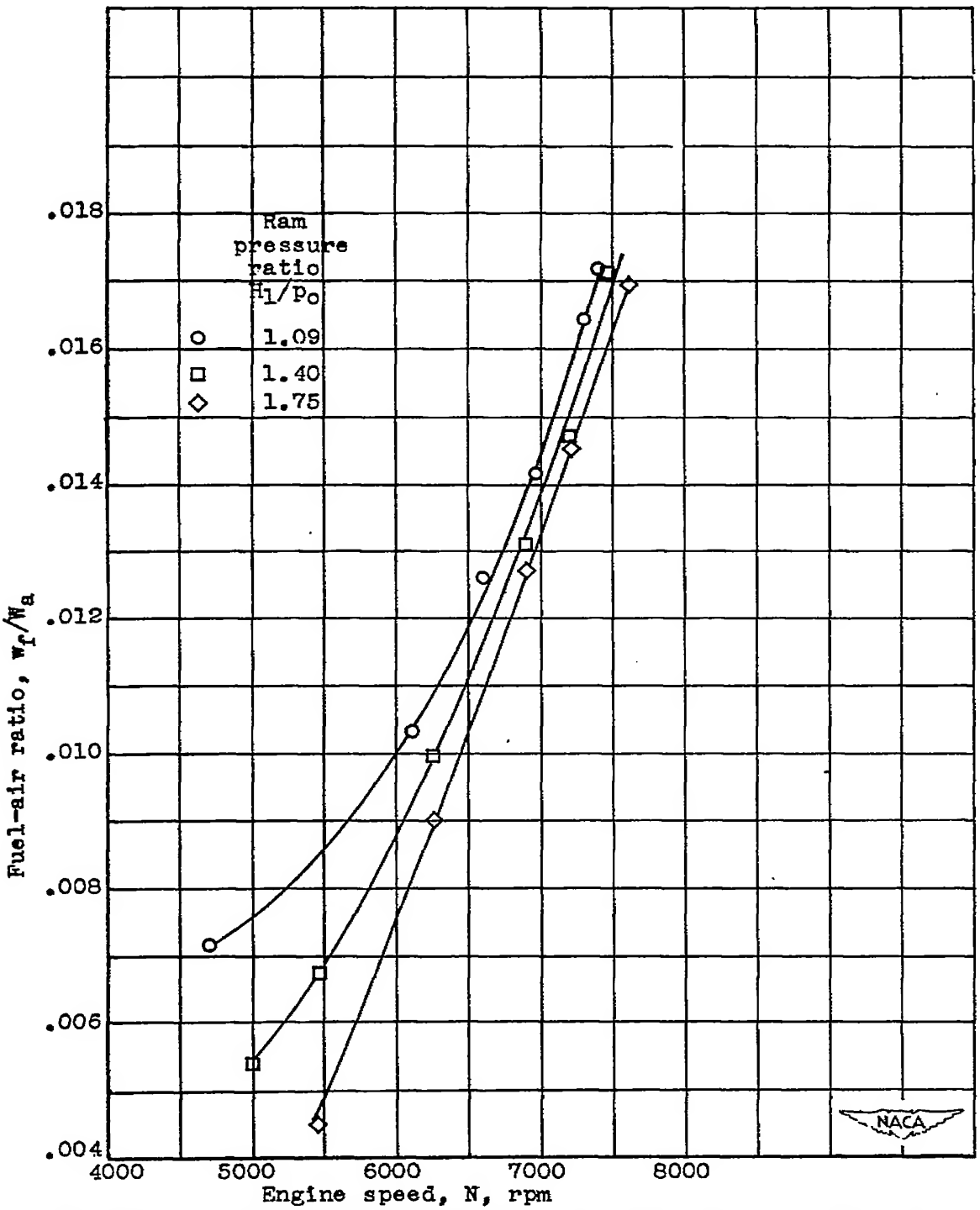

Figure 19.- Effect of engine speed and ram pressure ratio on fuel-air ratio at a pressure altitude of 30,000 feet with high-flow compressor and 18-inch-diameter tail-pipe nozzle.

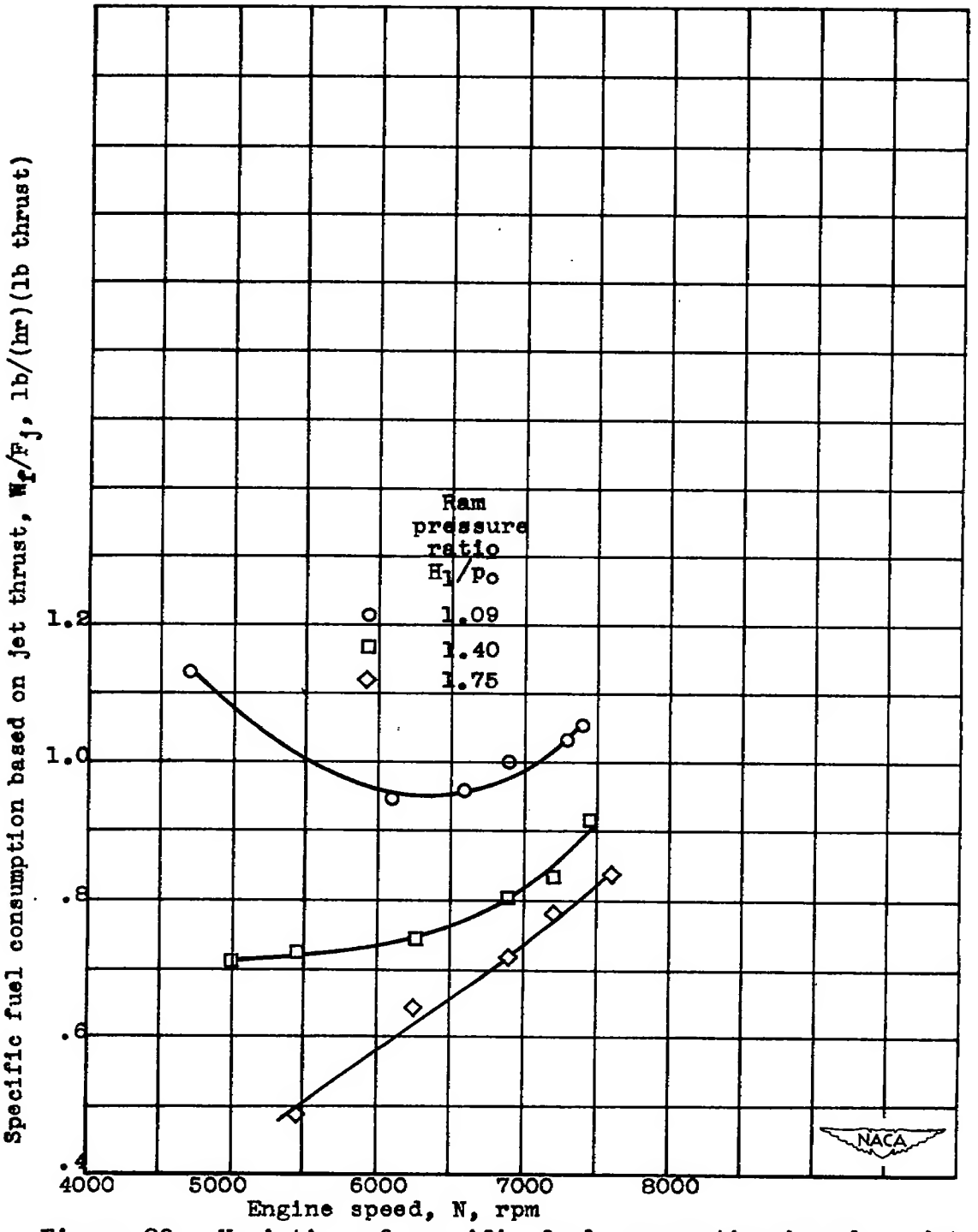

Figure 20.- Variation of specific fuel consumption based on jet thrust with engine speed and ram pressure ratio at a pressure altitude of 30,000 feet with high-flow compressor and 18-inch-diameter tail-pipe nozzle.

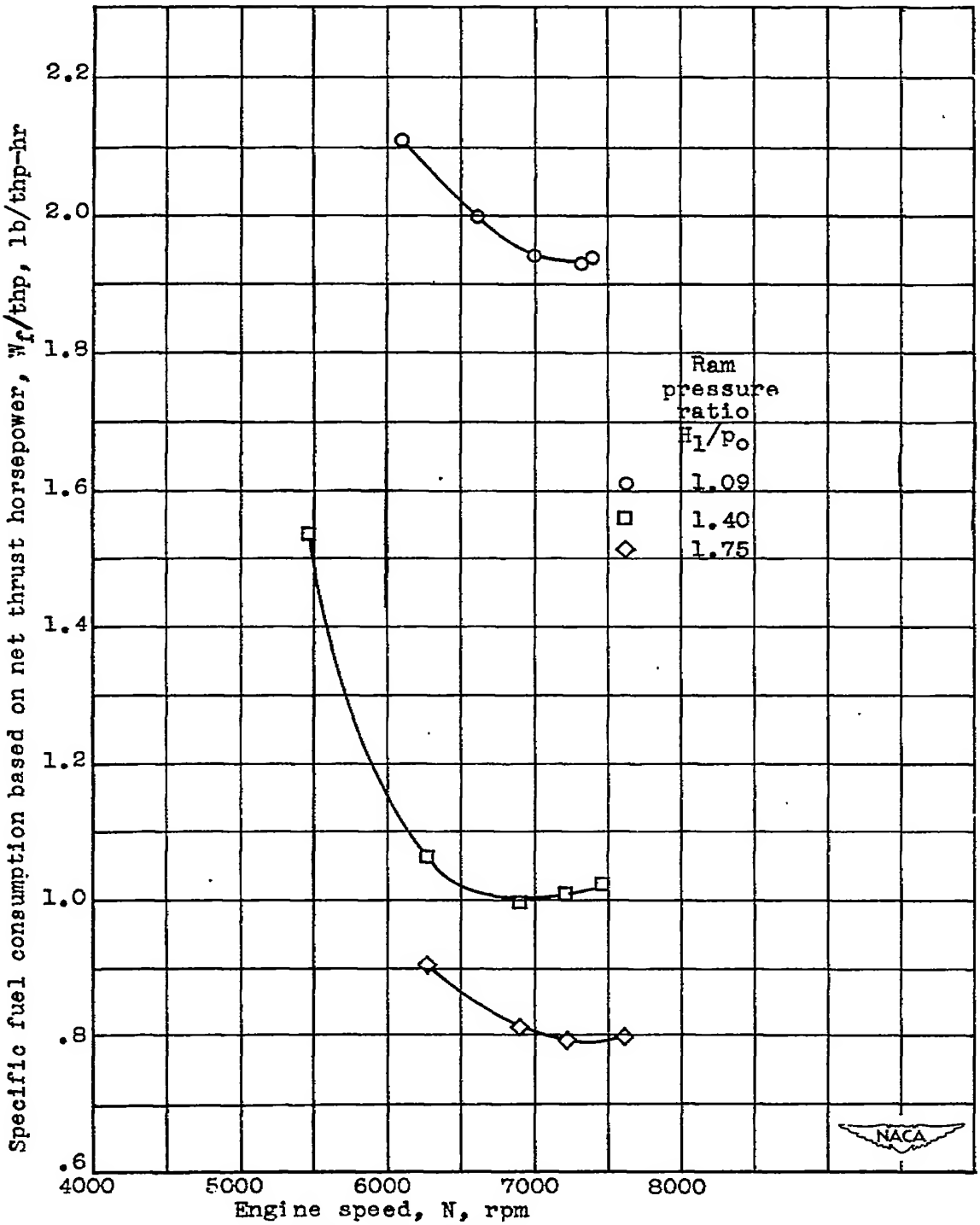

Figure 21.- Variation of specific fuel consumption based on net thrust horsepower with engine speed and ram pressure ratio at a pressure altitude of 30,000 feet with high-flow compressor and 18-inch-diameter tail-pipe nozzle.

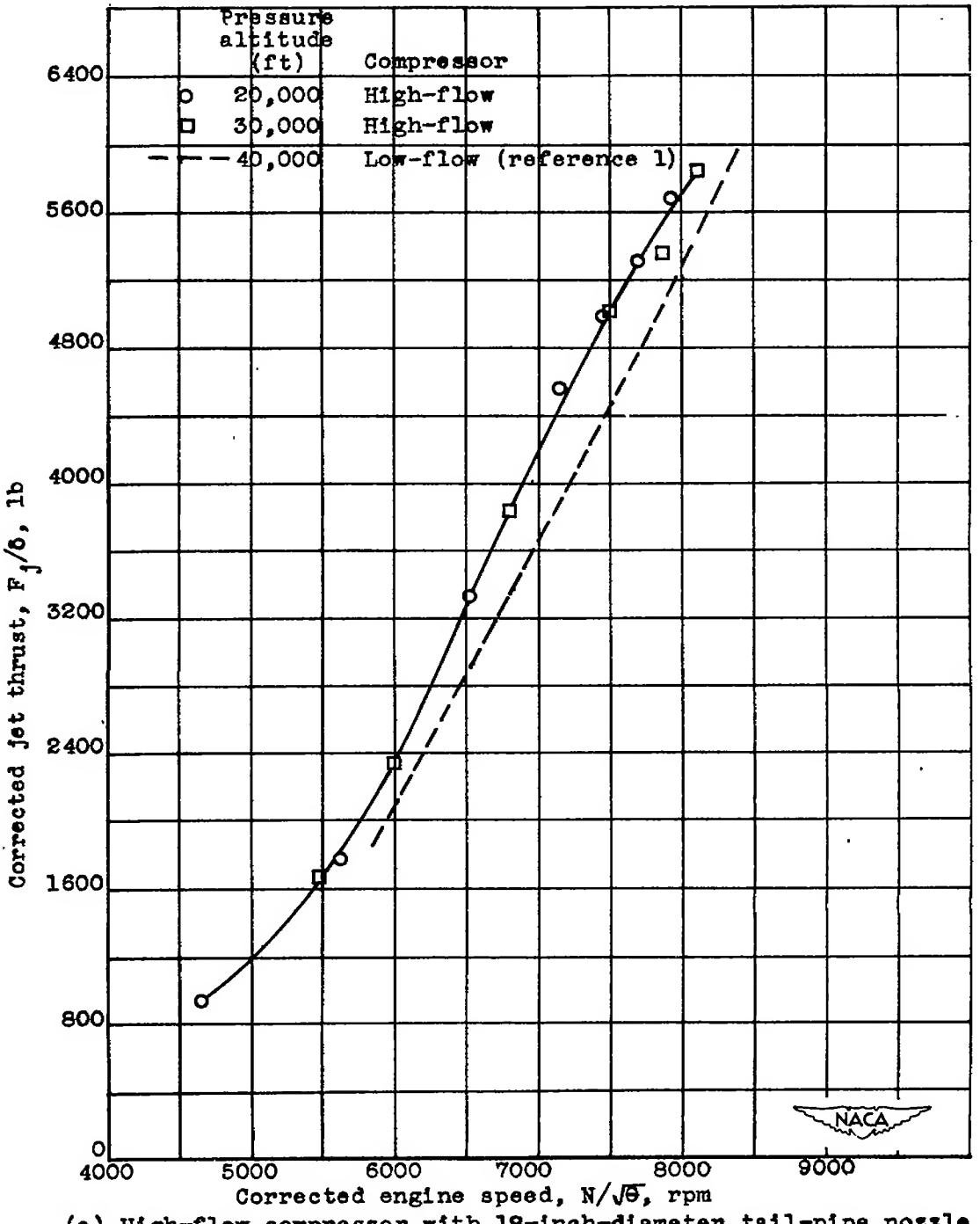

(a) High-flow compressor with 18-inch-diameter tail-pipe nozzle and low-flow compressor with 16¼-inch-diameter tail-pipe nozzle.

Figure 22.- Effect of corrected engine speed and pressure altitude on corrected jet thrust at a ram pressure ratio of approximately 1.40. Engine speed and jet thrust corrected to NACA standard atmospheric conditions at sea level.

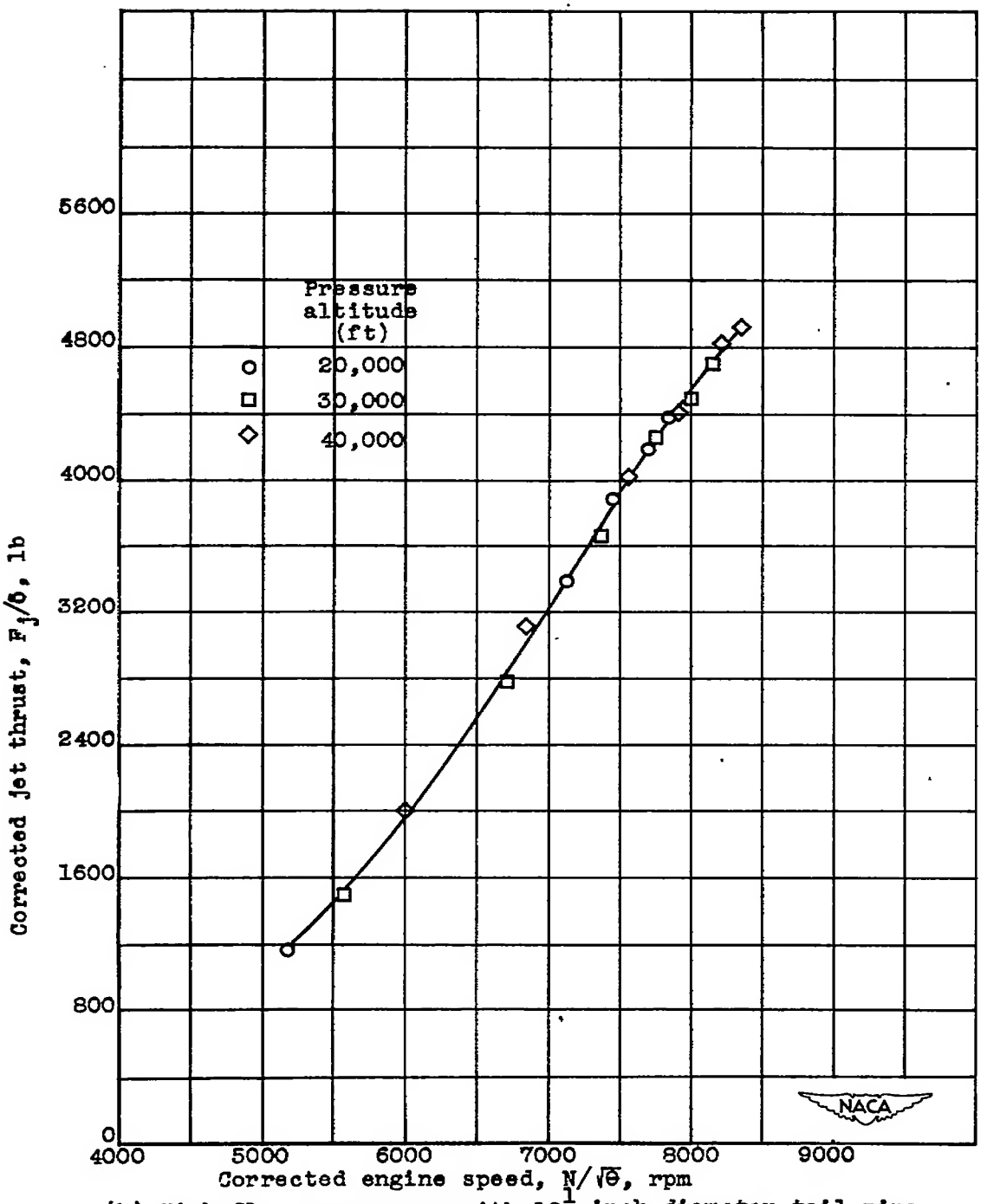

(b) High-flow compressor with 19$\frac{1}{2}$-inch-diameter tail-pipe nozzle.

Figure 22.- Concluded.

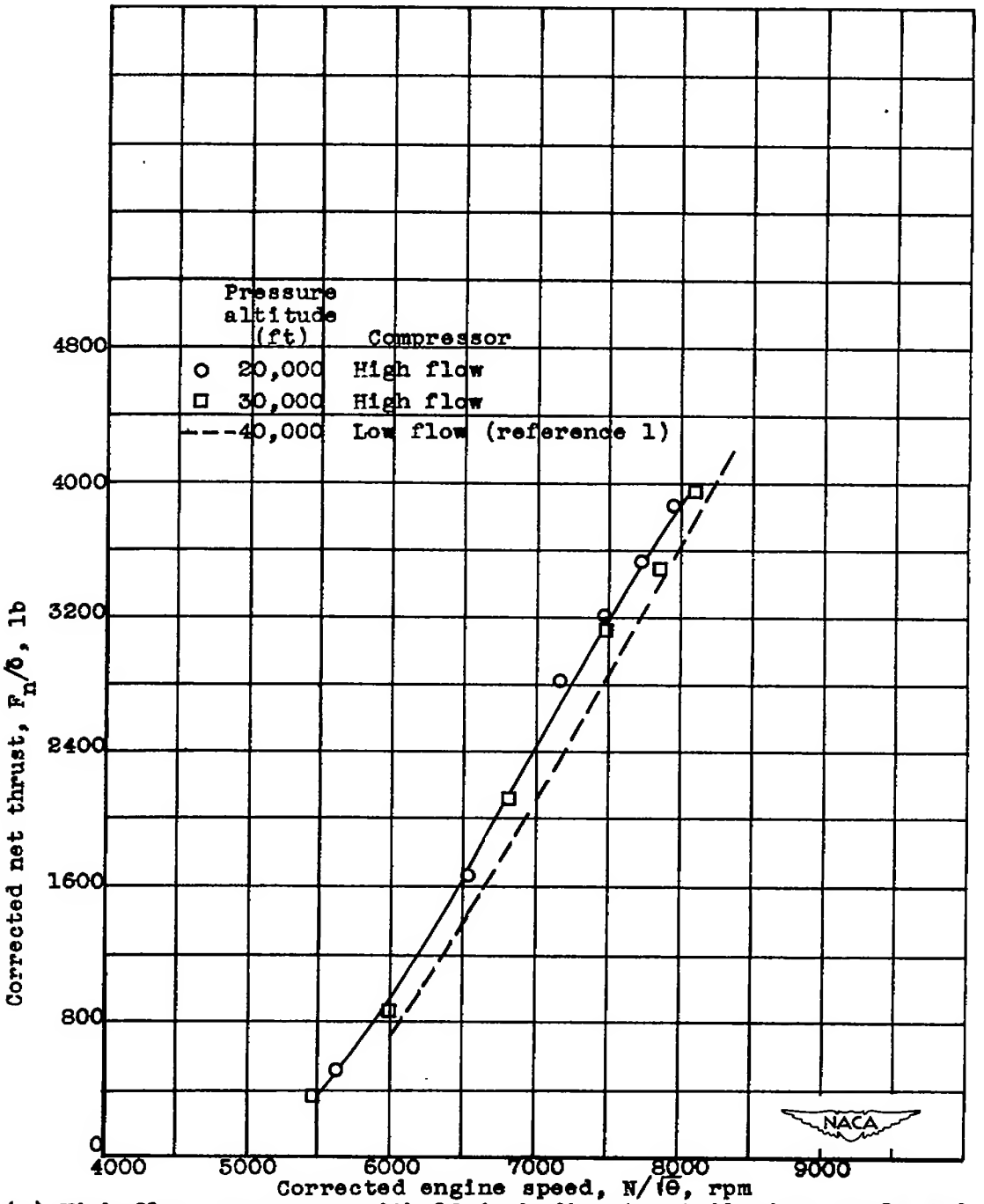

(a) High-flow compressor with 18-inch-diameter tail-pipe nozzle and low-flow compressor with $16\frac{3}{4}$-inch-diameter tail-pipe nozzle.

Figure 23.- Effect of corrected engine speed and pressure altitude on corrected net thrust at a ram pressure ratio of approximately 1.40. Engine speed and net thrust corrected to NACA standard atmospheric conditions at sea level.

553

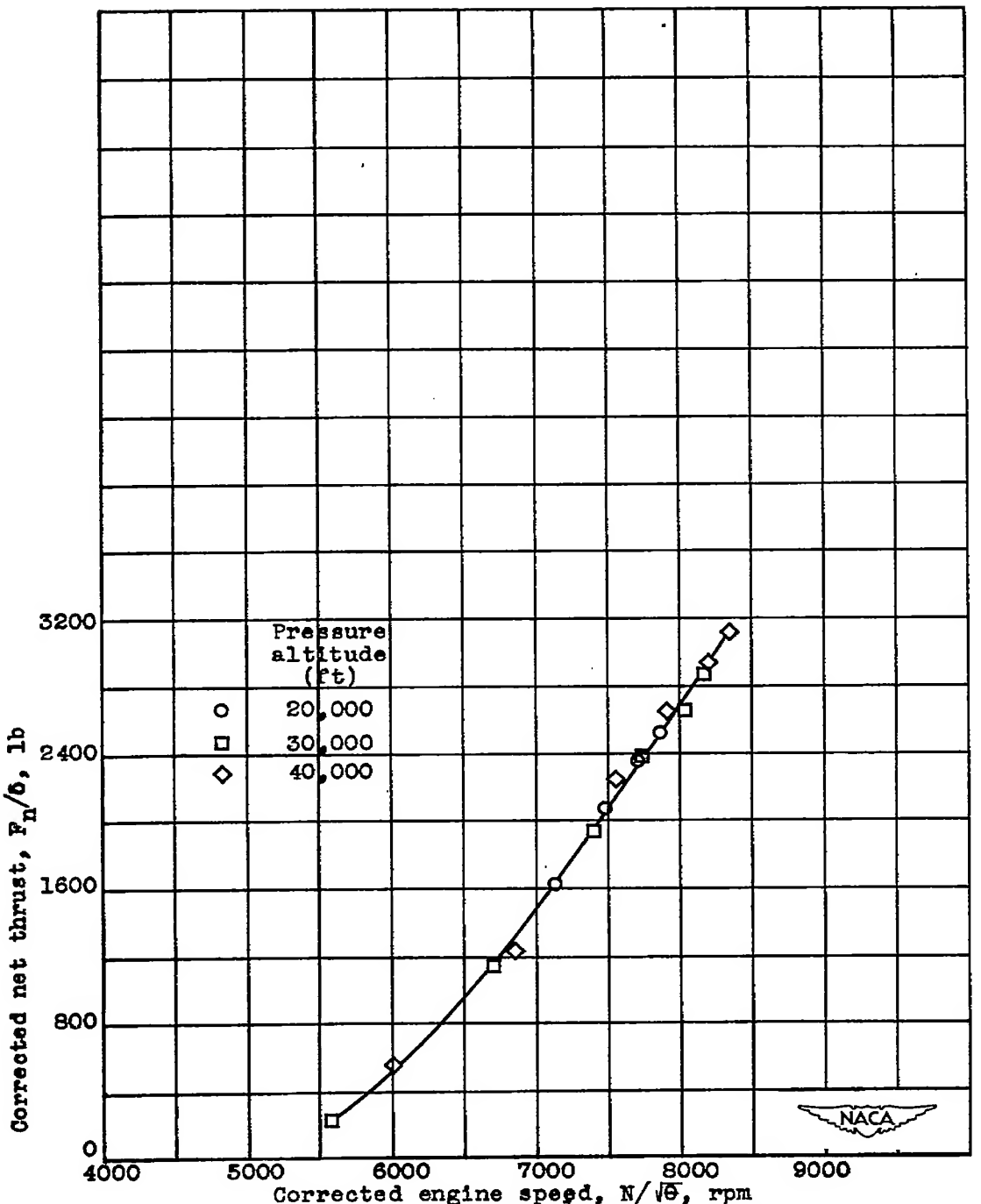

(b) High-flow compressor with $19\frac{1}{2}$-inch-diameter tail-pipe nozzle.

Figure 23.- Concluded.

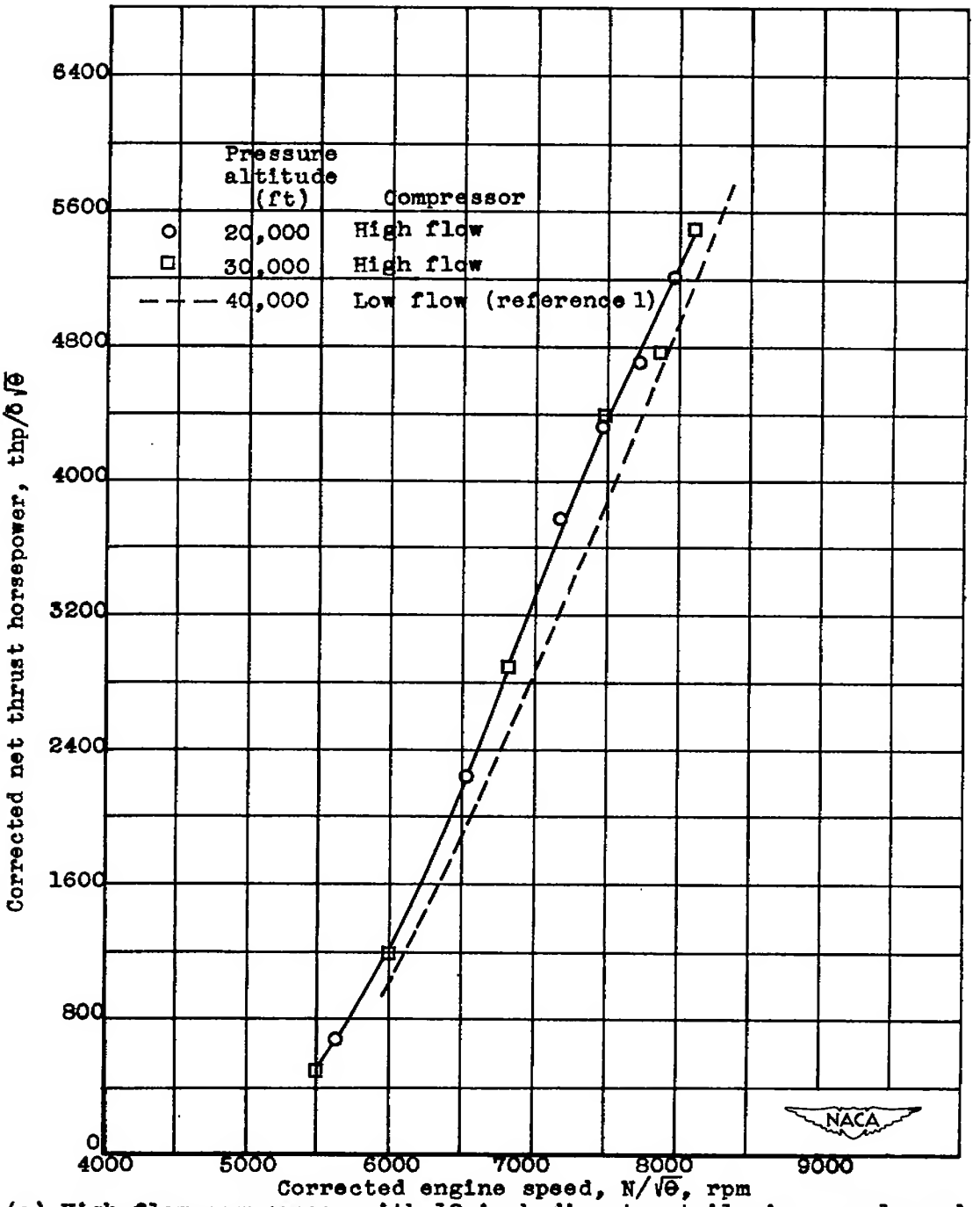

(a) High-flow compressor with 18-inch-diameter tail-pipe nozzle and low-flow compressor with $16\frac{3}{4}$-inch-diameter tail-pipe nozzle.

Figure 24.- Effect of corrected engine speed and pressure altitude on corrected net thrust horsepower at a ram pressure ratio of approximately 1.40. Engine speed and net thrust horsepower corrected to NACA standard atmospheric conditions at sea level.

553

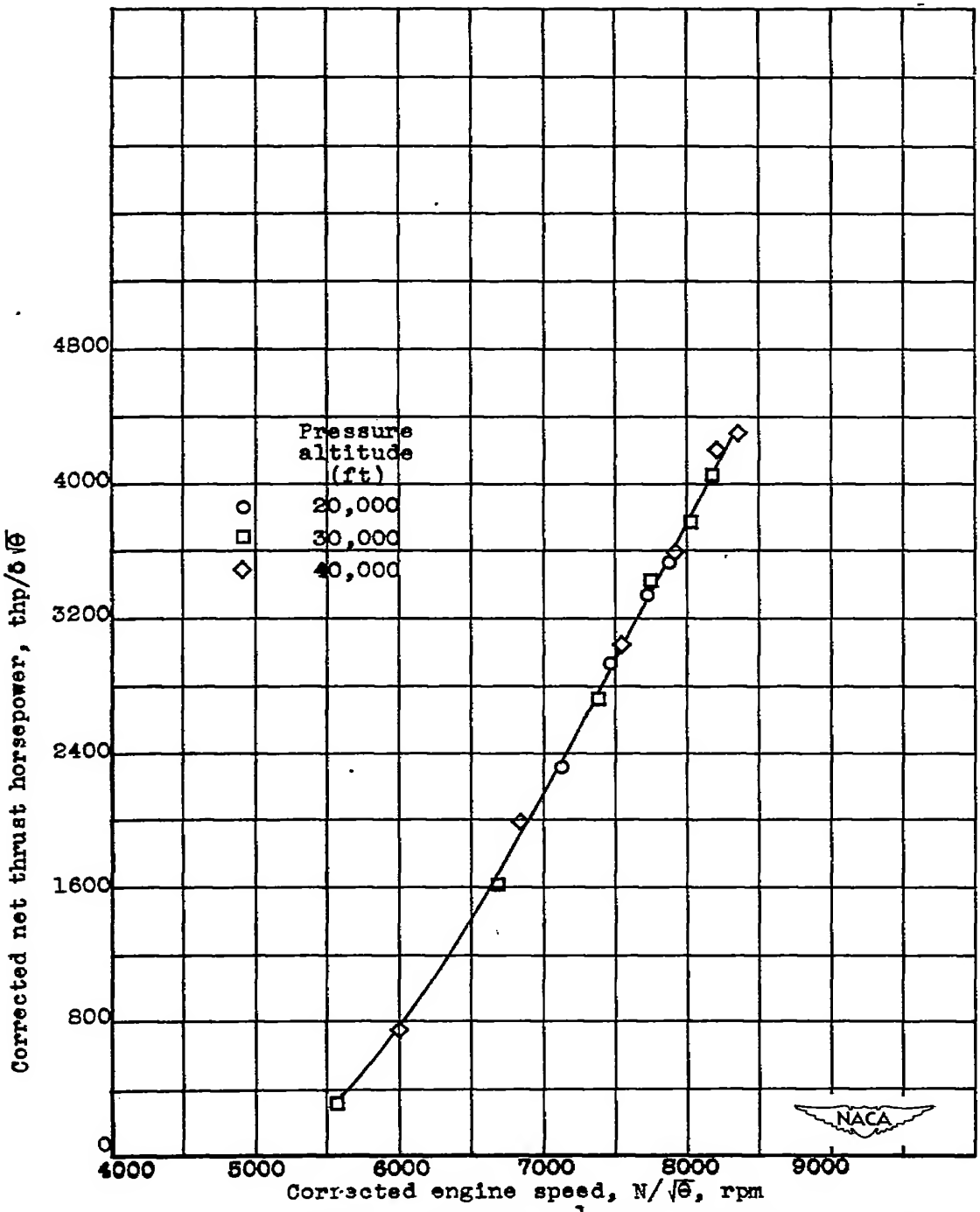

(b) High-flow compressor with 19$\frac{1}{2}$-inch-diameter tail-pipe nozzle.

Figure 24.- Concluded.

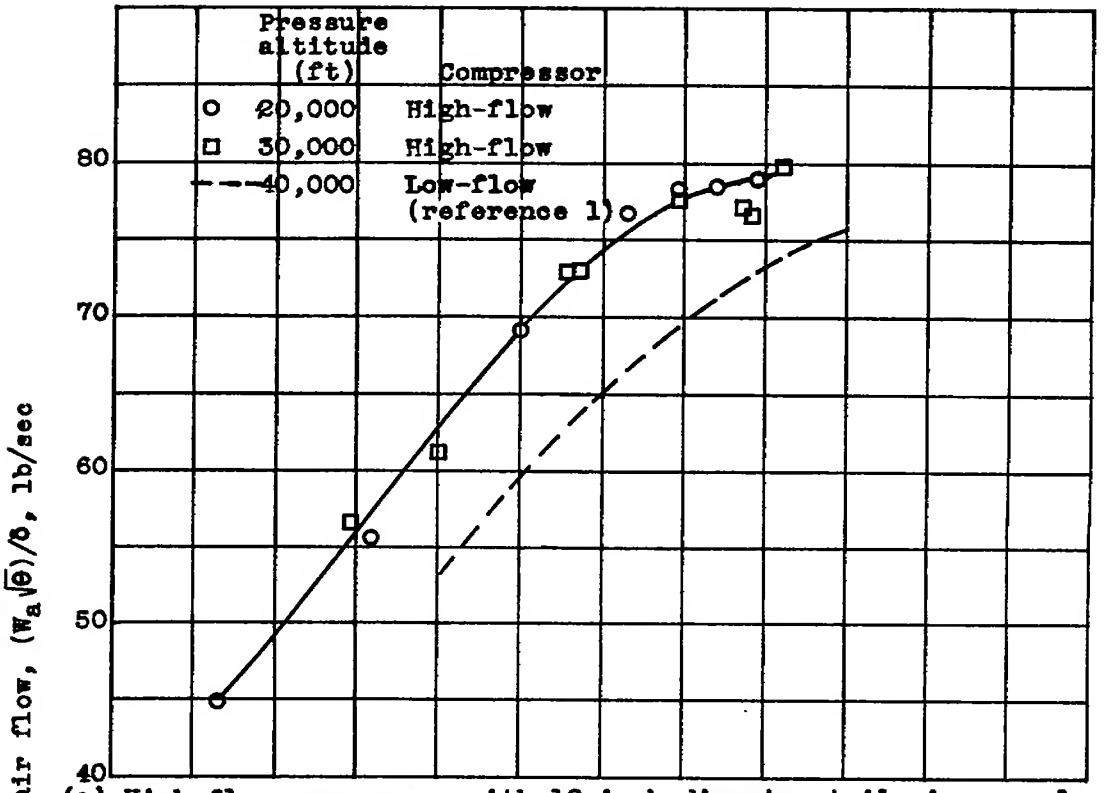

(a) High-flow compressor with 18-inch-diameter tail-pipe nozzle and low-flow compressor with $16\frac{3}{4}$-inch-diameter tail-pipe nozzle

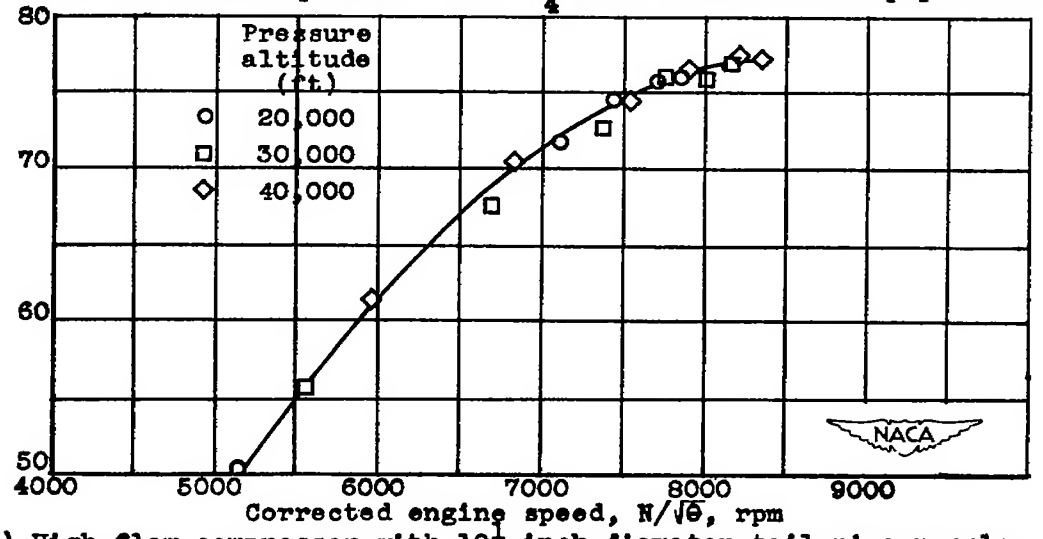

(b) High-flow compressor with $19\frac{1}{2}$-inch-diameter tail-pipe nozzle.

Figure 25.- Effect of corrected engine speed and pressure altitude on corrected air flow at a ram pressure ratio of approximately 1.40. Engine speed and air flow corrected to NACA standard atmospheric conditions at sea level.

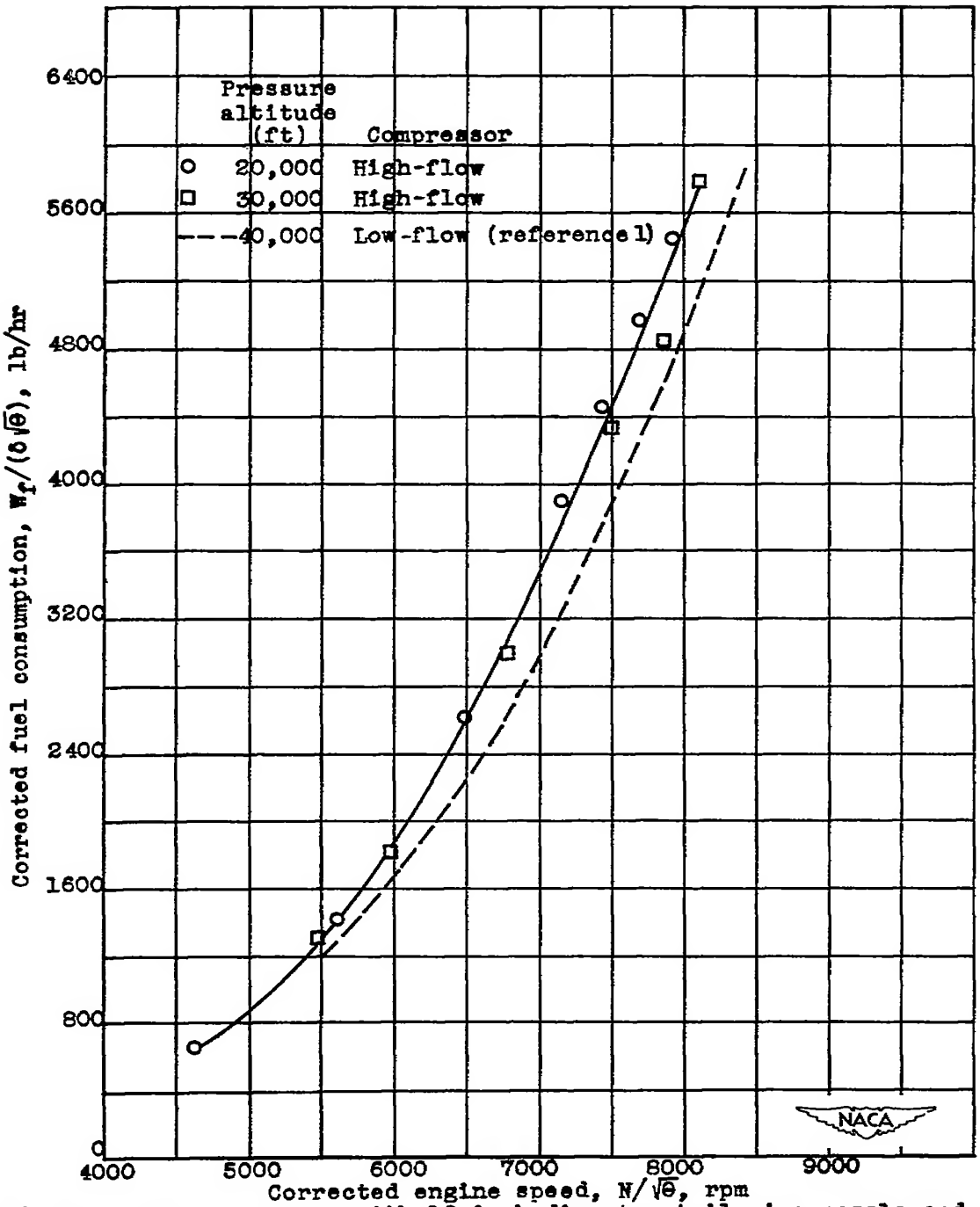

(a) High-flow compressor with 18-inch-diameter tail-pipe nozzle and low-flow compressor with $16\frac{3}{4}$-inch-diameter tail-pipe nozzle.

Figure 26.- Effect of corrected engine speed and pressure altitude on corrected fuel consumption at a ram pressure ratio of approximately 1.40. Engine speed and fuel consumption corrected to NACA standard atmospheric conditions at sea level.

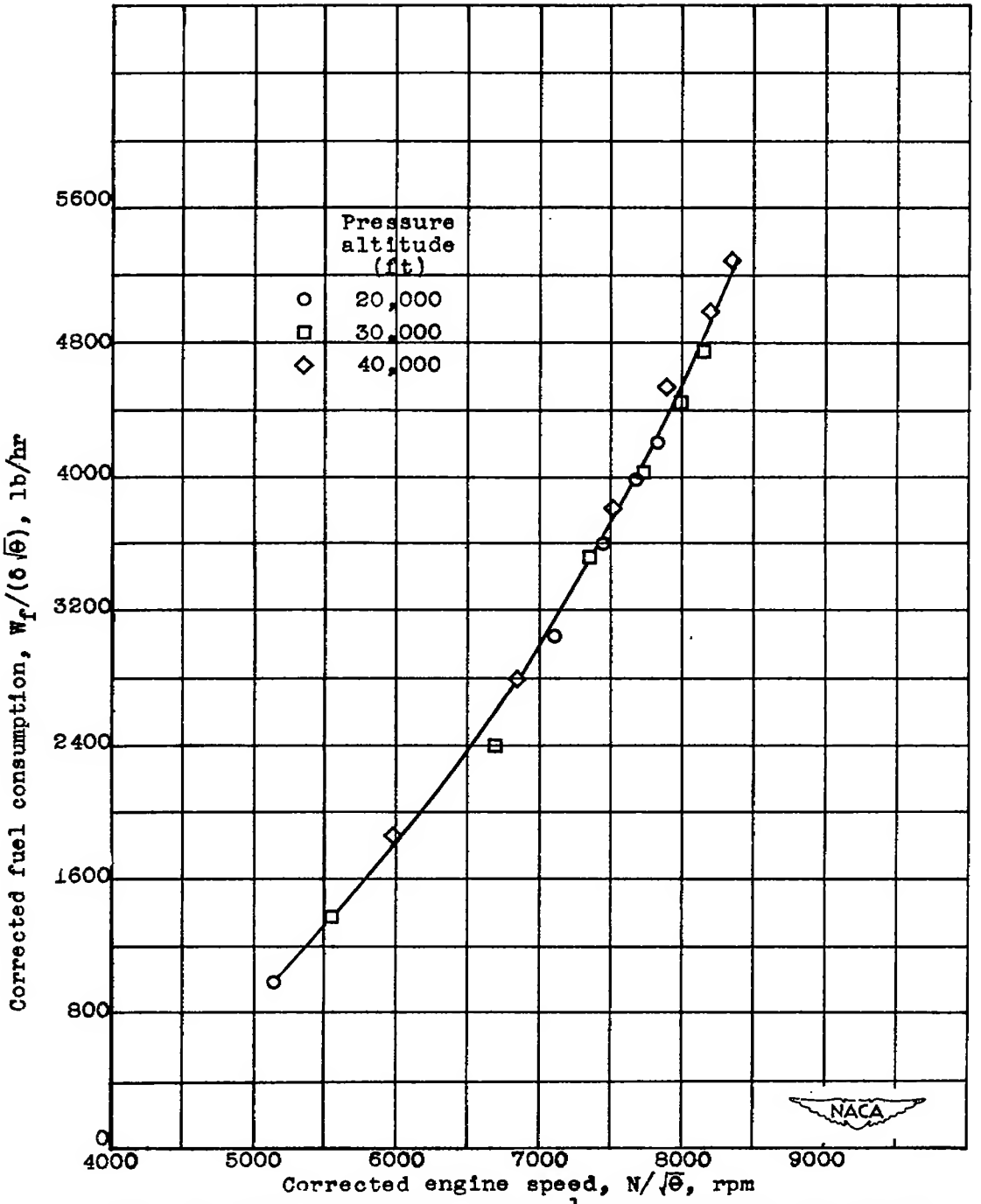

(b) High-flow compressor with $19\frac{1}{2}$-inch-diameter tail-pipe nozzle.

Figure 26.- Concluded.

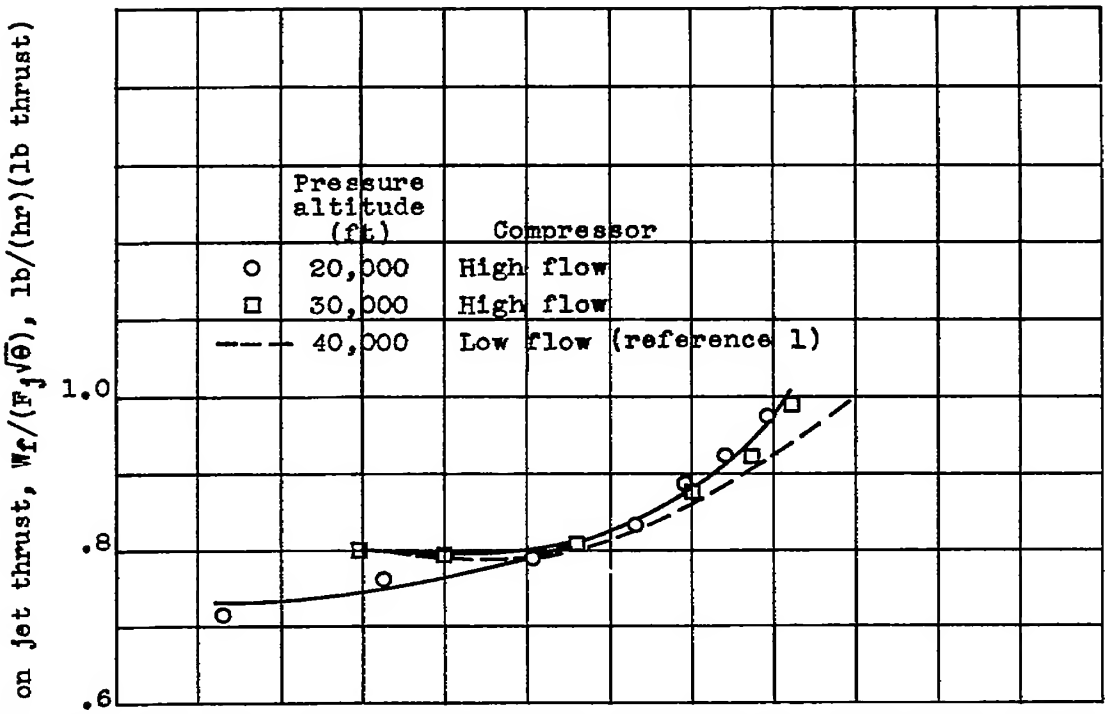

(a) High-flow compressor with 18-inch-diameter tail-pipe nozzle and low-flow compressor with 16$\frac{3}{4}$-inch-diameter tail-pipe nozzle.

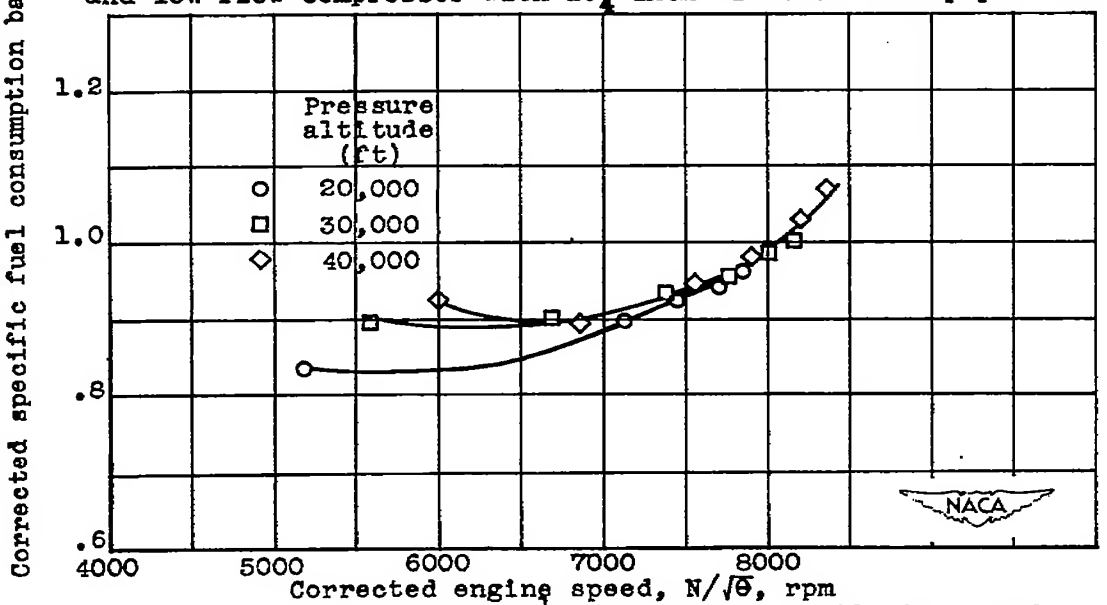

(b) High-flow compressor with 19$\frac{1}{2}$-inch-diameter tail-pipe nozzle.

Figure 27.- Variation of corrected specific fuel consumption based on jet thrust with corrected engine speed and pressure altitude at a ram pressure ratio of approximately 1.40. Specific fuel consumption and engine speed corrected to NACA standard atmospheric conditions at sea level.

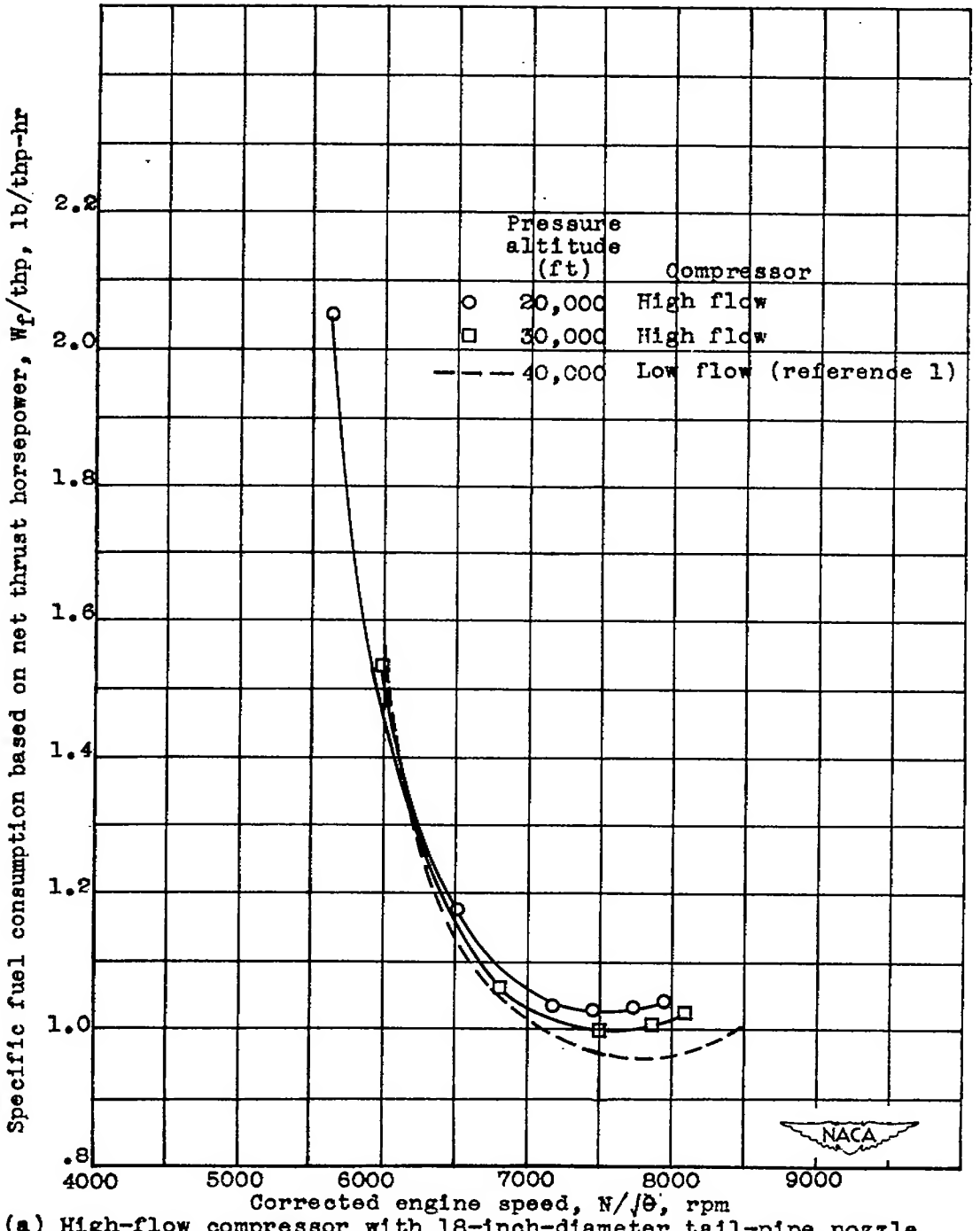

(a) High-flow compressor with 18-inch-diameter tail-pipe nozzle and low-flow compressor with $16\frac{3}{4}$-inch-diameter tail-pipe nozzle.

Figure 28.- Variation of specific fuel consumption based on net thrust with corrected engine speed and pressure altitude at a ram pressure ratio of approximately 1.40. Engine speed corrected to NACA standard atmospheric conditions at sea level.

553

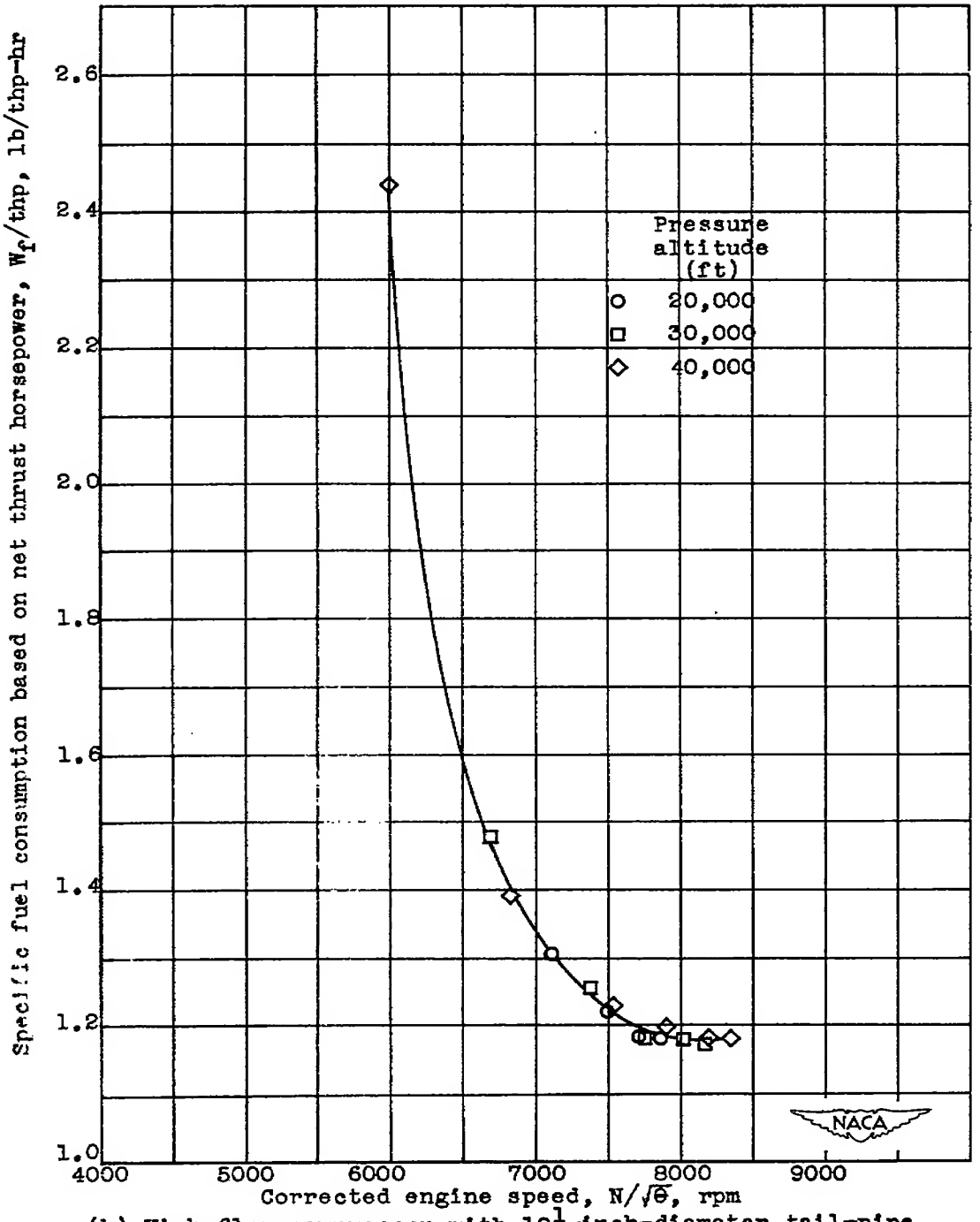

(b) High-flow compressor with $19\frac{1}{2}$-inch-diameter tail-pipe nozzle.

Figure 28.- Concluded.

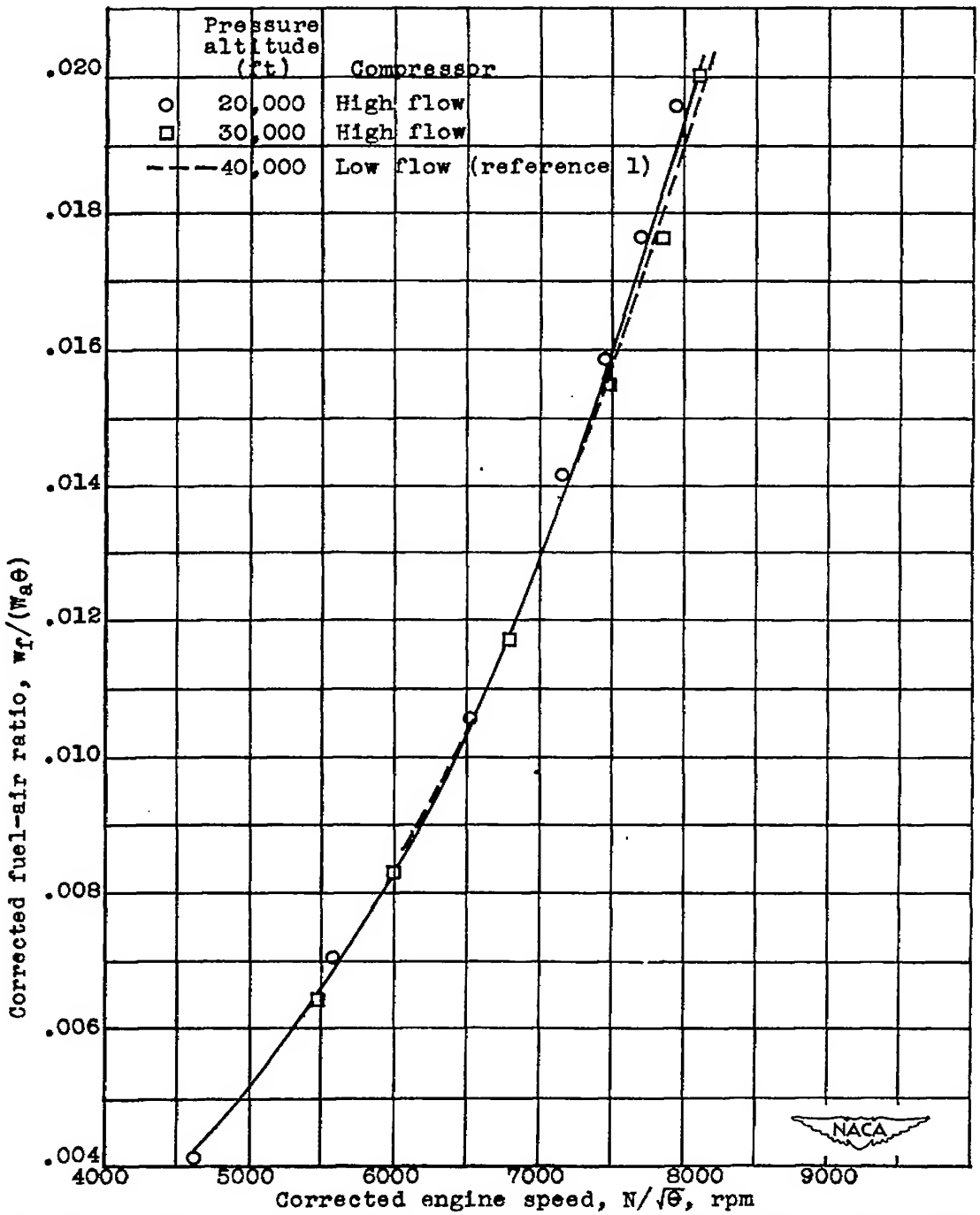

(a) High-flow compressor with 18-inch-diameter tail-pipe nozzle and low-flow compressor with $16\frac{3}{4}$-inch-diameter tail-pipe nozzle.

Figure 29.- Effect of corrected engine speed and pressure altitude on corrected fuel-air ratio at a ram pressure ratio of approximately 1.40. Engine speed and fuel-air ratio corrected to NACA standard atmospheric conditions at sea level.

553

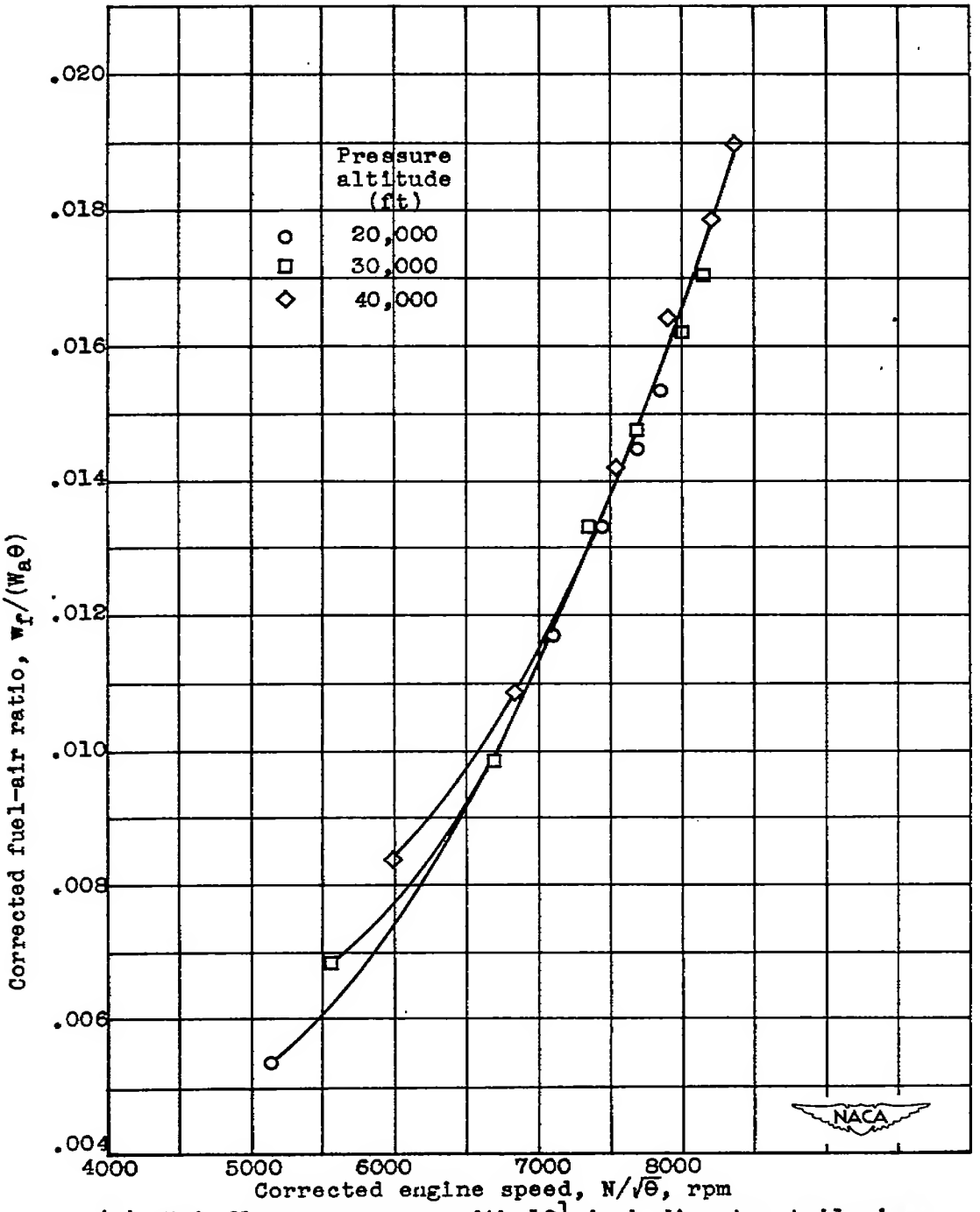

(b) High-flow compressor with $19\frac{1}{2}$-inch-diameter tail-pipe nozzle.

Figure 29.- Concluded.

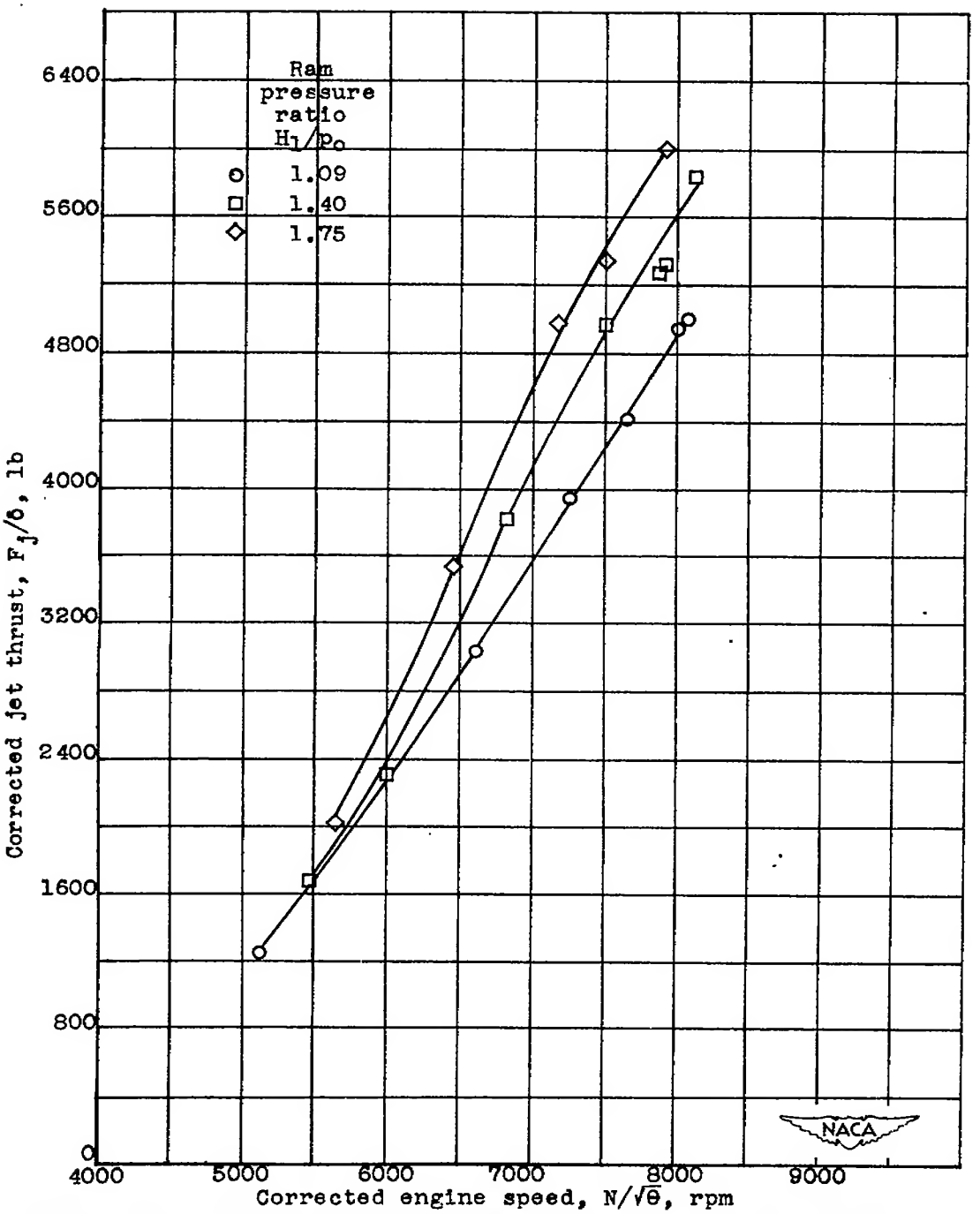

Figure 30.- Effect of corrected engine speed and ram pressure ratio on corrected jet thrust at a pressure altitude of 30,000 feet with high-flow compressor and 18-inch-diameter tail-pipe nozzle. Engine speed and jet thrust corrected to NACA standard atmospheric conditions at sea level.

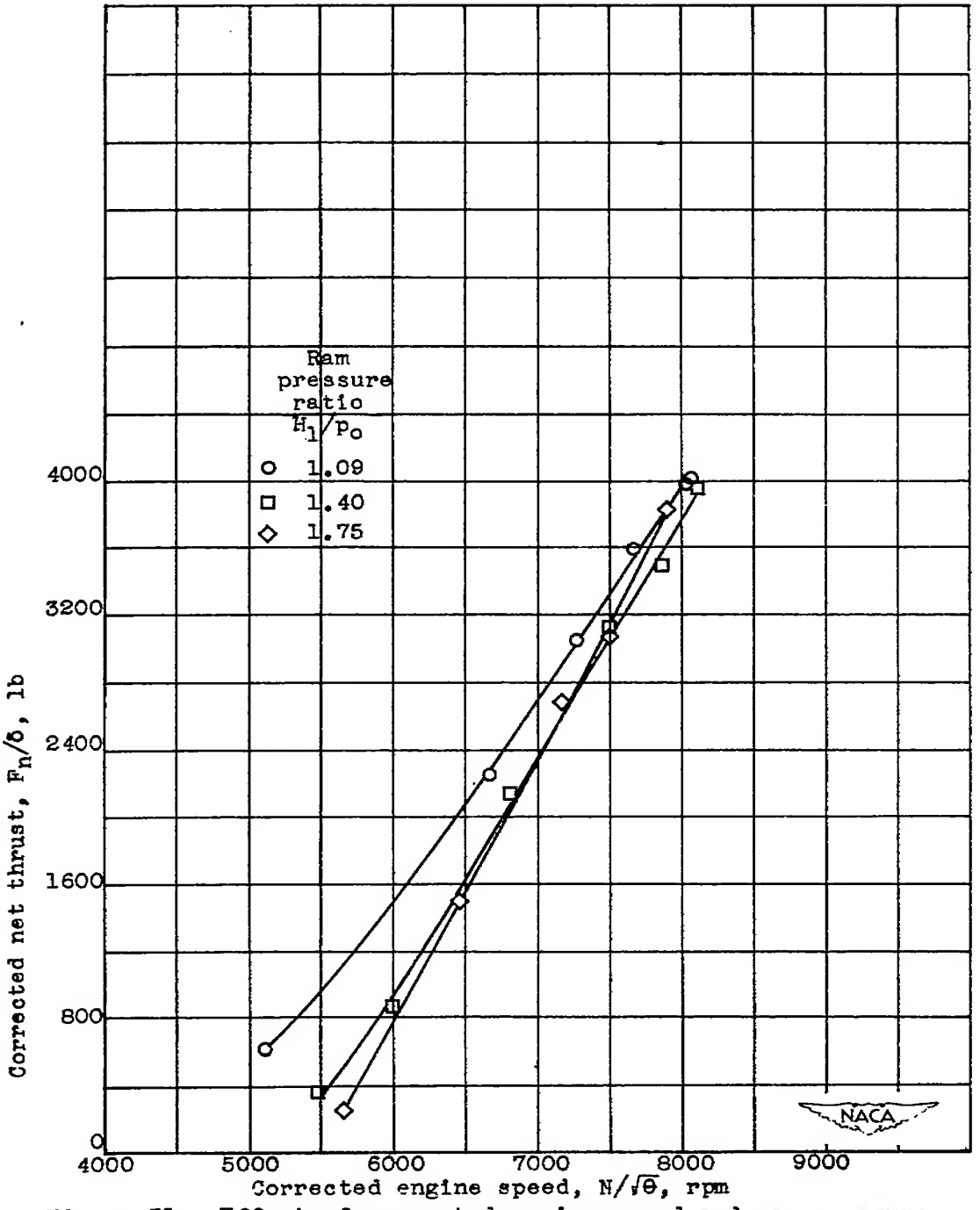

Figure 31.- Effect of corrected engine speed and ram pressure ratio on corrected net thrust at a pressure altitude of 30,000 feet with high-flow compressor and 18-inch-diameter tail-pipe nozzle. Engine speed and net thrust corrected to NACA standard atmospheric conditions at sea level.

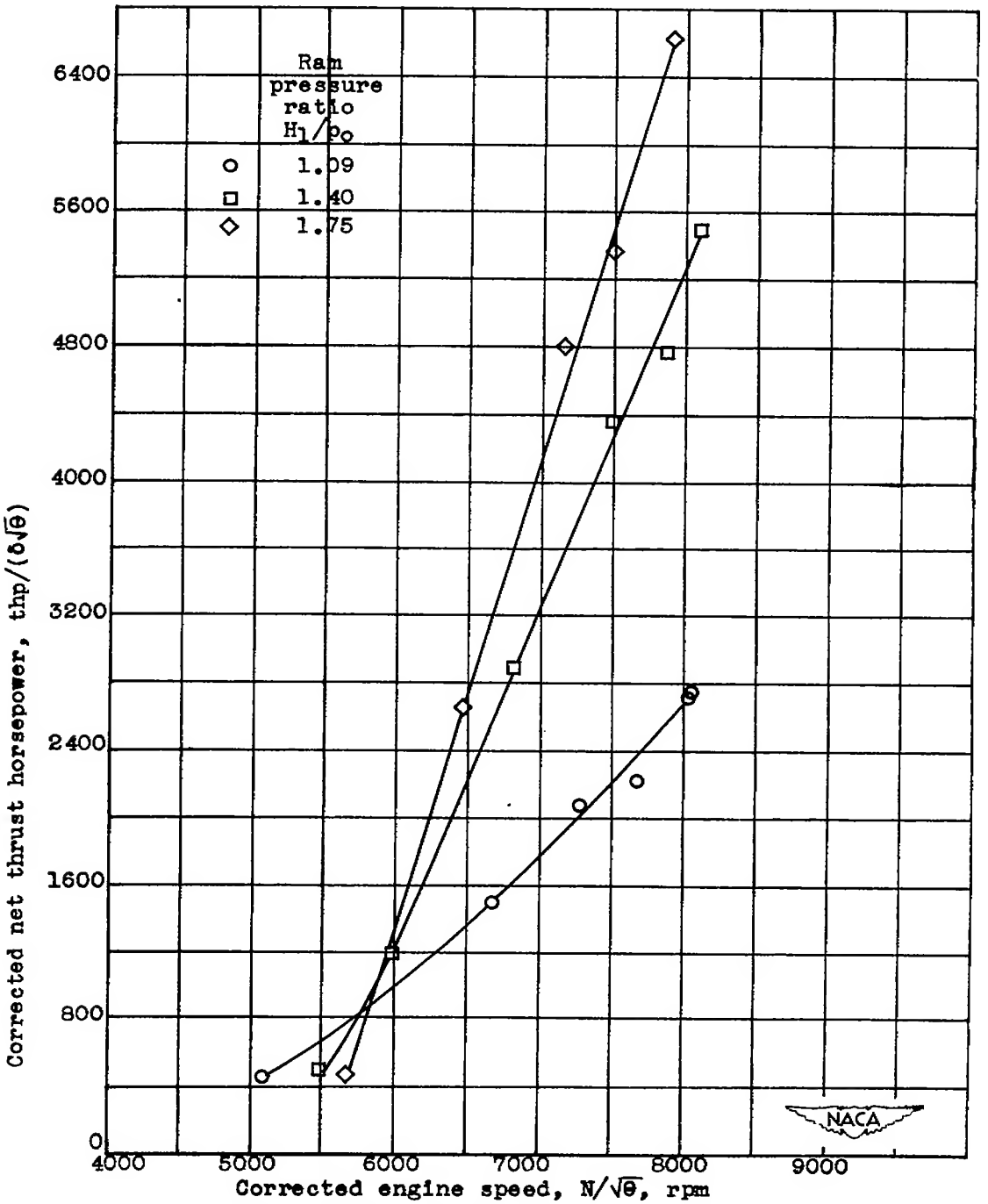

Figure 32.- Effect of corrected engine speed and ram pressure ratio on corrected net thrust horsepower at a pressure altitude of 30,000 feet with high-flow compressor and 18-inch-diameter tail-pipe nozzle. Engine speed and net thrust horsepower corrected to NACA standard atmospheric conditions at sea level.

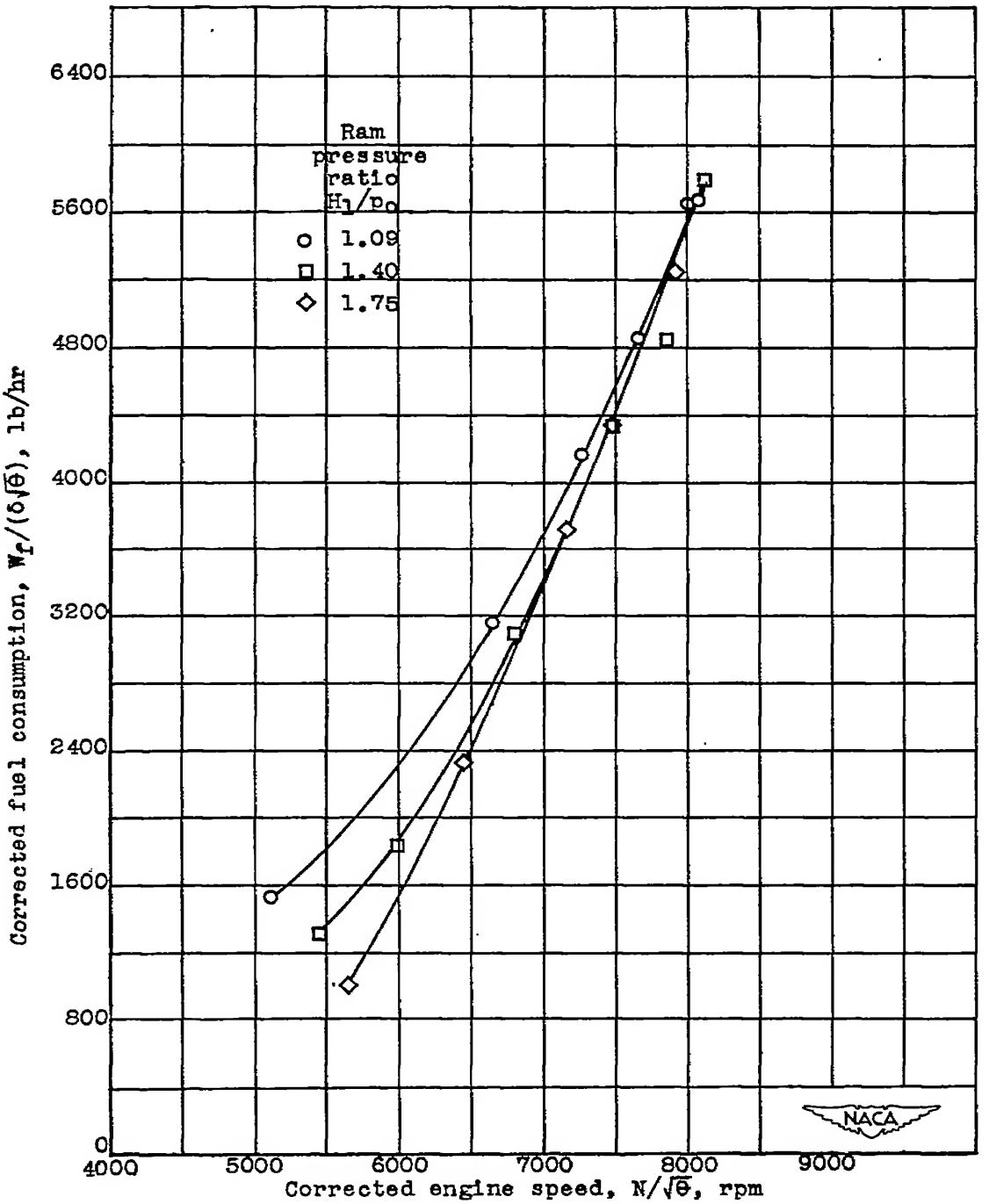

Figure 33.- Effect of corrected engine speed and ram pressure ratio on corrected fuel consumption at a pressure altitude of 30,000 feet with high-flow compressor and 18-inch-diameter tail-pipe nozzle. Engine speed and fuel consumption corrected to NACA standard atmospheric conditions at sea level.

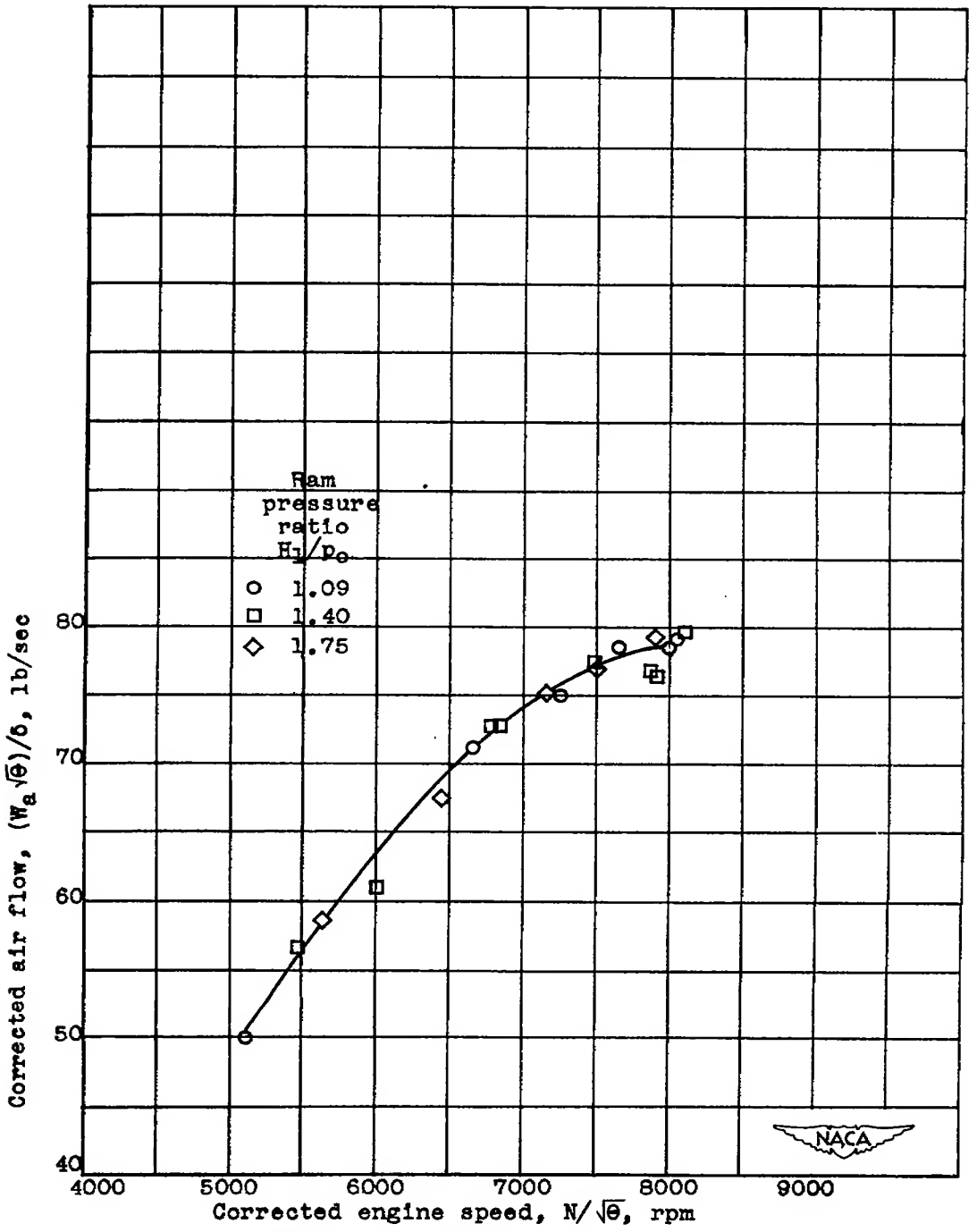

Figure 34.- Effect of corrected engine speed and ram pressure ratio on corrected air flow at a pressure altitude of 30,000 feet with high-flow compressor and 18-inch-diameter tailpipe nozzle. Engine speed and air flow corrected to NACA standard atmospheric conditions at sea level.

553

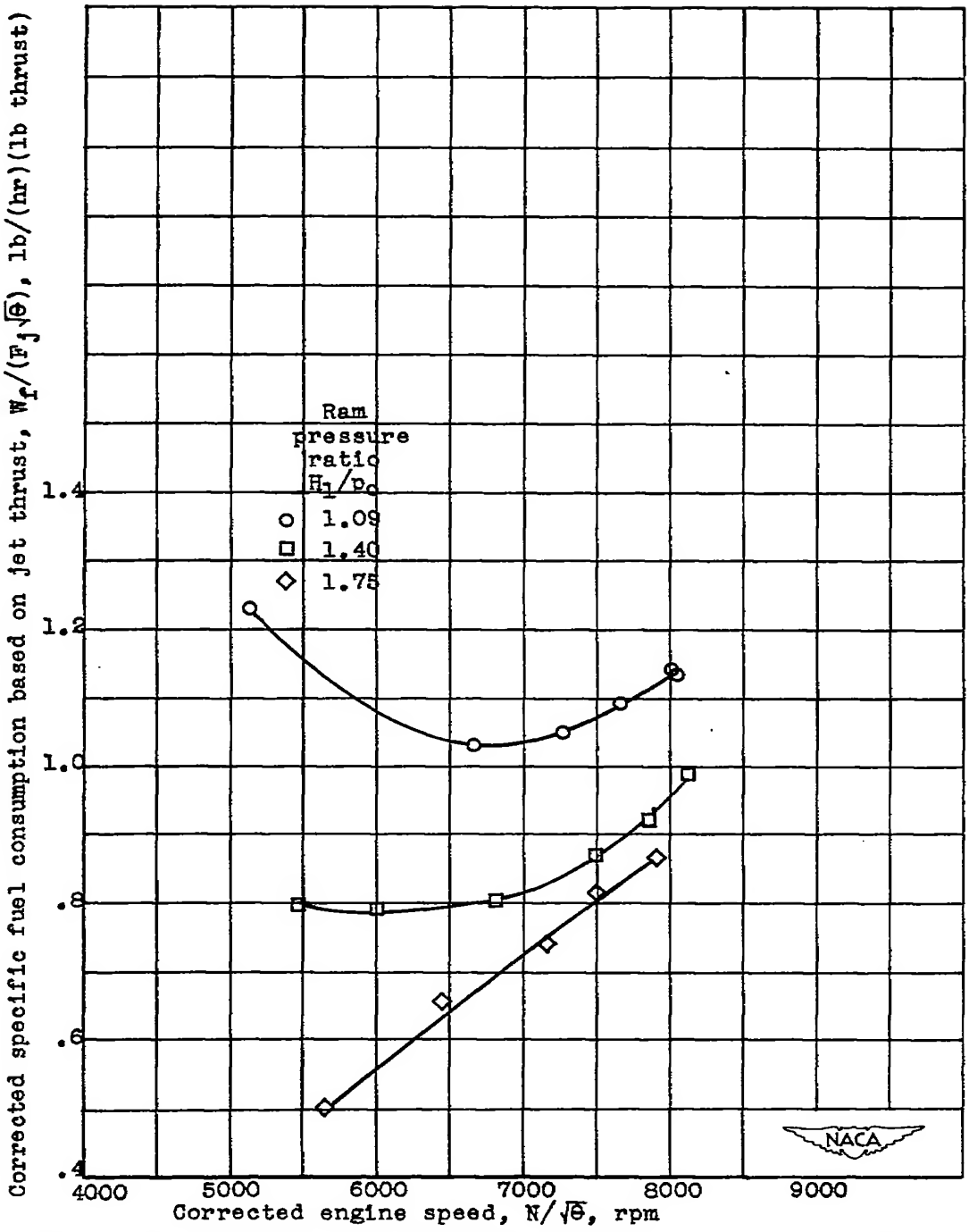

Figure 35.- Variation of corrected specific fuel consumption based on jet thrust with corrected engine speed and ram pressure ratio at a pressure altitude of 30,000 feet with high-flow compressor and 18-inch-diameter tail-pipe nozzle. Engine speed and specific fuel consumption corrected to NACA standard atmospheric conditions at sea level.

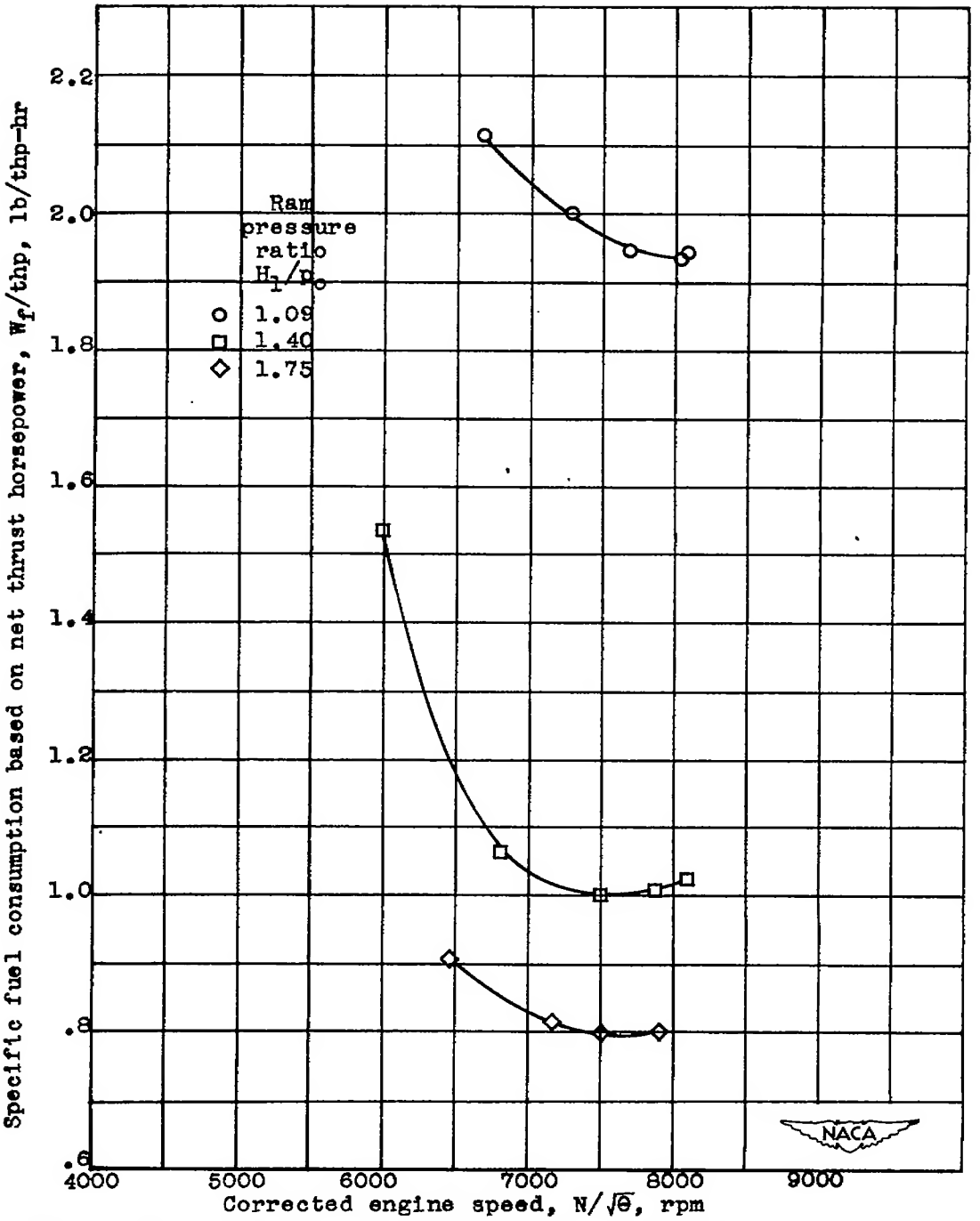

Figure 36.- Variation of specific fuel consumption based on net thrust horsepower with corrected engine speed and ram pressure ratio at a pressure altitude of 30,000 feet with high-flow compressor and 18-inch-diameter tail-pipe nozzle. Engine speed corrected to NACA standard atmospheric conditions at sea level.

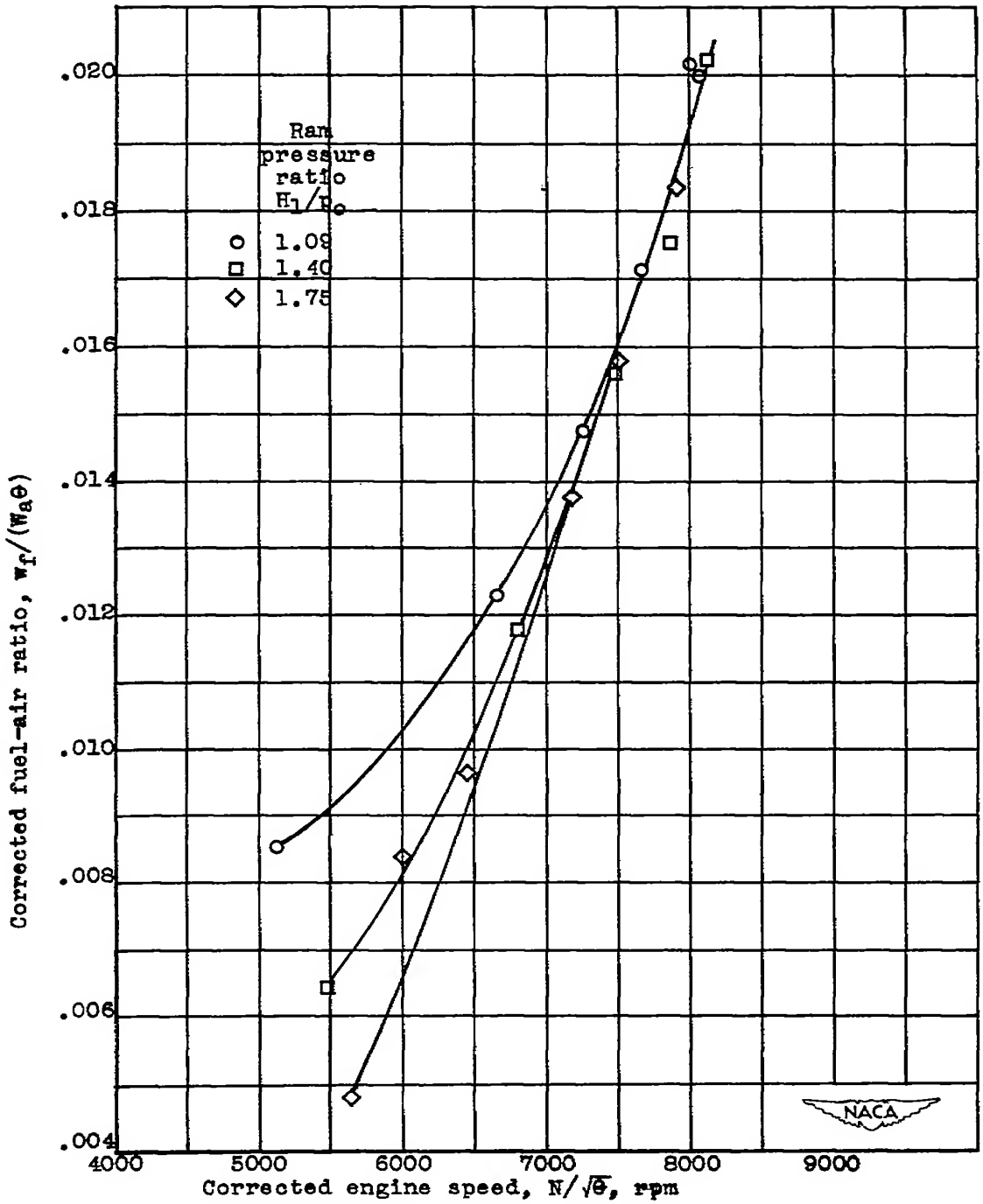

Figure 37.- Effect of corrected engine speed and ram pressure ratio on corrected fuel-air ratio at a pressure altitude of 30,000 feet with high-flow compressor and 18-inch-diameter tail-pipe nozzle. Engine speed and fuel-air ratio corrected to NACA standard atmospheric conditions at sea level.

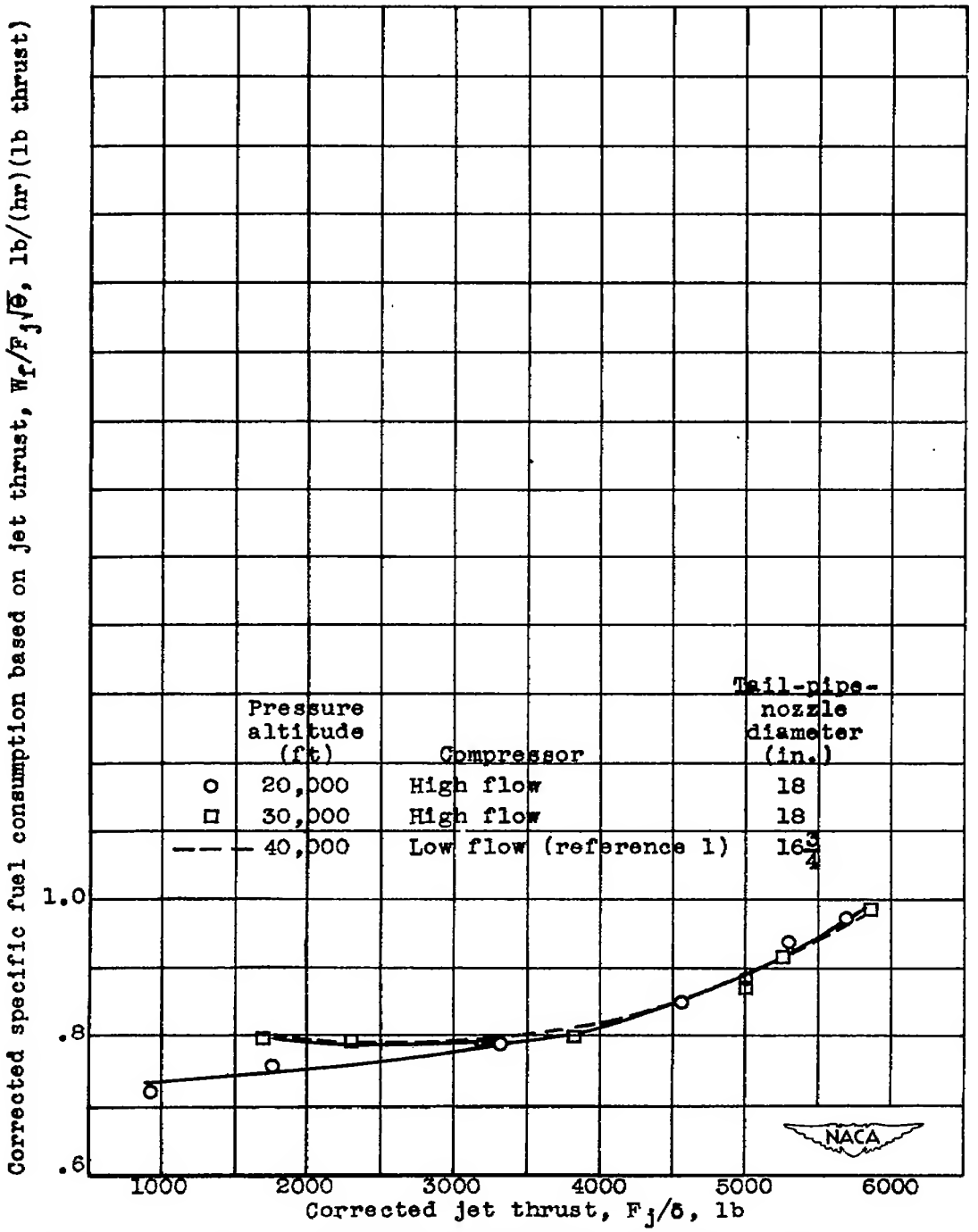

Figure 38.- Variation of corrected specific fuel consumption based on jet thrust with corrected jet thrust and pressure altitude at a ram pressure ratio of approximately 1.40. Jet thrust and specific fuel consumption corrected to NACA standard atmospheric conditions at sea level.

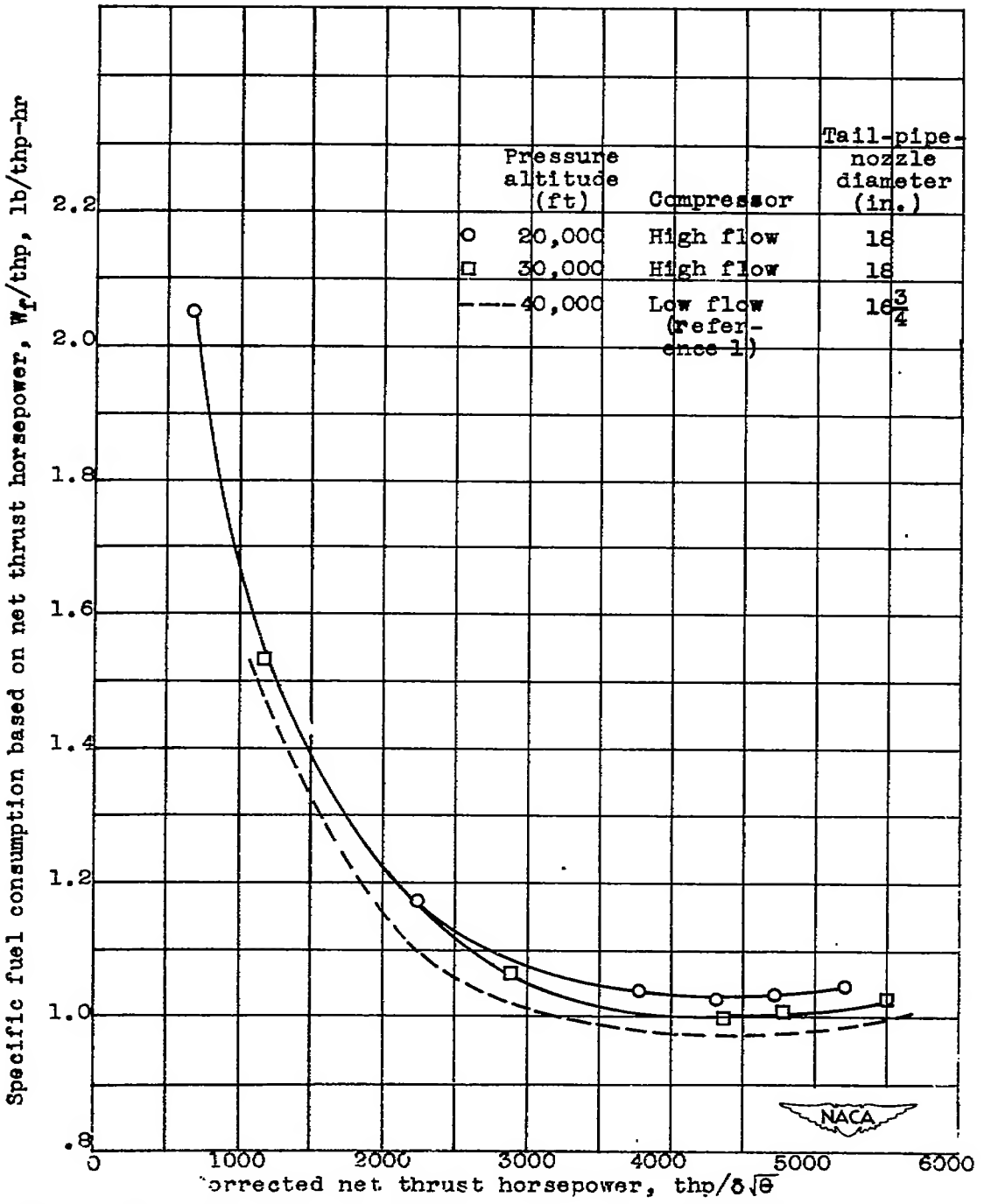

Figure 39.- Variation of specific fuel consumption based on net thrust horsepower with net thrust horsepower and pressure altitude at a ram pressure ratio of approximately 1.40. Net thrust horsepower corrected to NACA standard atmospheric conditions at sea level.

NASA Technical Library
3 1176 01435 5334